Aus der Klinik für Kardiologie und Pneumologie

(Prof. Dr. med. G. Hasenfuß)

der Medizinischen Fakultät der Universität Göttingen

Analysis of catecholamine-induced beta-adrenergic signaling in TTS by patient-specific pluripotent stem cell-derived cardiomyocytes

INAUGURAL-DISSERTATION

zur Erlangung des Doktorgrades

der Medizinischen Fakultät der

Georg-August-Universität zu Göttingen

vorgelegt von

Celina Isabelle Guessoum

aus Goslar

Göttingen 2020

Dekan:	Prof. Dr. rer. nat. H. K. Kroemer
Referent/in:	PD Dr. K. Streckfuß-Bömeke
Ko-Referent/in:	PD Dr. L. Zelarayan-Behrend
Drittreferent/in:	Prof. Dr. M. Oppermann

Datum der mündlichen Prüfung: 21. April 2020

Hiermit erkläre ich, die Dissertation mit dem Titel "Analysis of catecholamine-induced beta-adrenergic signaling in TTS by patient-specific pluripotent stem cell-derived cardiomyocytes“ eigenständig angefertigt und keine anderen als die von mir angegebenen Quellen und Hilfsmittel verwendet zu haben.

Göttingen, den 18. März 2020

Table of contents

Abbreviations ..... **IV**

List of Figures ..... **VII**

List of Tables ..... **VIII**

1 Introduction **1**

1.1 Takotsubo syndrome *1*

1.2 Pathophysiology of TTS *3*

1.2.1 Protective effect of estrogen 3

1.2.2 Neurogenic stunned myocardium 4

1.2.3 Vascular involvement 4

1.2.4 Genetic predisposition 5

1.2.5 High levels of catecholamines 5

1.2.6 Beta-adrenergic signaling 6

1.3 Human-induced pluripotent stem cells *7*

1.4 Directed cardiac differentiation of hiPSCs *9*

1.5 Disease modeling and drug screening with hiPSCs *10*

1.6 Aim of this thesis *12*

2 Material and methods **13**

2.1 Materials *13*

2.1.1 Cells and cell lines 13

2.1.2 Media, solutions and chemicals for cell culture 14

2.1.3 Chemicals, solutions and buffers for molecular biological and protein analyses 17

2.1.4 Antibodies used for immunofluorescence and western blot analyses 23

2.1.5 Oligonucleotides 24

2.2 Methods *26*

2.2.1 Cell culture 26

2.2.1.1 Cultivation and inactivation of mouse embryonic fibroblasts 26

2.2.1.2 Cultivation of hiPSCs on mouse embryonic fibroblasts 26

2.2.1.3 Cultivation of hiPSCs on Geltrex 26

2.2.1.4 Freezing and thawing of cultivated hiPSCs 27

2.2.1.5 Harvesting of cultivated cells for pellets 28

2.2.1.6 Spontaneous in vitro differentiation of hiPSCs cultivated on feeder-layer 28

2.2.1.7 Directed cardiac differentiation of hiPSCs cultivated on Geltrex 29

2.2.1.8 Digestion of hiPSC-derived cardiomyocytes 30

2.2.1.9 Selection of hiPSC-derived cardiomyocytes 30

2.2.1.10 Catecholamine treatment of hiPSC-derived cardiomyocytes 30

2.2.2 Alkaline phosphatase staining 31

2.2.3 Immunofluorescence staining 31
2.2.4 Metaphase preparation and karyotyping 32
2.2.5 Teratoma formation and analysis 33
2.2.6 Gene expression analyses 33
2.2.6.1 RNA isolation and purification 33
2.2.6.2 Reverse transcription reaction 34
2.2.6.3 Semi-quantitative PCR 35
2.2.6.4 Gel electrophoresis 36
2.2.6.5 Quantitative real-time PCR 36
2.2.7 Western blot analyses 37
2.2.7.1 Preparation of cell lysates 37
2.2.7.2 SDS-polyacrylamide gel electrophoresis 38
2.2.7.3 Protein transfer 38
2.2.7.4 Protein detection 39
2.2.8 Statistical analyses 39

3 Results 40

3.1 Proof of pluripotency 40
3.1.1 Morphology and alkaline phosphatase staining 40
3.1.2 Expression of pluripotency related markers 40
3.1.3 Differentiation potential *in vitro* and *in vivo* 42
3.1.4 Karyotyping 45
3.2 Generation of hiPSC-derived cardiomyocytes 45
3.3 Stress induction in hiPSC-derived cardiomyocytes 47
3.4 NR4A1 as a stress marker 48
3.4.1 Next Generation Sequencing 48
3.4.2 Detailed analysis of *NR4A1* expression 49
3.5 Influence of stress induction on sarcomeric structure 52
3.6 Influence of catecholamine treatment on beta-adrenergic signaling 52
3.7 Expression of possible NR4A1 targets after catecholamine treatment 55

4 Discussion 57

4.1 Successful generation of hiPSCs from TTS patients 57
4.2 Successful directed differentiation of hiPSCs into CMs 59
4.3 Generation of a humanized in vitro TTS-hiPSC-CMs model 60
4.3.1 Analysis of stress induction in hiPSC-CMs 61
4.3.2 Involvement of the β-adrenergic pathway in TTS 63
4.3.3 ERK activation 64
4.3.4 Targets of NR4A1 64
4.4 Limitations 65

4.5 Future perspectives *66*

5 Summary **68**

6 References **69**

Abbreviations

ACTN2	Alpha-actinin 2
AFP	Alpha-1-fetoprotein
α-MHC	Alpha-myosin heavy chain
ALB	Albumin
AMI	Acute myocardial infarction
ANP	Atrial natriuretic peptide
APS	Ammonium persulfate
bFGF	Basic fibroblast growth factor
BSA	Bovine serum albumin
BNP	Brain natriuretic peptide
CASQ2	Calsequestrine 2
cDNA	Complementary deoxyribonucleic acid
CDM3	Chemically defined medium, 3 components
CMs	Cardiomyocytes
C-MYC	v-myc avian myelocytomatosis viral oncogene homolog
CPT1C	Carnitine palmitoyltransferase 1C
cTNT	Cardiac troponin T
Cy3	Cyanine 3
DAPI	4’,6-diamidino-2-phenylindole dihydrochloride
DEPC	Diethylpyrocarbonate
DMEM	Dulbecco’s modified Eagle medium
DMSO	Dimethylsulfoxide
DNA	Deoxyribonucleic acid
DPBS	Dulbecco’s phosphate-buffered saline
DTT	Dithiothreitol
EBs	Embryoid bodies

ECG	Electrocardiogram
EDTA	Ethylenediaminetetraacetic acid
Epi	Epinephrine
ERK 1/2	Extracellular-signal regulated kinase
FBS	Fetal bovine serum
FITC	Fluorescein isothiocyanate
FOXD3	Forkhead box D3
GAPDH	Glyceraldehyde-3-phosphate dehydrogenase
GATA4	GATA-binding protein 4
GDF3	Growth differentiation factor 3
GFAT1	Glucosamine-fructose-6-phosphate-aminotransferase 1
HEPES	4-(2-hydroxyethyl)-1-piperazineethanesulfonic acid
hESCs	Human embryonic stem cells
hiPSCs	Human-induced pluripotent stem cells
hiPSC-CMs	hiPSC-derived cardiomyocytes
IgG/IgM	Immunoglobulin G/M
IF	Immunofluorescence
IMDM	Iscove's Modified Dulbecco's Medium
Iso	Isoprenaline
IWPs	Inhibitors of Wnt production
KLF	Kruppel-like factor 4
MACCE	Major adverse cardiac and cerebrovascular events
MEFs	Mouse embryonic fibroblasts
MTG	Monothioglycerol
NEAA	Non-essential amino acids
NFATc3	Nuclear factor of activated T-cells, cytoplasmic 3
NPPA	Natriuretic peptide precursor A
NPPB	Natriuretic peptide precursor B

NR4A1	Nuclear receptor subfamily 4 group A member 1
OCT4	Octamer-binding transcription factor 4
OGT	O-linked N-acetylglucosamine transferase
PCR	Polymerase chain reaction
PFA	Paraformaldehyde
RBM20	RNA binding motif protein 20
RPMI	Roswell Park Memorial Institute
RT-PCR	Reverse transcriptase PCR
RYR2	Ryanodine receptor 2
pRYR2-S2808	Ryanodine receptor 2 phosphorylated at Serine 2808
SAH	Subarachnoid hemorrhage
SDS	Sodium dodecyl sulfate
α-SMA	Alpha-smooth muscle actin
SNP	Single nucleotide polymorphism
SOX2	SRY (sex determining region Y)-box 2
SSEA4	Stage-specific embryonic antigen 4
STEMCCA	Stem cell cassette
SYP	Synaptophysin
TB buffer	Tris-borate buffer
TBS-T	Tris-buffered saline with Tween 20
TEMED	Tetramethylethylenediamine
TH	Tyrosine hydroxylase
Tris	Tris(hydroxymethyl)aminomethane
WB	Western blot
WES	Whole-exome sequencing

List of Figures

Figure 1. Angiogram of a left ventricle during a TTS event resembles Japanese octopus trap..... 1
Figure 2. Schematic overview of the β-adrenergic signaling pathyway. 7
Figure 3. General overview about cardiac differentiation of hiPSCs. 10
Figure 4. Schematic illustration of the spontaneous differentiation protocol used for in vitro differentiation of the generated hiPSCs. 28
Figure 5. Visualization of the directed cardiac differentiation protocol. 29
Figure 6. Morphology and alkaline phosphatase staining. 40
Figure 7. Gene expression analysis and immunostaining of two generated hiPSC lines of patient 1. 41
Figure 8. Gene expression analysis of in vitro differentiated TTS-hiPSCs. 42
Figure 9. Immunofluorescence staining and teratoma formation of spontaneously differentiated TTS-hiPSCs. 44
Figure 10. A representative karyogram of hiPSCs (1-TTS-1) cultivated for ≥ 25 passages. 45
Figure 11. Gene expression analysis, morphology and immunofluorescence staining of mature TTS-hiPSC-derived CMs. 46
Figure 12. Expression of *NPPB* and *NPPA* in control- and TTS-hiPSC-CMs after catecholamine treatment. 48
Figure 13. NGS data obtained after treating control- and TTS-hiPSC-CMs with 500 µmol/L Epi. 49
Figure 14. Gene expression of *NR4A1* in hiPSC-CMs after Epi, Iso and PE treatment. 50
Figure 15. *NR4A1* expression in control- and TTS-hiPSC-CMs after Iso and Epi treatment. 51
Figure 16. Immunostaining of TTS-hiPSC-CMs with or without catecholamine treatment. 52
Figure 17. Phosphorylation of RyR2 at Serine 2808 in TTS- and control-hiPSC-CMs after catecholamine treatment. 54
Figure 18. Phosphorylation of ERK in TTS- and control-hiPSC-CMs after catecholamine treatment. 55
Figure 19. Expression of *GFAT1* and *OGT* after catecholamine treatment. 56

List of Tables

Table 1. HiPS cell lines used in this work. 13
Table 2. Components for cell culture. 14
Table 3. Components for molecular biological methods and protein analyses. 18
Table 4. Primary antibodies used for immunofluorescence and western blot analyses. 23
Table 5. Secondary antibodies. 24
Table 6. Oligonucleotides used for PCR analyses. 25
Table 7. Catecholamine concentrations. 31
Table 8. RT reaction components. 34
Table 9. Thermocycler program for the RT reaction. 34
Table 10. Components for PCR. 35
Table 11. Thermocycler program for semi-quantitative PCR. 35
Table 12. Master mix for quantitative real-time PCR 36
Table 13. Quantitative PCR program 37
Table 14. Transfer arrangement. 38

1 Introduction

1.1 Takotsubo syndrome

Takotsubo syndrom (TSS) is a heart disease first described by Dr. Hikaru Sato and his colleagues in the early nineties (Sato et al. 1990, Dote et al. 1991). In his Japanese publication, Dr. Sato reported on patients with transient left ventricular dysfunction and described the shape of the patients' left ventricle in systole **(Fig. 1A)** as "tsubo"-shaped (meaning pot-shaped). Referring to the Japanese octopus trap "takotsubo" with a narrow neck and a round bottom **(Fig. 1B)**, his description was later modified to tako-tsubo-shaped. In 1991, a colleague of Dr. Sato published a detailed study report of 5 takotsubo cases, thereby creating awareness for this previously unknown cardiac disease (Dote et al. 1991). Over time, a growing number of TTS cases were reported in Japan and finally even outside of Japan (Pavin et al. 1997, Desmet et al. 2003). Nowadays, over 1000 articles concerning TTS have been published (Komamura et al. 2014).

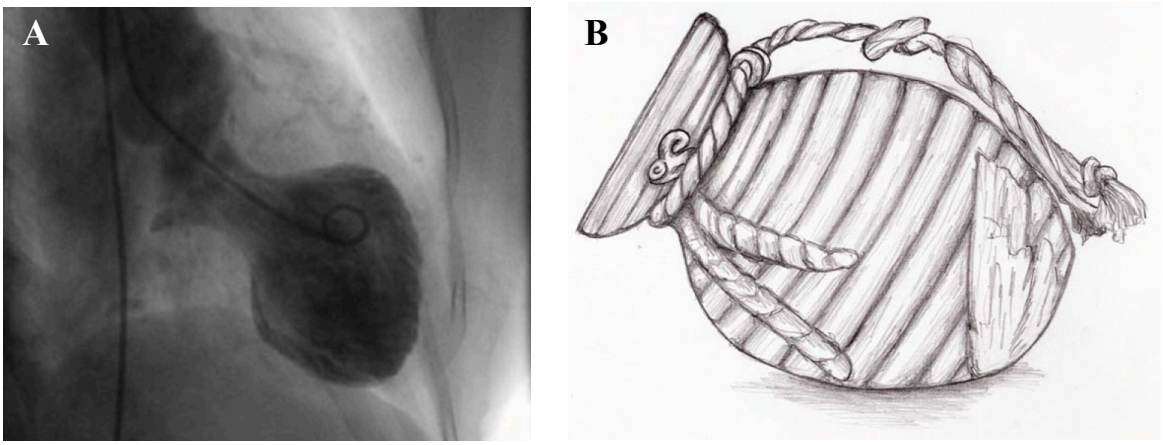

Figure 1. Angiogram of a left ventricle during a TTS event resembles Japanese octopus trap.

Angiogram of a TTS patient's left ventricle in systole during a TTS event **(A)** resembles the shape of the Japanese octopus trap "Takotsubo" **(B)** due to the transient hypokinesis of the left ventricular apex (Roshanzamir and Showkathali 2013). License number provided by the Copyright Clearance Center: 4564870311375

A variety of synonyms have occurred over the years (Sharkey et al. 2011) so that the Takotsubo syndrome is, among others, also known as ampulla cardiomyopathy (Ueyama et al. 2003), transient left ventricular apical ballooning (Tsuchihashi et al. 2001), apical ballooning syndrome (Elesber et al. 2007), stress-related cardiomyopathy (Sankri-Tarbichi et al. 2007) or broken heart syndrome (Soares-Filho et al. 2010). The latter two names refer to the noteworthy correlation between TTS and emotional or physical stress. More than two thirds of TTS patients show a preceding emotional or physical stressful event (Templin et al. 2015, Lyon et al. 2016). Although the synonym "broken heart syndrom" implies predominance of emotional triggers such as the death of a loved one, phys-

ical triggers like an asthma attack, a pneumothorax or an acute neurologic disorder are more prevalent (Templin et al. 2015).

Due to its clinical presentation, it is often said that the TTS mimics acute myocardial infarction (AMI). It has been estimated that about 2 % of the patients initially hospitalized with a suspected AMI eventually turn out to have TTS (Bybee et al. 2004, Prasad et al. 2008). Typical symptoms of patients with TTS include chest pain, dyspnea and syncope (Prasad et al. 2008, Templin et al. 2015). Additionally, ECG changes such as ST elevation or T wave inversion frequently occur in TTS patients (Bybee et al. 2007, Prasad et al. 2008, Frangieh et al. 2016). In contrast to AMI, these ECG changes as well as the ventricular wall motion abnormalities are not limited to the supply area of a single epicardial coronary artery. Coronary angiography of TTS patients confirms the absence of a significant coronary artery stenosis or evidence of an acute plaque rupture (Bybee et al. 2004, Prasad et al. 2008). Elevation of cardiac biomarkers such as Troponin T and CK-MB commonly occurs in TTS patients, although overall levels tend to be lower compared to AMI (Madhavan et al. 2009, Ramaraj et al. 2009). Another biomarker elevated in TTS patients is brain natriuretic peptide (BNP), which is known to be upregulated in patients with left ventricular dysfunction and whose serum concentrations can be used to determine the degree of heart failure in affected patients (Madhavan et al. 2009, Ahmed et al. 2012). To this day, no TTS-specific biomarker has yet been found. That is why the Mayo criteria, which were originally published in 2004 (Bybee et al. 2004) and updated in 2008 (Prasad et al. 2008), provide a guideline concerning the diagnosis of TTS and the differentiation to AMI. These criteria include the above-mentioned typical transient left ventricular wall motion abnormalities and evidence of myocardial ischemia in form of modest elevation of cardiac biomarkers and/or newly developed ECG abnormalities (such as ST elevations) without correlation to the perfusion territory of a single coronary artery. Furthermore, the absence of coronary artery stenosis, pheochromocytoma and myocarditis are also important criteria for the diagnosis of TTS (Bybee et al. 2007, Prasad et al. 2008). As the pathophysiology of TTS is still not fully understood, these criteria have been modified over time and will most likely continue to evolve. In the course of time, for example, it became apparent, that left ventricular dysfunction does not always involve apical (81.7 %) or midventricular (14.6 %) segments, which create the typical apical ballooning phenomenon first described in the early nineties (Dote et al. 1991, Templin et al. 2015). Although less common, hypo- or akinesis of basal segments (2.2 %) has been described and leads to the so-called reverse or basal TTS (Song et al. 2011, Templin et al. 2015). The least common type of all four TTS variants is focal TTS, which only occurs in 1.5 % of TTS patients (Templin et al. 2015).

No specific treatment of TTS has been developed so far. Due to the clinical similarities, TTS patients are initially treated for AMI until proven otherwise. Once the diagnosis has been confirmed, treatment of TTS mainly concentrates on monitoring of vital parameters and supportive care. Angiotensin-converting-enzyme inhibitors (ACE-inhibitors), beta-blockers, aspirin and diuretics are

among the drugs, which have been suggested for treatment of haemodynamically stable TTS patients (Amsterdam et al. 2014). Haemodynamically unstable patients can benefit from an intra-aortic balloon pump (Anders et al. 2011) and in case of apical thrombosis due to ventricular akinesis, anticoagulant therapy is required (Kurisu et al. 2011).

Remarkably, a lot of patients recover relatively quickly from a TTS event and regain their systolic ventricular function within months or even days after a TTS event, sometimes even without any kind of treatment (Akashi et al. 2003, Lyon et al. 2016). Nevertheless, TTS still remains a life-threatening disease. A recent detailed study of Templin and colleagues showed that approximately 22 % of TTS patients experience serious in-hospital complications such as cardiogenic shock, cardiopulmonary resuscitation or death (Templin et al. 2015). Further complications, especially during the acute phase of TTS, include arrhythmia (Brown et al. 2015), ventricular rupture (Akashi et al. 2004), intraventricular thrombi and embolic events (Sharkey et al. 2010). Recurrence of TTS amounts to approximately 2 % per patient-year while the rate of major adverse cardiac and cerebrovascular events (MACCE) amounts approximately 10 % per patient-year (Templin et al. 2015).

Patients of both sexes and nearly every age group can develop TTS. However, a wide range of studies has shown that the majority of TTS cases occur in postmenopausal women over the age of 55 (Bybee et al. 2004, Deshmukh et al. 2012). About 90 % of TTS patients are women with a mean age of 67 years (Templin et al. 2015), which led to the discussion of whether estrogen might play a protective role in the development of TTS (Kuo et al. 2010, Ueyama et al. 2003). Although progress has been made since the initial mention in 1990, substantial aspects of the pathophysiology of TTS still remain unexplained.

1.2 Pathophysiology of TTS

Several hypotheses have been suggested for the pathophysiology of TTS over the past 20 years. Although the exact mechanism that leads to the development of TTS still remains unclear, some hypotheses are considered more likely than others (Lyon et al. 2016, Kato et al. 2017).

1.2.1 Protective effect of estrogen

The above-mentioned large percentage of postmenopausal women affected by TTS did not go unnoticed by scientists studying the pathophysiology of TTS. Ueyama and colleagues were among the first to suggest a potentially protective effect of estrogen (Ueyama et al. 2003, Ueyama et al. 2007). They demonstrated that ovariectomized rats with estrogen supplementation showed less cardiac dysfunction and an increase of cardioprotective components such as heat shock protein 70 or atrial natriuretic peptide (ANP) after exposure to immobilization stress compared to ovariectomized rats

without estrogen supplementation (Ueyama et al. 2007). Additionally, their studies showed lower mRNA expression of cellular activity marker *c-fos* in the heart, brain and adrenal gland of ovariectomized rats with estrogen supplementation compared to those without, thereby suggesting that estrogen downregulates the stress-induced sympatho-adrenal activity (Ueyama et al. 2008). A notable lack of estrogen replacement therapy in TTS patients further supports this hypothesis (Kuo et al. 2010) and a recent study by El-Battrawy and colleagues verified the electrophysiological protective effect of estradiol to isoprenaline-treated hiPSC-CMs (El-Battrawy et al. 2018).

1.2.2 Neurogenic stunned myocardium

Although no TTS specific biomarker exists so far, Jaguszweski et al. were able to present four microRNAs that differentiate TTS from AMI (Jaguszweski et al. 2014). Two of these microRNAs, miR-16 and miR-26a, are associated with depression and stress response (Katsuura et al 2012, Rinaldi et al. 2010). Additionally, Templin et al. showed that more than half of the TTS patients in their study demonstrated the occurrence of a psychiatric or neurologic disorder in their past or present medical history (Templin et al. 2015). Acute heart failure occurring during (acute) neurologic diseases, in particular subarachnoid hemorrhage (SAH), has been reported in various cases and was named neurogenic stunned myocardium. Previous studies have discussed the clinical findings in patients with neurogenic stunned myocardium due to SAH and their resemblance to TTS (Guglin and Novotorova 2011). Patients with subarachnoid hemorrhage show ECG changes similar to those of TTS patients, including ST elevations and T inversions (Brouwers et al. 1989). Histological findings in neurogenic stunned myocardium are also similar to those found in TTS patients (Samuels 2007, Guglin and Novotorova 2011). In addition, ventricular wall motion abnormalities have been reported in patients with SAH (Pollick et al. 1988). In contrast to TTS patients, who predominantly show apically located ventricular dysfunction, patients with SAH mostly show basal, midventricular or global dysfunction (Banki et al. 2006, Guglin and Novotorova 2011, Templin et al. 2015). An increase of sympathetic stimulation and catecholamine serum concentration has been suggested as main pathophysiological factor behind neurogenic stunned myocardium (Kawahara et al. 2003, Shimizu et al. 2008). Whether and to which extent TTS and neurogenic stunned myocardium are two names for the same syndrome will be the subject of future research. The connection between TTS and neurologic or psychiatric disorders also needs further clarification.

1.2.3 Vascular involvement

As coronary angiography of TTS patients serves to confirm the absence of an obstructive coronary artery disease and thereby differentiates TTS from AMI (Bybee et al. 2004, Prasad et al. 2008), other vascular causes for TTS were considered. Multivessel epicardial coronary artery spasm was

among the first suggestions for the mechanism behind the reversible left ventricular dysfunction of TTS (Sato et al. 1990). A small study showed the provocation of coronary artery spasm in 10 out of 14 TTS patients (Kurisu et al. 2002). However, reports of coronary artery spasm in TTS patients are infrequent and the majority of TTS patients do not show any form of coronary artery spasm (Bybee et al. 2004, Gianni et al. 2006).

Another suggestion for the pathophysiology of TTS was coronary microvascular disturbances. A study by Elesber and colleagues showed abnormal myocardial perfusion in 69 % of TTS patients, who also presented higher troponin levels and showed ECG changes more frequently (Elesber et al. 2006). Other studies also reported microcirculation abnormalities in TTS patients, supporting the theory that TTS is associated with microvascular dysfunction (Kume et al. 2005, Abdelmoneim et al. 2009, Galiuto et al. 2010). To date, it is unclear whether the microvascular disturbances are a result or the cause of the left ventricular dysfunction (Akashi et al. 2008).

1.2.4 Genetic predisposition

It is not yet clear whether a genetic predisposition of TTS patients exists. Several cases of TTS in family members have been reported involving two sisters or mother and daughter (Pison et al. 2004, Kumar et al. 2010, Subban et al. 2012). Furthermore, small studies analyzing genetic mutations in TTS patients and healthy donors have suggested potential gene mutations associated with TTS. For example, a recent study by d'Avenia *et al.* sequenced the Bcl2-associated athanogene 3 (*BAG3*) gene in 70 TTS patients and 81 healthy controls revealing that 62.8 % of TTS patients carried the g2252c single nucleotide polymorphism (SNP) resulting in binding loss of microRNA-371a-5p (d'Avenia et al. 2015). Analysis of SNPs of β_1- and β_2-adrenergic receptors showed significant differences between TTS patients and healthy controls (Vriz et al. 2011) and L14Q polymorphism of G protein coupled receptor kinase 5 (GRK5) was also associated with TTS (Spinelli et al. 2010). Recently, Borchert and colleagues identified SNPs in the two cardiac genes *RBM20* (RNA binding motif protein 20) and *CASQ2* (calsequestrine 2) while analyzing cellular material of TTS patients (Borchert et al. 2017). All these findings are mostly based on small cohorts of TTS patients and healthy controls. Further research will be necessary to verify the genetic predisposition of TTS patients.

1.2.5 High levels of catecholamines

A first breakthrough in further understanding the pathophysiology of TTS occurred in 2005, when Wittstein et al. published their hypothesis that high catecholamine concentrations might be the primary cause behind the pathophysiology of TTS (Wittstein et al. 2005). In their study, Wittstein and his colleagues showed significantly increased serum concentrations of epinephrine, norepinephrine

and dopamine in TTS patients. Moreover, the group of TTS patients had two to three times higher catecholamine serum concentrations than the comparison group of AMI patients and up to 34 times higher catecholamine serum concentrations than the normal range (Wittstein et al. 2005). This data is supported by case reports of patients with pheochromocytoma (a catecholamine-secreting tumor) and patients with iatrogenic epinephrine overdose, who also showed TTS-like ventricular dysfunction (Litvinov et al. 2009, Marcovitz et al. 2010). Additionally, myocard biopsies of TTS patients showed, among others, contraction band necrosis and fibrosis similar to the histological findings in myocard biopsies obtained after exposure to elevated catecholamine concentrations (Movahed et al. 1994, Reichenbach and Benditt 1970).

Thereafter, several research groups were able to induce a TTS event in animal *in vivo* and *in vitro* models after exposure to high catecholamine concentrations (Ellison et al. 2007, Paur et al. 2012, Shao et al. 2013, Redfors et al. 2014). Mainly rats and mice or their isolated CMs were treated with isoprenaline, epinephrine, phenylephrine or other catecholamines in different concentrations. Especially *in vivo* animal models were able to show via echocardiography that the different tested catecholamine concentrations induced TTS-like ventricular dysfunction (Redfors et al. 2014, Shao et al. 2013).

1.2.6 Beta-adrenergic signaling

The various catecholamines used during the TTS disease modeling all possess different adrenoreceptor subtype affinities. For example, epinephrine is a $\beta_1/\beta_2/\alpha$-adrenoreceptor agonist and isoprenaline is a β_1/β_2-adrenoreceptor agonist, whereas phenlyephrine is a selective α_1-adrenoreceptor agonist (Hoffmann et al. 2004, Redfors et al. 2014). Hence, Redfors and colleagues tried to determine with an *in vivo* rat model, whether the relevance of each adrenoreceptor for the TTS pathophysiology could be determined via the respective catecholamine's ability to induce a TTS event. In their study, they were unable to find any indication that ventricular dysfunction could be traced back to the stimulation of a specific adrenergic receptor subtype (Redfors et al. 2014).

Each adrenoreceptor is coupled to a heterotrimeric G protein. Stimulation of, for example, a β_2-adrenoreceptor also leads to stimulation of the coupled G_s protein, whose α-subunit then exchanges its bound GDP for GTP. The resulting conformation change leads to the release of the receptor-bound G_s protein and its division into a α- and a β/γ-subunit. The α-subunit releases its GDP and instead binds GTP. Afterwards, the α-subunit activates the adenylate cyclase. The membrane-bound adenylate cyclase catalyzes the conversion of ATP into cAMP. Protein kinase A (PKA), in turn, is a cAMP-dependent enzyme that phosphorylate its various target proteins, among others ryanodine receptor 2 at Serine 2808 (Wehrens et al. 2006, Löffler 2008) (**Fig. 2**).

The most common form of TTS is an apically located ventricular dysfunction (Templin et al. 2015). It is known that an apical-basal gradient of β-adrenoreceptor density exists in the mammali-

an heart and that the density of β-adrenoreceptors is highest in the apex (Mori et al. 1993, Paur et al. 2012). Previous publications have shown in animal models, that epinephrine can activate both G_s and G_i protein signaling pathways via β_2-adrenoreceptor stimulation depending on its concentration (Heubach et al. 2004). High epinephrine concentrations lead to a switch from G_s to G_i protein (Heubach et al. 2004), that probably occurs to prevent excessive induction of the G_s protein-signaling pathway, which would lead to apoptosis of the CMs (Chesley et al. 2000). Lyon et al. were the first to propose that a catecholamine-triggered switch from G_S to G_i protein after β_2-adrenoreceptor stimulation might be the cause of TTS (Lyon et al. 2008, Paur et al. 2012). The proposed hypothesis implies that the switch from the positive inotropic pathway of the G_s protein to the negative inotropic pathway of the G_i protein after β_2-adrenoreceptor stimulation would especially affect the apex with its higher density of β-adrenoreceptors and lead to the apically located dysfunction during a TTS event (Lyon et al. 2008, Paur et al. 2012).

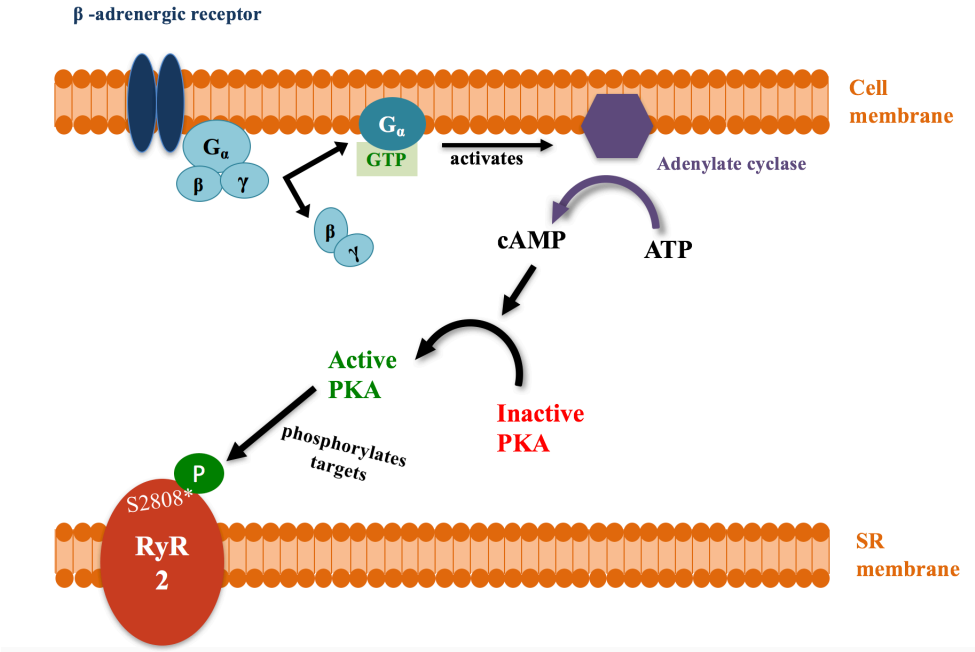

Figure 2. Schematic overview of the β-adrenergic signaling pathyway.

Stimulation of the β-adrenergic receptor leads – via enabled alpha subunit of the coupled G protein – to activation of the adenylate cylase. The membrane-anchored enzyme adenylate cyclase catalyzes the conversion of ATP into cAMP, which in turn activates the PKA. Function of the active PKA is phosphorylation of its various targets, such as ryanodine receptor 2 (RyR2) at Serine 2808 (S2808).

1.3 Human-induced pluripotent stem cells

The concept of human-induced pluripotent stem cells (hiPSCs) was first developed and published by the working group of Shinya Yamanaka (Takahashi et al. 2007). In 2012, his discovery earned him the Nobel Prize alongside of Sir John B. Gurdon in the category Physiology or Medicine. Ya-

manaka showed that overexpression of certain transcription factors in human somatic cells (here: dermal fibroblasts) can be used to generate human pluripotent stem cells. These hiPSCs are able to differentiate into all three germ layers (ectoderm, mesoderm and endoderm) both *in vitro* and *in vivo*. They also show other characteristics similar to those of human embryonic stem cells (hESCs), e.g. similar morphology, gene expression, surface markers or telomerase activities (Takahashi et al. 2007). The working group tested 24 genes and identified OCT3/4 (octamer-binding transcription factor), SOX2 (SRY (sex determining region Y)-box 2), C-MYC (v-myc avian myelocytomatosis viral oncogene homolog), and KLF4 (Kruppel-like factor 4) as the four reprogramming factors necessary for a sufficient induction of pluripotency in human somatic cells (Takahashi et al. 2007). However, expression of each factor has been associated with different types of tumors (Hochedlinger et al. 2005, Okita et al. 2007, Park et al. 2008). As an example, KLF4 expression is elevated in breast cancer (Pandya et al. 2004) and 70% of all human tumors show a conspicuous C-MYC expression (Kuttler and Mai 2006). Seeing as hiPSCs might one day play a big role in regenerative medicine, e.g. in the form of autologous (cell) treatment, any carcinogenic factors need to be avoided. Therefore, a less carcinogenic set of genes was introduced for reprogramming which still included OCT4 and SOX2, but replaced KLF4 and C-MYC with NANOG and LIN28 (Yu et al. 2007).

Yamanaka and his colleagues used retroviral and lentiviral transduction to introduce each transcription factor into human dermal fibroblasts (Takahashi et al. 2007). Usage of multiple viral vectors (one for each transcription factor) was required for successful reprogramming. Development of a single polycistronic lentiviral vector, which expresses a “stem cell cassette” (STEMCCA) containing all four initial factors (OCT4, SOX2, KLF4, C-MYC), simplified the process of reprogramming (Sommer et al. 2009). Although these transductions were efficient enough, retroviruses and lentiviruses offer the problem of (randomly) integrating into the host cell genome (Medvedev et al. 2010). Integration decreases as soon as the somatic cells turn into hiPSCs, but the amount of initial integration varies unpredictably and the integrated virus could alter transcription, therefore potentially leading to loss of gene function or oncogene activation (Okita et al. 2007, Mátrai et al. 2010). Over time, non-integrating systems were developed to bypass this problem. Reprogramming via protein transduction (Kim et al. 2009), plasmids (Okita et al. 2011), adenoviruses (Stadtfeld et al. 2008), synthetic mRNA (Warren et al. 2010) and Sendai viruses (Fusaki et al. 2009, Ye et al. 2013) are examples for feasible integration-free reprogramming methods. In general, viral systems require elaborate safety precautions and are often costlier compared to non-viral methods (Diecke et al. 2015). HiPSCs used for this work were generated with either plasmid vectors or sendai viruses applying previously published protocols respectively (Okita et al. 2011, Churko et al. 2013). Sendai virus is a negative sense, single-stranded RNA virus. In contrast to lenti- or retrovirus, Sendai viruses do not integrate into the host cell genome as they replicate in the cytoplasm (Fusaki et al. 2009). Plasmid vectors are another non-integrating system used for the generation of hiPSCs.

Similar to hESCs, hiPSCs were initially cultivated on a feeder layer composed of mouse embryonic fibroblasts (MEFs) (Ghasemi-Dehkordi et al. 2015). However, cultivation of hiPSCs on feeder layer was time-consuming and culture quality sometimes varied due to unwanted spontaneous differentiation. Over time, feeder-free culture systems such as Matrigel, Geltrex or laminin-511 were developed to improve cell culture quality (Xu et al. 2001, Rodin et al. 2010, Stover and Schwartz 2011, Kogut et al. 2014, Ghasemi-Dehkordi et al. 2015). Laminin-511 is a recombinant extracellular matrix protein, whereas both Matrigel and Geltrex are a mixture of extracellular matrix proteins secreted by Engelbreth-Holm-Swarm mouse sarcoma cells (Rodin et al. 2010, Stover and Schwartz 2011). HiPSCs used for this work were initially cultivated on feeder layer before being transferred onto Geltrex. Analogous to the matrices, cultivation medium for hiPSCs changed from hESC medium to the more reliable and stable option of chemically defined media such as Essential 8 medium (Chen et al. 2011).

1.4 Directed cardiac differentiation of hiPSCs

Using hiPSCs for the analysis of a cardiac disease such as TTS requires the differentiation of hiPSCs into cardiomyocytes (CMs). Initially, hiPSC-derived CMs were obtained via spontaneous *in vitro* differentiation, a method first described for hESCs (Itskovitz-Eldor et al. 2000, Zhang et al. 2009). Cultivated hiPSCs were transferred onto non-adherent plates to prevent cell adhesion so that three-dimensional aggregates, the so-called embryoid bodies (EBs), could form in suspension culture (Zhang et al. 2009, Zwi et al. 2009). After a few days, these EBs were plated onto gelatin-coated culture dishes and spontaneously differentiated into tissues of all three germ layers including CMs. Successful generation of CMs was confirmed via molecular and functional analysis of contracting EBs appearing from the fourth day after plating. However, this method was effortful and often inefficient due to the uncontrollable, spontaneous aspect of the differentiation (Zhang et al. 2009, Mummery et al. 2012). Therefore, further research concentrated on developing protocols for a directed cardiac differentiation of hiPSCs. One approach focused on the role of the wnt/β-catenin signaling pathway during cardiac differentiation (Paige et al. 2010, Lian et al. 2012, Lian et al. 2013). Wnt/β-catenin signaling plays a biphasic role in the process of human cardiac differentiation. At first, the wnt/β-catenin signaling pathway is activated in order to enhance differentiation into mesoderm **(Fig. 3)**. At a later stage, inhibition of wnt/β-catenin signaling is necessary to induce cardiac differentiation as continued activation of the wnt/β-catenin pathway would inhibit cardiac differentiation (Paige et al. 2010). In order to apply these findings to cardiac differentiation of hiPSCs, Lian and colleagues first treated hiPSCs with a medium supplemented with a GSK3-inhibitor (here: CHIR99021) to activate the wnt/β-catenin signaling pathway. This was followed by the application of inhibitors of Wnt production (IWPs) to induce cardiac differentiation via inhibition of the wnt/β-catenin pathway (Lian et al. 2013).

By applying this protocol, the working group was able to generate 80-98% pure, functional CMs (Lian et al. 2013), whereas Zhang et al. had only been able to generate 10% CMs via EB formation (Zhang et al. 2009). In contrast to the three-dimensional aggregates forming during EB cultivation, two-dimensional monolayer methods are currently used for cultivation of hiPSCs during directed cardiac differentiation. Monolayer methods allow the generation of larger quantities of cells and additionally provide the possibility of a scalable cardiac differentiation unlike EB formation (Lian et al. 2013, Burridge et al. 2014).

Chemically defined media are used for monolayer cultivation of hiPSC-CMs. Following hESC cultivation, RPMI 1640 supplemented with B-27 was first used as cardiac cultivation medium to which differentiation efficiency-increasing molecules such as GSK3-inhibitors could be added (Laflamme et al. 2007, Lian et al. 2012). After the discovery of insulin's inhibiting influence on cardiac differentiation, a switch to B-27 supplement without insulin took place to further optimize and stabilize the cardiac differentiation process (Lian et al. 2013). In 2014, it was shown that a chemically defined medium containing merely three components (CDM3) was sufficient enough to produce a usable cardiac cultivation medium (Burridge et al. 2014). CDM3 consisted of RPMI 1640 combined with recombinant human albumin and L-ascorbic acid 2-phosphate. Wnt/β-catenin signaling activators and inhibitors were added to CDM3 for two days respectively and produced up to 95% CMs (Burridge et al. 2014).

To further purify hiPSC-CMs after differentiation, cardiac cultivation medium was enriched with lactate and deprived of glucose. In contrast to other cell types, cardiomyocytes are able to utilize lactate as an energy source, thereby being able to survive during glucose-depleted conditions (Tohyama et al. 2013).

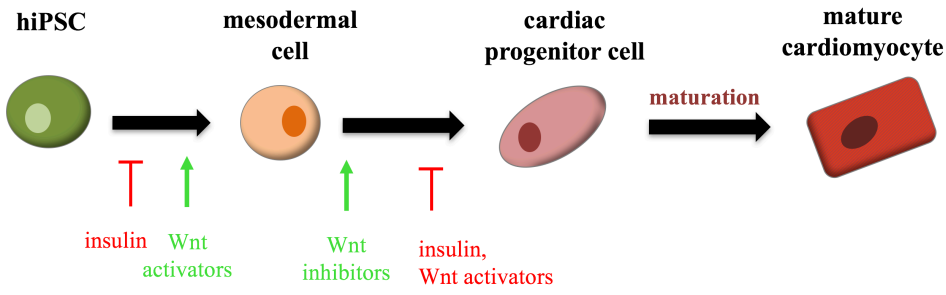

Figure 3. General overview about cardiac differentiation of hiPSCs.

During the differentiation of hiPSCs into mature cardiomyocytes wnt/β-catenin signaling is initially activated and enhances the differentiation of hiPSCs into mesodermal cells. At a later stage, the wnt/β-catenin signaling pathway is inhibited in order to induce differentiation into cardiac progenitor cells.

1.5 Disease modeling and drug screening with hiPSCs

Animal models are only suitable to a limited extend for disease modeling and drug screening as no animal's physiology is identical to the human one. Therefore, their validity is reduced and they are

unable to provide detailed insight into the patient's pathophysiological features. HiPSCs overcome these limitations and provide the possibility of a human patient-specific disease model. Since their development, hiPSCs have been widely used for disease modeling as they also offer the possibility to work with human pluripotent stem cells without the ethical conflict hESC usage entails. HiPSCs generated from somatic cells of a patient are able to differentiate into any type of tissue while maintaining the patient's genetic background. Many diseases with a genetic cause or predisposition have already been studied with the help of hiPSCs. Among others, hiPSCs were successfully generated from patients with Amyotrophic lateral sclerosis, Diabetes mellitus and Down syndrome (Fujikura et al. 2012, Toli et al. 2015, M Lee et al. 2017).

The difficulties concerning obtaining and cultivation of human CMs always complicated cardiac disease modeling in the past. In contrast, hiPSCs provide an unlimited source of patient-specific CMs. Several cardiac diseases have already been successfully modeled with the help of hiPSCs. Especially channelopathies like Brugada syndrome or catecholaminergic polymorphic ventricular tachycardia (CPVT), which are based on genetic mutations in genes coding for ion channels, provide fitting examples for the usefulness of hiPSC-CMs as a patient-specific disease model (Fatima et al. 2011, Liang et al 2016). Apart from that, cardiomyopathies such as dilated and hypertrophic cardiomyopathy have also been effectually studied with the help of hiPSC-CMs (Sun et al. 2012, Lan et al. 2013).

There is a certain limitation of the hiPSC disease model due to the degree of maturity of the generated hiPSC-CMs. Studies have shown that the phenotype of hiPSC-CMs resembles embryonic CMs rather than mature CMs (Yang et al. 2014a). This is shown, among others, in the lack of transverse tubules or multinucleation, the smaller cell size and smaller number of mitochondria as well as the metabolic dependence on glycolysis and the shorter sarcomere length (Gherghiceanu et al. 2011, Yang et al. 2014a, Kadota et al. 2017). That is why modeling of late onset disorders such as Parkinson's disease is more difficult than modeling of childhood diseases or those occurring during embryonic development (Miller et al. 2013). However, studies have shown that there are ways to influence the degree of maturity. Prolonged cultivation of 80 to 120 days, addition of tri-iodo-l-thyronine or cultivation on a mattress of undiluted matrigel increases maturation of the hiPSC-CMs (Lundy et al. 2013, Yang et al. 2014b, Feaster et al. 2015). Despite these options, the phenotype of hiPSC-CMs is still closer to embryonic CMs than to mature, adult CMs. Further research will be necessary to optimize the maturity level of the cultivated hiPSC-CMs. Nevertheless, previous disease models of various cardiac and non-cardiac disorders have proven the usefulness of this human *in vitro* disease model.

In addition, the use of hiPSCs provides new possibilities for drug discoveries and toxicity tests. During the preclinical phase of drug development, research often relies on *in vivo* animal models, which do not necessarily reflect the human physiology correctly and give rise to ethical concerns, while also being costly and difficult to automate (Gunaseeli et al. 2010). Usage of hiPSCs instead

offers the ability to receive more accurate results during toxicological testings and might thereby provide a greater degree of safety for the clinical stages of drug development. An evaluation of over 40 drugs, whose effects on the human heart are well known, showed promising results concerning drug response prediction of the tested hiPSC-CMs (Dick et al. 2010). Furthermore, a recent study by Liang et al. suggested that disease-specific hiPSC-CMs might be best suited for the prediction of adverse drug responses as their study showed differences in the susceptibilities between the hiPSCs obtained from patients and healthy controls (Liang et al. 2013). Toxicity tests with hiPSCs could be simplified and automated with the help of high-throughput platforms. As an *in vitro* model, hiPSCs are currently unable to completely replace the need for *in vivo* animal models, but they complement the existing models as they most accurately reflect the human physiology.

1.6 Aim of this thesis

Taking into account the potential underlying genetic predisposition of TTS and the fact that all previous TTS disease models either worked with animal CMs or faced the difficulty of cultivation and proliferation of human CMs, there is a need for a patient-specific disease model to successfully study the pathophysiology of TTS. Therefore, the aim of this thesis was the exploration of whether hiPSC-CMs can serve as a patient-specific disease model for TTS and offer the possibility to further study the pathomechanism of TTS. This includes:

(1) Detailed characterization of the generated hiPSCs from TTS patients with proof of their pluripotency.
(2) Directed differentiation of TTS- and control-hiPSCs into CMs.
(3) Establishment of catecholamine-dependent stress induction in TTS- and control-hiPSC-CMs.
(4) Exploration of TTS-specific stress markers.
(5) Analysis of the phosphorylation status of PKA targets after beta-adrenergic stimulation.
(6) Expression of possible NR4A1 targets after catecholamine treatment.

2 Material and methods

2.1 Materials

2.1.1 Cells and cell lines

Mouse embryonic fibroblasts (MEFs): isolated from 15- to 17-day-old embryos of NMRI mice (Institute for Cellular and Molecular Immunology, University Medical Center Göttingen)

Human-induced pluripotent stem cells (hiPSCs): generated from skin fibroblasts or perinuclear blood cells with Sendai virus, plasmid or STEMCCA lentivirus; approved by the Institutional Ethical Committee (21/1/11), University Medical Center Göttingen **(Table 1)**.

Table 1. HiPS cell lines used in this work.

Cell line	Cell source
1-TTS-1	hiPS cell line 1 generated from skin fibroblasts of TTS patient 1
1-TTS-2	hiPS cell line 2 generated from skin fibroblasts of TTS patient 1
5-TTS-1	hiPS cell line 1 generated from skin fibroblasts of TTS patient 5
8-TTS-1	hiPS cell line 1 generated from skin fibroblasts of TTS patient 8
8-TTS-2	hiPS cell line 2 generated from skin fibroblasts of TTS patient 8
1-C-1	hiPS cell line 1 generated from perinuclear blood cells of healthy control 1
1-C-2	hiPS cell line 2 generated from perinuclear blood cells of healthy control 1
2-C-1	hiPS cell line 1 generated from skin fibroblasts of healthy control 2
2-C-2	hiPS cell line 2 generated from skin fibroblasts of healthy control 2
1-F	skin fibroblasts of TTS patient 1
iC133	hiPS cell line (proof of pluripotency published in: Dudek et al. 2016)
iFB3	hiPS cell line generated from anonymous healthy fibroblasts (proof of pluripotency published in: Streckfuss-Bömeke et al. 2013)

The TTS patients 1, 5 and 8, which are used in this work, are not related to each other and were selected from the International Takotsubo Registry. They fulfil the Mayo Clinic Diagnostic Criteria for TTS **(Table 1)**. The healthy control 1 used in this work is a post-menopausal female without any diagnosed cardiovascular disease. The second healthy control is a 25-year-old female. Additionally, an anonymized healthy donor (iFB3) was also used as a control for the experiments.

2.1.2 Media, solutions and chemicals for cell culture

All media, solutions and chemicals used for cell culture along with the name of the supplier and the catalogue number are listed below in **Table 2**.

Table 2. Components for cell culture.

Component	Supplier, catalogue number
Albumin, human recombinant	Sigma-Aldrich, #A02347
B-27 serum free supplement (50x)	Thermo Fisher Scientific, #17504044
Basic fibroblast growth factor (bFGF)	PeproTech, #100-18B
CHIR99021 (CHIR)	Merck Millipore, #361559
Collagenase B	Worthington Biochemical, #CLS-AFB
Collagenase IV	Worthington Biochemical, #CLS-4
Dimethylsulfoxide (DMSO)	Sigma-Aldrich, #D2650
Dulbecco's modified Eagle medium (DMEM)	Thermo Fisher Scientific, #11960044
DMEM/F12	Thermo Fisher Scientific, #31331028
Dulbecco's phosphate-buffered saline (DPBS)	Thermo Fisher Scientific, #14190169
Epinephrine hydrochloride	Sigma-Aldrich, # E4642-5G
Essential 8 Medium	Thermo Fisher Scientific, #A1517001
Fetal bovine serum (FBS)	Sigma-Aldrich, #F7524
Gelatin	Sigma-Aldrich, #48720
Geltrex (Growth Factor Reduced)	Thermo Fisher Scientific, #A1413302
Hydrochloric acid (HCl) fuming 37 %	Merck Millipore, #100317
Iscove's modified Dulbecco's medium (IMDM)	Thermo Fisher Scientific, #31980022
Isoprenaline hydrochloride	Sigma-Aldrich, # I5627-5G
IWP2	Merck Millipore, #681671
KnockOut Serum	Thermo Fisher Scientific, #10828028
L-ascorbic acid 2-phosphate	Sigma-Aldrich, #A8960
L-glutamine (200mM, 100x)	Thermo Fisher Scientific, #25030024
Mitomycin C	Serva Electrophoresis, #29805.02

Monothioglycerol (MTG)	Sigma-Aldrich, #M6145-25ML
Non-essential Amino Acid (NEAA, 100x)	Thermo Fisher Scientific, #11140035
Penicillin-streptomycin solution (P/S) (100x)	Thermo Fisher Scientific, #15140112
RPMI 1640 with HEPES with GlutaMAX	Thermo Fisher Scientific, #724000021
RPMI 1640 without HEPES without Glucose	Thermo Fisher Scientific, #11879020
Sodium DL-lactate solution 60% (w/w)	Sigma-Aldrich, #L4263
Thiazovivin (TZV)	Merck Millipore, #420220
Trypsin/EDTA (0.25%)	Thermo Fisher Scientific, #2520056
Versene Solution (0.48 mM EDTA)	Thermo Fisher Scientific, #15040066

bFGF: 100 µg bFGF dissolved in 1ml Tris (5 mM) and stored at -20 °C; working solution: 5ng/µl, diluted 1:20 in 0.1% BSA/DPBS

β-mercaptoethanol (100x)

7 µl diluted in 10 ml DPBS and sterile-filtered, stored at 4 °C

BSA (1%)

1 ml of 7.5 % BSA added to 6.5 ml DPBS, stored at 4 °C

Cardio Culture Medium

500 ml RPMI 1640 with HEPES with GlutaMAX, 10 ml B-27 supplement with insulin, stored at 4 °C

Cardio Differentiation Medium

500 ml RPMI 1640 with HEPES with GlutaMAX, 250 mg albumin (human recombinant), 100 mg L-ascorbic acid 2-phosphate, sterile-filtered and stored at 4 °C

Cardio Digestion Medium

80 ml Cardio Culture Medium, 20 ml FBS, 100 µl Thiazovivin (final concentration 2 µM), stored at 4 °C

Cardio Selection Medium

500ml RPMI 1640 without HEPES without GlutaMAX, 2 ml lactate/HEPES (1 M), 250 mg albumin (human recombinant), 100 mg L-ascorbic acid 2-phosphate, stored at 4 °C

CHIR99021 (12 mM)

5 mg CHIR99021 dissolved in 0.894 ml DMSO, stored at –20 °C

Collagenase B (400 U/ml)

dissolved in RPMI medium to a working solution of 400 U/ml, sterile-filtered and stored at 4 °C

Collagenase IV (200 U/ml)

dissolved in DMEMD/F12 to a working solution of 200 U/ml, sterile-filtered and stored at 4 °C

Cryopreservation Medium (10 ml)

2 ml DMSO, 8 ml Essential 8 Medium, 20 µl TZV (2 mM), stored at 4 °C for one week

Epinephrine

Dissolved in sterile H_2O, stored at -20 °C, working solution (100 nmol/L, 10 μmol/L, 500 μmol/L, 1 mol/L) diluted in Cardio Culture Medium

Essential 8 Medium

500 ml Essential 8 basal Medium, 10 ml Essential 8 supplement

Fetal bovine serum

heat inactivated for 30 min at 56 °C

Feeder layer Medium

84 ml DMEM, 15 ml FBS (heat inactivated), 1 ml L-glutamine

Freezing Medium

18 ml DMEM, 5 ml FBS (heat inactivated), 2 ml DMSO

Gelatin (0.1%)

5 g gelatin dissolved in 5 l distilled water, autoclaved and stored at 4 °C

Geltrex

2 mg Geltrex aliquoted and stored at -20 °C; dissolved in 12 ml cold DMEM/F12 before use

Human Embryonic Stem Cell (hESC) Medium

500 ml DMEM/F12, 90 ml KnockOut Serum, 6 ml NEAA, 6 ml β-Mercaptoethanol (100x), 10 ng/ml bFGF (freshly added), stored at 4 °C

Iscove Medium (100 ml)

79 ml IMDM, 20 ml FBS, 1 ml NEAA, 450 µM MTG (freshly prepared), stored at 4 °C

Isoprenaline

Dissolved in sterile H_2O, stored at -20 °C, working solution (100 nmol/L, 10 µmol/L, 5 mmol/L) diluted in Cardio Culture Medium

IWP2 (5 mM)

10 mg dissolved in 4.28 ml DMSO and incubated at 37 °C for 10 min, stored at –20 °C

Lactate/HEPES (1 M stock solution)

3 ml of 60 % sodium DL-lactate solution diluted in 18 ml of 1 M HEPES sodium salt solution, stored at –20 °C

Mitomycin C

dissolved in DPBS (200 µg/ml) and stored at –20 °C

MTG (150 mM)

13 µl MTG diluted in 1 ml IMDM and sterile-filtered; freshly prepared before use

Phenylephrine

Dissolved in sterile H_2O, stored at -20 °C, working solution (100 nmol/L, 1 μmol/L, 10 μmol/L) diluted in Cardio Culture Medium

TZV (2 mM)

10 mg diluted in 6.8 ml DMSO, stored at -20 °C

2.1.3 Chemicals, solutions and buffers for molecular biological and protein analyses

All chemicals, solutions, enzymes and kits used for molecular biological and protein analyses along with the name of the supplier and the catalogue number are listed below in **Table 3**.

Table 3. Components for molecular biological methods and protein analyses.

Component	Supplier, catalogue number
2-Propanol	Merck Chemicals, 1096341000
4', 6-diamidino-2-phenylindole dihydrochloride (DAPI)	Sigma-Aldrich, #D9542
Acetic acid (glacial)	Th. Geyer, #2234-25L
Agarose, peq Gold universal Agarose	Peqlab, #732-2789
Alkaline Phosphatase staining kit	Sigma-Aldrich, #86R-1KT
Ammonium persulfate (APS)	Roth, #9178
β -Mercaptoethanol	Sigma-Aldrich, #M3148
Boric acid	Sigma-Aldrich, #15663
Bovine serum albumin (BSA), pH 7.0	Sigma-Aldrich, #A2153
Coomassie Brilliant Blue G-250	Serva Electrophoresis, #17524
cOmplete (protease inhibitor cocktail tablets), EDTA-free	Roche, #11873580001
Demecolcine (10 µl/ml)	Sigma-Aldrich, #D1925
Dithiothreitol (DTT)	Roth, #6908
dNTP Mix	Bioline, #BIO-39029
DEPC-treated water	Ambion, #AM9915G
ε-aminocaproic acid	AppliChem, #A2266,0500
Ethanol 99%, denatured	WALTER CMP GmbH, #WAL10503 1000
Formalin 37 %	Merck Millipore, #1039991000
GeneRuler 100bp DNA ladder	Thermo Fisher Scientific, #0321
Giemsa stain	Sigma-Aldrich, #GS500
Glacial acetic acid	Merck Millipore, #1.00063.1000
Glycine	Serva Electrophoresis, #23391
GoTaq G2 DNA Polymerase	Promega, #M7841
Green GoTaq reaction buffer 5x	Promega, #M7911

HEPES	Roth, #9105
Hydrogen peroxide solution	Sigma-Aldrich, #216763-100ML
IGEPAL CA-630	Sigma-Aldrich, #I3021
Loading buffer	Applichem, #A3481
Magnesium chloride, 25mM	Thermo Fisher Scientific, #N8080010
Methanol	Merck Millipore, #106009
Microscope slide	Nunc, #177380
Microscope slide, SuperFrost Ultra Plus	Menzel, #J3800AMNZ
Midori Green Advance	Biozym, #617004
MuLV Reverse Transcriptase (50 U/µl)	Thermo Fisher Scientific, #N8080018
Nonfat dry milk	Roth, #T145
Nuclease-free water	Thermo Fisher Scientific, #AM9932
Oligo d(T)16 Primer	Thermo Fisher Scientific, #N8080128
Paraformaldehyde (PFA)	Sigma-Aldrich, #158127
PCR buffer II 10x	Thermo Fisher Scientific, #N8080010
PeqGold protein marker V	Peqlab, #27-2210
PhosSTOP (phosphatase inhibitor cocktail tablets)	Roche, #04906837001
Pierce BCA potein assay kit	Thermo Fisher Scientific, #23225
PVDF membrane, pore size 0.45 µm	Roth, #T830.1
Ponceau S solution	Sigma-Aldrich, # P7170-1L
Potassium chloride (KCl)	Sigma-Aldrich, #P9541
QIAquick Gel Extraction kit	Qiagen, #28706
RNase Inhibitor	Thermo Fisher Scientific, #N8080199
Rotiphorese gel 30	Roth, #3029
Sodium azide	Sigma-Aldrich, #S2002
Sodium chloride (NaCl)	Roth, #9265.1
Sodium dihydrogen phosphate ($NaH_2PO4 \cdot H_2O$)	Merck Millipore, #1.06345
Sodium dodecyl sulphate (SDS)	Roth, #2326

Sodium fluoride (NaF)	Roth, #P756
Sodium hydrogen phosphate (Na_2HPO_4)	Merck Millipore, #567547
Sodium orthovanadate	Sigma-Aldrich, #S6508
SuperSignal West Pico Chemiluminescent Substrate	Thermo Scientific Fisher, #34080
SV Total RNA isolations kit	Promega, #Z3100
SYBR Green PCR master mix	Thermo Fisher Scientific, #4309155
Tetramethylethylenediamine	Roth, #2367
Tricine BioChemica	AppliChem GmbH, #A1085,0100
Tris	Roth, #5429
Tris buffer pure	Roth, #1022840
Triton X-100	Sigma-Aldrich, #3051.3
TrypLE Express Enzyme (1X), no phenol red	Thermo Fisher Scientific, #12604013
Tween 20	Bio-Rad, #170-6531
VECTASHIELD Antifade Mounting Medium	Vector Laboraties, #H-1000

Anode buffer

36.34 g Tris, 17.9 g Tricine, filled up to 1000 ml with dH_2O, pH adjusted to 8.8 with HCl

Agarose gel (1.5 %)

2.25 g peq Gold universal Agarose dissolved in 150 ml 1x TBE buffer by boiling in a microwave, 6 µl of Midori Green Advance were added to 100 ml agar gel for visualization of DNA under ultraviolet light

APS (10 %)

10 g APS dissolved in 100 ml dH_2O, sterile filtrated, and stored at –20 °C

Blue loading buffer (5x)

38 ml 0.313 M Tris-HCl (pH 6.8), 10 g SDS, 1 ml 5 % bromphenol blue, 50 ml glycerin, 1000 µl 0.5 M EDTA, 2.313 DTT, filled up to 100 ml with dH_2O; stored at -20 °C

Cathode buffer

39.35 g ε-aminocaproic acid and 3.63 g Tris filled up to 1000 ml with dH_2O, pH adjusted to 8.7 with HCl

Cell lysis buffer (1.25 ml)

12.5 µl 2 M Tris-HCl (pH 7.4), 62.5 µl 4 M NaCl, 125 µl 200 mM NaF, 62.5 µl 20 % Triton, 62.5 µl 20% IGEPAL® CA-630, 12.5 µl 1 mM Na_3VO_4, 12.5 µl 1mM DTT, 125 µl PhosSTOP, 125 µl cOmplete EDTA-free, 650 µl dH_2O

Coomassie Brilliant Blue

150 mg Coomassie Brillant Blue G-250 dissolved in 200 ml methanol, stored at room temperature

Dithiothreitol [100 mM]

0.386 g dithiothreitol dissolved in 25 ml dH_2O

EDTA-free, cOmplete

1 tablet dissolved in 2 ml, aliquoted and stored at -20 °C

Fixation buffer for karyotyping

methanol mixed in a ratio 3:1 with acetic acid (glacial), freshly prepared and cooled at –20 °C

Nonfat dry milk (5 %)

0.5 g nonfat dry milk mixed in 100 ml 1x TBS-T buffer

PFA (4 %)

4 g PFA dissolved in 100 ml DPBS, stored at -20 °C

Phosphate-buffered formalin

4.6 g $NaH_2PO_4 \cdot H_2O$ and 6.5 g Na_2HPO_4 dissolved in 900 ml dH_2O, pH adjusted to 7.0 with HCl; 89.2 ml of phosphate buffer added to 10.8 ml 37 % formalin; stored at 4 °C

PhosSTOP

1 tablet dissolved in 1 ml, aliquoted and stored at -20 °C

PVDF destain solution

100 ml acetic acid, 400 ml ethanol, 500 ml dH_2O

RNA lysis buffer (10 ml)

10 ml cell lysis buffer (part of the SV total RNA isolation kit) and 200 µl β-mercaptoethanol (freshly added each time)

Running buffer (10x)

60.4 g Tris, 288 g glycine, 20 g SDS filled up to 2000 ml with dH_2O

SDS (10 %)

10 g SDS dissolved in 100 ml dH_2O and stored at 4 °C

Separation gel (10 %, 12 ml)

4 ml Rotiphorese gel 30, 5 ml dH_2O, 3 ml Tris/SDS (4x, pH 8.8), 48 µl APS (10 %), 18 µl TEMED

Sodium chloride (4 M)

46.74 g sodium chloride dissolved in 200 ml dH_2O

Sodium fluoride (200 mM)

0.8398 g sodium fluoride dissolved in 100 ml dH_2O

Sodium orthovanadate (100 mM)

10.7356 g sodium orthovanadate dissolved in 40 ml dH_2O, stored at -20 °C

Stacking gel (7.5 ml)

1 ml Rotiphorese gel 30, 4.62 ml dH_2O, 1.88 ml Tris/SDS (4x, pH 6.8), 37.5 µl APS (10 %), 15 µl TEMED

TBE buffer [5x]

54 g Tris, 27.5 g boric acid, 20 ml 0.5 M EDTA (pH 8.0) and 1 l dH_2O

TBS buffer (10x, pH 7.6)

80 g NaCl, 24 g Tris, filled up to 1000 ml with dH_2O, pH adjusted to 7.6 with HCl

TBS-T buffer (1x)

900 ml dH_2O, 100 ml TBS buffer (10x), 500 µl Tween

Tris (2 M, pH 7.4)

24.228 g Tris dissolved in 200 ml dH_2O; pH adjusted to 7.4 with HCl

Tris/SDS (4x, pH 6.8)

6.05 g Tris and 0.4 g SDS diluted in 100 ml dH_2O; pH adjusted to 6.8 with HCl

Tris/SDS (4x, pH 8.8)

45.54 g Tris and 1 g SDS diluted in 250 ml dH_2O; pH adjusted to 8.8 with HCl

Triton X-100 (0.1 %)

10 µl Triton X-100 diluted in 990 µl DPBS, stored at 4 °C

2.1.4 Antibodies used for immunofluorescence and western blot analyses

All primary and secondary antibodies used for immunofluorescence (IF) and western blot (WB) analyses are listed in the tables below (**Table 4** and **5**).

Table 4. Primary antibodies used for immunofluorescence and western blot analyses.

Antibody, type	Host	Dilution	Supplier, catalogue number
AFP	rabbit (IgG)	1:800 (IF)	DAKO, #A0008
α-actinin	mouse (IgG_1)	1:1000 (WB) 1:1000 (IF)	Sigma Aldrich, #A7811
α-SMA	mouse (IgG_{2A})	1:3000 (IF)	Sigma Aldrich, #A2547
class III β-TUBULIN	mouse (IgG_{2A})	1:2000 (IF)	Covance, #MMS-435P
ERK 1	rabbit	1:1000 (WB)	Cell Signaling Technology, #4372
ERK2 (D-2)	mouse (IgG_{2B})	1:200	Santa Cruz Biotechnology, #SC-1647
GAPDH	mouse (IgG_1)	1:5000 (WB)	Merck Millipore, #MAB374
LIN28	goat (IgG)	1:300 (IF)	R&D Systems, #AF3757
NANOG	goat (IgG)	1:200 (IF)	Abcam, #PA5-18406
OCT4	goat (IgG)	1:40 (IF)	R&D Systems, #AF1759
pERK 1/2 Thr202/Tyr204	rabbit	1:1000 (WB)	Cell Signaling Technology, #9101

RYR2	polyclonal rabbit	1:15 000 (WB)	Sigma Aldrich, #HPA020028
pRYR2-S2808	rabbit (IgG)	1:5000 (WB)	Badrilla, #A010-30
SOX2	mouse (IgG_{2A})	1:50 (IF)	R&D Systems, #MAB2018
SSEA4	mouse (IgG_3)	1:200 (IF)	Abcam, #MC813
TRA-1-60	mouse (IgM)	1:200 (IF)	Abcam, #ab16288

Table 5. Secondary antibodies.

Antibody	Host	Dilution	Supplier, catalogue number
Alexa Fluor 488-anti-mouse	Donkey (IgG)	1:1000	Thermo Fisher Scientific, #A21202
Alexa Fluor 555- anti-goat	Donkey (IgG)	1:1000	Thermo Fisher Scientific, #A21432
Cy3-anti-mouse	Goat (IgG+IgM)	1:300	Jackson ImmunoResearch, #115-165-068
FITC-anti-mouse	Goat (IgM)	1:200	Jackson ImmunoResearch, #115-096-072
HRP-anti-rabbit	Donkey (IgG)	1:10 000	Thermo Fisher Scientific, #A16023
HRP-anti-mouse	Donkey (IgG)	1:10 000	Thermo Fisher Scientific, #A16011

2.1.5 Oligonucleotides

All oligonucleotides used for PCR were purchased from Microsynth. The sequences are listed in alphabetical order **(Table 6)** together with the length of the amplified fragment (F), as well as the annealing temperature (T_A) and the number of cycles (C).

Table 6. Oligonucleotides used for PCR analyses.

Gene	Sequence	F [bp]	T_A [°C]	C
ACTN2	for: AGG AGG AAG AAT GGC CTG AT rev: GAT GCA GTA CTG GGC CTG AT	291	60	30
AFP	for: ACT CCA GTA AAC CCT GGT GTT G rev: GAA ATC TGC AAT GAC AGC CTC A	255	60	33
ALB	for: CCT TTG GCA CAA TGA AGT GGG TAA CC rev: CAG CAG TCA GCC ATT TCA CCA TAG	355	62	35
α-MHC	for: GTC ATT GCT GAA ACC GAG AAT G rev: GCA AAG TAC TGG ATG ACA CGC T	413	60	40
β-MHC	for: AGA CTG TCG TGG GCT TGT ATC AG rev: GCC TTT GCC CTT CTC AAT AGG	101	63	30
cTNT	for: GAC AGA GCG GAA AAG TGG GA rev: TGA AGG AGG CCA GGC TCT AT	305	56	35
FOXD3	for: 5'-GTG AAG CCG CCT TAC TCG TAC rev: CCG AAG CTC TGC ATC ATG AG	353	60	38
GAPDH	for: AGA GGC AGG GAT GAT GTT CT rev: TCT GCT GAT GCC CCC ATG TT	258	60	30
LIN28	for: AGT AAG CTG CAC ATG GAA GG rev: ATT GTG GCT CAA TTC TGT GC	410	52	30
NANOG	for: AGT CCC AAA GGC AAA CAA CCC ACT TC rev: ATC TGC TGG AGG CTG AGG TAT TTC TGT CTC	164	64	36
NPPA	for: GTG AGC CGA ATG AAG AAG CG rev: GCT CCA ATC CTG TCC ATC CT	229	52	31
NPPB	for: ATG GTG CAA GGG TCT GGC T rev: TCT TAA TGC CGC CTC AGC	92	52	31
NR4A1	for: CCC TGT ATC CAA GCC CAA TA rev: AGG AAG GTG TCA AAC TCT CCT G	130	57	36
OCT4	for: AGT TTG TGC CAG GGT TTT TG rev: ACT TCA CCT TCC CTC CAA CC	113	54	34
OGT	for: ATC CTG ATT TGT ACT GTG TTC GC rev: AAG CTA CTG CAA AGT TCG GTT	123	54	38
SOX2	for: ATG CAC CGC TAC GAC GTG A rev: CTT TTG CAC CCC TCC CAT TT	437	60	34
TH	for: GCG GTT CAT TGG GCG CAG G rev: CAA ACA CCT TCA CAG CTC G	215	60	34

2.2 Methods

2.2.1 Cell culture

All cells were cultivated under humidified air conditions with 5 % carbon dioxide and 20 % oxygen at 37 °C (incubator from Labotect). All cell culture work was performed under sterile conditions using a laminar flow cabinet (Heraeus Instruments) to avoid microbiological contamination. HiPSC lines were generated with the help of non-integrating systems such as Sendai viruses (MOI of 5/5/3 (KOS/hc-myc/hKLF4)) or plasmids (pCXLE-hSK, pCXLE-hUL and pCXLEhOct3/4-shp53-F) using previously described protocols (Okita et al. 2011, Churko et al. 2013). HiPS cell lines (passage range 6-10) were defrosted and cultivated for proof of pluripotency and further experiments.

2.2.1.1 Cultivation and inactivation of mouse embryonic fibroblasts

After being isolated from 15- to 17-day-old embryos of NMRI mice, MEFs were cultivated on 0.1 % gelatin-coated culture dishes in Feeder layer Medium (see 2.1.2). At around 95 % confluency, the MEFs were inactivated by incubation with mitomycin C (300 µl in 8 ml Feeder layer Medium) at 37 °C for 3 hours in order to stop cell proliferation. After being washed thrice with DPBS, the MEFs were further incubated in 0.25 % Trypsin/EDTA for a maximum of 5 minutes until the cells started to detach. The single cells were resuspended in Feeder layer Medium and counted under a light microscope with the help of a Thoma cell counting chamber. A number of 3 x 10^5 cells along with 3 ml Feeder layer Medium was then distributed to each 6-cm dish, which had been coated with 0.1 % gelatin at least one hour in advance to its use.

2.2.1.2 Cultivation of hiPSCs on mouse embryonic fibroblasts

HiPSCs were cultured on mitomycin C-treated MEFs in hESC Medium (see 2.1.2). The medium was replaced daily along with the removal of spontaneously differentiated areas. Depending on density and size of the hiPSC colonies, the cells were passaged every 4 to 5 days. Therefore, the cells were washed once with DMEM/F12 and subsequently incubated in Collagenase IV (200 U/ml) at 37 °C for approximately 5 minutes. After another washing step with DMEM/F12, the cells were mechanically split into smaller clusters by using a sterile cell scraper. After resuspension in HESC Medium an appropriate percentage of cells was transferred onto new 6 cm culture dishes containing the mitomycin C-treated MEFs.

2.2.1.3 Cultivation of hiPSCs on Geltrex

Geltrex is a reduced growth factor basement membrane extract used for feeder-free culture of hiPSCs. Frozen Geltrex aliquots were stored at -20 °C and dissolved in 24 ml cold DMEM/F12. The

required 6-well or 12-well plates were coated at least one hour in advance to their use. At about 90 % confluency the cells were passaged onto new dishes. Therefore, the cells were washed twice with 2 ml Versene Solution and subsequently incubated in another 2 ml Versene Solution at 37 °C for 3 to 5 minutes. Afterwards, the cells were resuspended in 2 ml Essential 8 Medium (see 2.1.2) supplemented with Thiazovivin (final concentration 2 µM) before an appropriate percentage of cells was transferred to a new Geltrex-coated 6-well or 12-well plate. Daily medium change was performed using Essential 8 Medium.

2.2.1.4 Freezing and thawing of cultivated hiPSCs

For long-term availability of the cultivated cell lines, hiPSCs were frozen at different passages. Therefore, cells cultivated on Geltrex were washed twice and subsequently incubated in Versene Solution as described above (see 2.2.1.3). Thereafter, the medium was quickly replaced by 1 ml Essential 8 Medium and a 1000-µl pipette was used to detach the cells. In a dropwise manner 1 ml of Cryopreservation Medium (see 2.1.2) was added. The cell suspension was carefully mixed before 1 ml was transferred into a cryovial (STARLAB). Each labelled cryovial was frozen at -80 °C in an isopropanol freezing container, allowing controlled freezing at -1 °C per minute overnight. The following day, the cryovials were stored in liquid nitrogen.

To thaw cryo-frozen hiPSCs for further cultivation or as a control for a successful freezing procedure, the frozen cryovials were first placed in a 37 °C warm water bath. After a couple of minutes, when only a small ice particle was left within the Cryopreservation Medium, the cryovials were taken out of the water bath to continue further work under the laminar flow cabinet. The content of each vial was carefully transferred into a falcon tube filled with 10 ml DMEM/F12 and centrifuged at 200 x *g* for 3 minutes. The resulting pellets were resuspended in 2 ml Essential 8 Medium supplemented with Thiazovivin (final concentration 2 µM) and transferred onto a Geltrex-coated 6-well plate for further cultivation.

Freezing and thawing of hiPSCs cultivated on MEFs succeeded in a similar manner as described for hiPSCs cultivated on Geltrex. Cells were washed with DMEM/F12 and incubated with Collagenase IV (200 U/ml) for several minutes. After an additional washing step with DMEM/F12, the cells were mechanically split with a cell scraper and each culture was transferred into a 15-ml falcon tube. After centrifugation at 200 x *g* for 3 minutes, each pellet was carefully resuspended in 1 ml Freezing Medium (see 2.1.2) and transferred into a cryovial. The cryovials were frozen in an isopropanol freezing container at -80 °C and stored in liquid nitrogen the following day. For thawing, the frozen cryovials were incubated in a 37 °C water bath. Afterwards, the content of each thawed cryovial was transferred into 10 ml DMEM/F12 and centrifuged at 200 x *g* for 3 minutes. The resulting pellets were resuspended in HESC Medium supplemented with 10 ng/ml bFGF and transferred onto 6 cm culture dishes containing mitomycin C-treated MEFs.

2.2.1.5 Harvesting of cultivated cells for pellets

Cultivated hiPSCs or hiPSC-CMs were washed twice with DPBS. Then, another 1.3-1.5 ml DPBS were added to each well so that the cells could be mechanically split and detached with the help of a sterile cell scraper. The content of each well was transferred into a 1.5 ml Eppendorf tube and centrifuged at 13 000 x *g* for one minute. After aspiration of the supernatant, the tubes were flash frozen in liquid nitrogen and stored at -80 °C until further use.

2.2.1.6 Spontaneous *in vitro* differentiation of hiPSCs cultivated on feeder-layer

For spontaneous *in vitro* differentiation hiPSCs with around 80 % confluence were washed with DMEM/F12 and incubated with Collagenase IV (200 U/ml) as described above. After an additional washing step with DMEM/F12, HESC Medium supplemented with 10 ng/ml bFGF was added to the cells. Thereafter, the hiPSC colonies were dissected with the help of a sterile cell scraper. The generated cell clusters were bigger than those produced during passaging of hiPSCs. Cell clusters of at least 3 to 4 culture dishes were collected and transferred to an uncoated bacteriological dish and incubated at 37 °C overnight so that embryoid bodies could form (see 1.4). On the following day, the medium including the newly formed embryoid bodies was transferred into a 15-ml falcon tube for 5 minutes until the majority of the embryoid bodies settled at the bottom of the tube. The supernatant was carefully aspirated and Iscove Medium (see 2.1.2) with freshly supplemented MTG was added to transfer the cells to a new uncoated bacteriological dish. The embryoid bodies were cultivated in suspension at 37 °C for 7 more days. Iscove Medium was changed every other day. On the eights day, the embryoid bodies were plated on a 0.1 % gelatin-coated TC-treated 6-cm culture dish (Greiner) and cultivated for another 24 days in Iscove Medium (**Fig. 4**).

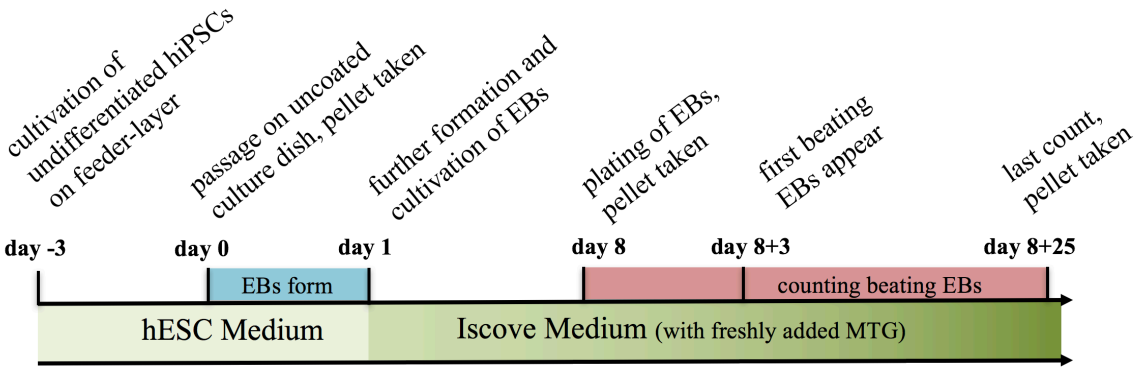

Figure 4. Schematic illustration of the spontaneous differentiation protocol used for in vitro differentiation of the generated hiPSCs.

The undifferentiated hiPSCs were cultivated in Iscove Medium (freshly supplemented with MTG) so that embryoid bodies (EBs) could form. On day 8, these embryoid bodies were transferred from uncoated culture dishes onto gelatin-coated culture dishes. Cultivation continued for another 25 days. The number of beating embryoid bodies was counted every three days (modified from Stauske 2014).

If necessary, glass coverslips (18 mm x 18 mm, Thermo Scientific) were added into each culture dish for subsequent immunofluorescence staining. The clusters of beating cardiomyocytes appearing during the spontaneous *in vitro* differentiation were counted every two to three days before medium change. Cell pellets were taken for PCR analysis (see 2.2.1.5) and immunofluorescence staining was performed for germ layer-specific markers (see 2.2.3).

2.2.1.7 Directed cardiac differentiation of hiPSCs cultivated on Geltrex

HiPSCs were cultivated on Geltrex-coated 6-well or 12-well plates (see 2.2.1.3) until they reached about 90 % confluence. Correct cell density was crucial for efficient differentiation. In order to start the directed cardiac differentiation (= day 0), the Essential 8 Medium was replaced with Cardiac Differentiation Medium (see 2.1.2) freshly supplemented with CHIR99021 (final concentration 4 µM). Two days later (= day 2), the medium was carefully replaced with Cardiac Differentiation Medium containing freshly added IWP2 (final concentration 5 µM). After another two days, medium change was performed with non-supplemented Cardiac Differentiation Medium every two or three days **(Fig. 5)**. At day 8, the Cardiac Differentiation Medium was replaced with Cardiac Culture Medium (see 2.1.2). From that point on, medium change was performed every two to three days with Cardiac Culture Medium.

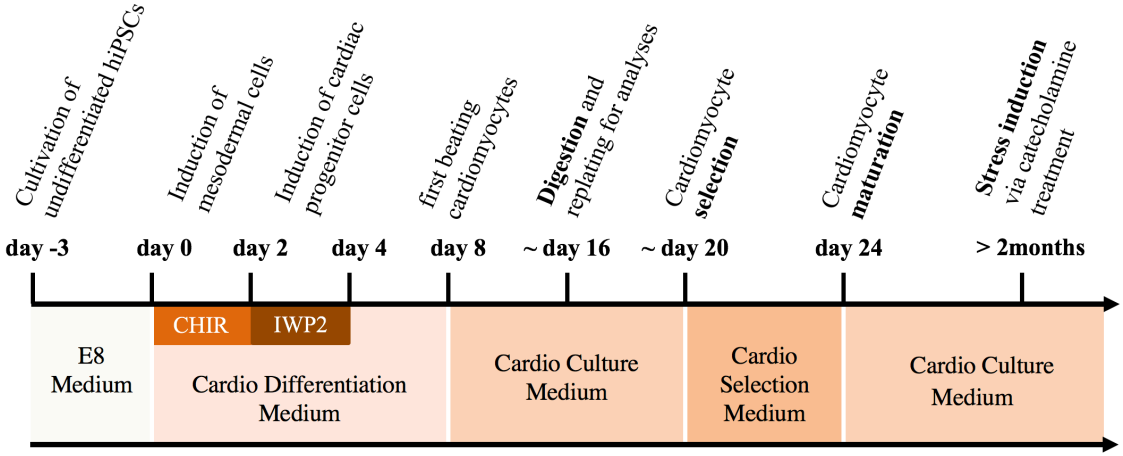

Figure 5. Visualization of the directed cardiac differentiation protocol.

After cultivated hiPSCs reached about 90 % confluency, Essential 8 Medium was replaced with Cardio Differentiation Medium supplemented with CHIR99021 and IWP2 for two days each in order to start the directed cardiac differentiation. Around day 16, the generated hiPSC-CMs were digested and replated in a lower cell density. Cardio Selection Medium containing lactate led to further purification. The generated hiPSC-CMs matured for two to three months before stress induction was performed (modified from Stauske 2014).

2.2.1.8 Digestion of hiPSC-derived cardiomyocytes

Ideally after two or three weeks of cultivation, the hiPSC-CMs were replated in a lower cell density. Therefore, the suitable 6-well or 12-well plate was washed once with 2 ml Versene Solution and subsequently incubated with Collagenase B (400 U/ml) at 37 °C for two hours. Afterwards, the cell clusters in suspension were carefully transferred into a 15-ml falcon tube and centrifuged at 200 x *g* for 5 minutes. The resulting pellet was carefully dissolved in 2 ml 0.25 % Trypsin/EDTA and incubated for 6 minutes at 37 °C. To singularize the cells, the falcon tube was cautiously given a shake every other minute during incubation. Resuspension with a 1000-µl pipette after incubation was kept to a minimum. When no cell clusters were visible anymore, 4 ml Cardio Digestion Medium (see 2.1.2) were added to each falcon tube followed by another centrifugation step (200 x *g* for 5 minutes). Thereafter, the pellet was resuspended in 1-2 ml Cardio Digestion Medium (depending on the size of the pellet) before the required number of cells was transferred onto new Geltrex-coated plates. The transferred volume was kept low (about 400 µl) so that the cells could attach quickly. After 30 minutes of incubation at 37 °C another 2 ml Cardio Digestion Medium were added to each well. After 2 days, medium was changed back to Cardio Culture Medium.

2.2.1.9 Selection of hiPSC-derived cardiomyocytes

Cardiac selection was performed at the earliest one week after digestion of the hiPSC-CMs, so that the cells had enough time to recover. Ideally, cardiac selection took place between day 20 and day 40 due to the cells' highly proliferate state and consequently high sensitivity to lactate. Therefore, Cardio Culture Medium was replaced with Cardio Selection Medium (see 2.1.2). Medium change was performed every second day for 4-6 days. After the end of the selection period medium change continued with Cardio Culture Medium as described above.

2.2.1.10 Catecholamine treatment of hiPSC-derived cardiomyocytes

In order to induce a TTS event in hiPSC-CMs, the cells were treated with different catecholamines in different concentrations (Table 7) for either 2 or 20 hours. Every experiment was performed with at least 2- to 3-month-old cardiomyocytes. Exactly 2 ml Cardio Culture Medium were added to each well one day before the experiment. After catecholamine treatment for 2 or 20 hours the following day, each well was washed twice with DPBS. The wells intended for a three-week recovery after catecholamine treatment were subsequently treated with 2-3 ml Cardio Culture Medium for further incubation at 37 °C. Medium change the following three weeks proceeded as described above.

Samples taken for PCR analyses were dissolved in 400 µl lysis buffer (see 2.1.2), detached with a sterile cell scraper and transferred into a 1.5 ml Eppendorf tube for storage at -80 °C. Samples tak-

en for western blot analyses were dissolved in up to 1.3 ml DPBS and detached with the help of a cell scraper. The content of each well was transferred into a 1.5 ml Eppendorf tube and centrifuged at 13 000 x *g* for one minute. After aspiration of the supernatant, the tubes were stored at -80 °C until further use.

Table 7. Catecholamine concentrations.

Catecholamine	Concentrations
Epinephrine	100 nmol/L, 10 µmol/L, 500 µmol/L, 1 mmol/L
Isoprenaline	100 nmol/L, 10 µmol/L, 5 mmol/L
Phenylephrine	100 nmol/L, 1 µmol/L, 10 µmol/L

2.2.2 Alkaline phosphatase staining

Alkaline phosphatase levels are significantly elevated in undifferentiated pluripotent stem cells. Therefore, alkaline phosphatase staining was performed to provide first evidence of a successful somatic cell reprogramming. At the beginning, undifferentiated hiPSC colonies cultivated on feeder layer or Geltrex were washed twice with DPBS and subsequently fixated for 30 seconds using the fixing solution provided by the alkaline phosphatase staining kit (see 2.1.3). After being washed twice with distilled water (dH_2O), the cells were incubated with the alkaline phosphatase staining solution for 15 minutes at 37 °C. The stained colonies were then washed two times with dH_2O and left to dry at room temperature. Alkaline phosphatase positive cells are stained in red.

2.2.3 Immunofluorescence staining

The expression of pluripotency-related proteins in undifferentiated hiPSCs as well as the expression of germ layer-specific proteins in spontaneously differentiated hiPSCs was shown by immunostaining, which was also used to demonstrate the expression of cardiac-specific proteins in hiPSC-CMs. For immunostaining, hiPSCs and hiPSC-CMs were cultivated on glass cover slips (Thermo Fisher Scientific). Beforehand, these cover slips were treated with 37 % HCl overnight, cleaned with the help of 70 % ethanol and lint-free paper the following day and autoclaved before use. The cover slips were inserted into the necessary culture dishes or 6-/12-well plates and coated with 0.1 % gelatine for at least one hour before being covered with feeder layer, Geltrex or a suspension of embryoid bodies as described above. The hiPSC colonies, embryoid bodies or hiPSC-CMs were cultivated on these cover slips until they reached the appropriate size and age. Then, the cells were washed twice with DPBS and fixated at room temperature by incubation with 4 % paraformaldehyde for 20 minutes. The fixated cells were washed thrice with DPBS before being

blocked in 1 % BSA overnight at 4 °C. If staining did not proceed the following day, the fixated cells stayed in parafilm-sealed dishes at 4 °C until further use.

Prior to antibody incubation, the cells being stained for nuclear transcription factors (OCT4, SOX2 and NANOG) or cardiac-specific proteins (α-actinin) were additionally treated with 0.1 % Triton X-100 (see 2.1.4) for 10 minutes at room temperature. For staining, each cover slip was incubated overnight at 4 °C with 100 µl primary antibody diluted in 1 % BSA **(Table 4)**. The following day, the cover slips were washed carefully for 10 minutes with DPBS before being incubated at 37 °C for one hour with 100 µl secondary antibody specifically diluted in 1 % BSA **(Table 5)**. After another washing step with DPBS, the samples were stained with 100 µl DAPI (1:5000, diluted in DPBS) for 10 minutes at room temperature. The stained cover slips were washed with DPBS for another 10 minutes before the final washing step was performed with dH_2O to avoid salt residues after drying. VECTASHIELD Mounting Medium was used for mounting the completed cover slips. Finally, the dried samples were sealed with nail polish. Fluorescent images were taken with a fluorescence microscope (Carl Zeiss Axio Observer.Z1).

2.2.4 Metaphase preparation and karyotyping

Undifferentiated hiPSCs with a high number of passages (25 passages or older) were used for karyotyping to confirm that long-term cultivation did not lead to numerical chromosome aberrations. HiPSCs cultivated on Geltrex with around 55 % confluence were treated with Demecolcine (final concentration 100 ng/ml) for 16 hours in order to induce a metaphase arrest via microtubules depolymerisation. Thereafter, the supernatant of the culture dishes was collected into a 15-ml falcon tube. The adherent cells were washed once with DPBS before being treated with TrypLE Express for 1 minute at 37 °C. The dissociated cells were collected in the 15-ml falcon tube. After centrifugation at 200 x *g* for 3 minutes, the majority of the supernatant was discarded leaving only 500 µl within the falcon tube for careful resuspension of the pellet. A hypotonic KCl solution (0.075 M), prewarmed at 37 °C, was added dropwise up to 8 ml while slightly shaking the falcon tube. After 45 minutes of incubation in a 37 °C water bath, allowing the cells to swell, the falcon tube was centrifuged (200 x *g*, 3 minutes) followed by aspiration of the supernatant leaving only 500 µl to resuspend the pellet as described above. Freshly prepared and precooled fixation buffer (see 2.1.3) was added in a dropwise manner up to 5 ml while slightly shaking the falcon tube. The cells were incubated on ice for 10 minutes and then centrifuged (200 x *g*, 3 minutes). This fixation step was repeated twice. After the final centrifugation, the majority of supernatant was discarded. Depending on the pellet size, 1-2 ml solution were left in the falcon tube to carefully resuspend the pellet. The cells were then dropped from different heights onto cold microscope slides, which were left to dry for 24 hours. The chromosomes were stained with Giemsa solution (1:20, diluted in dH_2O) for 5 minutes at room temperature and subsequently washed with dH_2O for another 5 minutes. After

drying, the stained chromosomes were counted under a light microscope (Zeiss Axio Imager.M2) using a 63x magnification and oil immersion. Karyotyping analysis was documented with the help of the Case Data Manager 6.0 software (Applied Spectral Imaging, ASI).

2.2.5 Teratoma formation and analysis

To determine the spontaneous *in vivo* differentiation ability, the generated hiPSCs were injected into an immunodeficient mouse to form teratomas. Therefore, the hiPSC colonies cultivated on feeder-layer were washed once with DMEM/F12 and incubated with Collagenase IV (200 U/ml) for 5 minutes. After another washing step with DMEM/F12, the cells were detached and dissected with the help of a sterile cell scraper. After adding 200-300 µl DPBS, the cell clusters were transferred into a 1.5 ml Eppendorf tube and carefully transported to the Institute for Cellular and Molecular Immunology of the University Göttingen, where the cells were injected subcutaneously into a 8-week-old severe combined immunodeficiency (SCID) mouse. After two to three months, the formed teratomas were cut out of the mice and fixed in phosphate-buffered formalin (see 2.1.3) for 4 hours at room temperature or overnight at 4 °C. Thereafter, the teratomas were washed with distilled water and dehydrated. Both embedding the teratomas into paraffin and finely slicing the samples into 6 µm sections with the help of a microtome (Leica Biosystems) were performed by technical assistants of Dr. Streckfuß-Bömeke's lab. The hematoxylin and eosin stainig was performed at the Department of Pathology of the University Medical Center Göttingen. The stained sections were analysed using light microscopy.

2.2.6 Gene expression analyses

2.2.6.1 RNA isolation and purification

In order to isolate RNA from hiPSCs cultivated either on feeder-layer or Geltrex, the cells in each well or culture dish were lysed in 400 µl RNA lysis buffer as described above (see 2.1.2 and 2.2.1.10). After additionally detaching the cells with a sterile cell scraper, the lysed cells were transferred into a 1.5 ml Eppendorf tube and stored at -80 °C. For further use, the samples were thawed on ice before RNA isolation and purification was performed with the help of the SV total RNA Isolation System (see 2.1.3). At first, 95 % ethanol was added in a 1:1 ratio to each sample. The solution was thoroughly mixed, transferred into a Spin Column Assembly and centrifuged at 13,000 x *g* for 1 minute. The eluate was discarded and 600 µl RNA Wash Solution were added to each Spin Basket. After another centrifugation step and disposal of the eluate, 50 µl freshly prepared DNase incubation mix (40 µl Yellow Core Buffer, 5 µl 0.09 M $MnCl_2$ and 5 µl DNase I) were added into each Spin Basket and incubated for 15 minutes at room temperature. Thereafter, 200 µl DNase Stop Solution were added, followed by another centrifugation step. Two washing

steps were subsequently performed. At first, 600 µl RNA Wash Solution were added and centrifuged for one minute, before another 250 µl RNA Wash Solution were added and centrifuged for 2 minutes. Each Spin Basket was then transferred into a 1.5 ml capped Elution Tube before 55-100 µl nuclease-free water were added depending on the size of the initial pellet. After the last centrifugation (13,000 x *g*, 1 minute), the concentration of the isolated RNA was measured at 260/280 nm with either an Eppendorf biophotometer or a NanoDrop 2000c/2000 Spectrophotomer (Thermo Fisher Scientific). The measured RNA was either used directly for reverse transcription (RT) reaction (see 2.2.6.2) or stored at -80 °C until further use.

2.2.6.2 Reverse transcription reaction

During reverse transcription reaction, the isolated RNA was transcribed into complementary DNA (cDNA). The required quantity of RNA (100 ng or 200 ng) was diluted in DEPC-treated water and added to a master mix containing the components listed below **(Table 8)**, resulting in a final volume of 20 µl per reaction. Everything was pipetted on ice.

Table 8. RT reaction components.

RT reaction components	20 µl final volume
100 or 200 ng RNA diluted in DEPC-treated water	10,2 µl
10x PCR buffer II	2 µl
25 mM $MgCl_2$	4 µl
100 mM dNTPs	0.8 µl
RNAse inhibitor (20 U/µl)	1 µl
50 µM Oligo $d(T)_{16}$	1 µl
MuLV reverse transcriptase (50 U/µl)	1 µl

A preset program **(Table 9)** was run in a thermocycler (SensoQuest) to perform the RT reaction. The resulting cDNA was either used for PCR analyses or stored at -20 °C until further use.

Table 9. Thermocycler program for the RT reaction.

	Step 1	Step 2	Step 3	Step 4
Temperature [°C]	22	42	95	4
Time [min]	10	50	10	∞

2.2.6.3 Semi-quantitative PCR

One way of gaining sequence specific amplification of the obtained cDNA was semi-quantitative PCR. Therefore, 1-2 µl cDNA were added to a master mix containing the components listed in the table below **(Table 10)**, resulting in a final volume of 25 µl per reaction. Everything was pipetted on ice.

Table 10. Components for PCR.

Components for PCR	25 µl final volume
cDNA	1 µl
Nuclease-free water	15.05 µl
5x Green GoTaq reaction buffer	5 µl
10 mM dNTPs	1.6 µl
Sense primer (10 µM)	1 µl
Antisense primer (10 µM)	1 µl
GoTaq DNA polymerase	0.1 µl
DMSO	0.25 µl

For every primer pair, the basic thermocycler program used for semi-quantitative PCR **(Table 11)** was adapted in regards to annealing temperature and number of amplification cycles **(Table 6)**. The obtained PCR product was stored at 4 °C until gel electrophoresis was performed.

Table 11. Thermocycler program for semi-quantitative PCR.

Step	Temperature [°C]	Duration	Repeats
Initial denaturation	95	3 minutes	1
Denaturation	94	15 seconds	(see 2.1.5, Table 6)
Annealing	(see 2.1.5, Table 6)	30 seconds	
Elongation	72	30 seconds	
Final elongation	72	10 minutes	1
Final step	4	∞	1

2.2.6.4 Gel electrophoresis

The resulting PCR products were loaded on a 1.5-2 % agarose gel prepared with 6 µl Midori Green Advance and run at 100 V for 30-45 minutes, submerged in 1x TBE buffer (see 2.1.3). The GeneRuler 100 bp DNA ladder was loaded next to the samples to confirm the amplified product's size. After a sufficient electrophoretic separation was achieved, the results were visualized under ultraviolet light with the help of a MultiImage Light Cabinet (Alpha Innotech Corporation). The generated images were quantified by using the AlphaEaseFC and GraphPad Prism 6 or 7 (GraphPad Software, Inc.) softwares.

2.2.6.5 Quantitative real-time PCR

Another option for gaining a sequence specific amplification of the produced cDNA was quantitative real-time PCR, which also offered the possibility of a more exact quantitation of the examined samples. In order to establish a standard curve in advance, a semi-quantitative PCR was run with the required primer pair (**Table 11**, T_A: 60 °C; cycles: 40). The obtained PCR product was loaded completely (25 µl) on a 1.5 % agarose gel and run for one hour at 100 V as described above (see 2.2.6.4). The resulting PCR product band was cut out of the gel under ultraviolet light. DNA purification was performed with the QIAquick Gel Extraction Kit according to the manufacturer's instructions. For gaining the standard curve, the purified DNA fragment was diluted in different ratios in a yeast t-RNA solution (30 µl/ml dH_2O). Triplicates of selected standard concentrations along with triplicates of the required cDNA samples (1 µl each) were added into the wells of a sterile 96-well plate (Firma). A freshly prepared master mix **(Table 12)** was additionally added into each well. The 96-well plate was sealed with an adhesive film and centrifuged at 500 x *g* for 2 minutes. The quantitative PCR was performed in a real-time PCR detection system (Bio-Rad iQ5 Multicolor Real-Time PCR Detection System) using the program listed below **(Table 13)**.

Table 12. Master mix for quantitative real-time PCR

Components for quantitative PCR	19 µl final volume
SYBR Green PCR master mix	10 µl
Nuclease-free water	7 µl
Sense primer (10 µM)	1 µl
Antisense primer (10 µM)	1 µl

Table 13. Quantitative PCR program.

Cycle	Step	Temperature	Duration	
Cycle 1	Step 1	95 °C	2 min	
Cycle 2	Step 1	95 °C	15 s	
	Step 2	60 °C	10 s	40 times
	Step 3	72 °C	20 s	
Cycle 3	Step 1	95 °C	15 s	
Cycle 4	Step 1	60 °C	10 s	72 times
				Melting curve
Cycle 5	Step 1	10 °C	∞	

The resulting data was analysed with the help of the Bio-Rad iQ5 Standard Edition Optical System Software 2.0 and the fluorescent dye SYBR Green (see **Table 12**), which binds to double-stranded DNA. As DNA is amplified during PCR, fluorescence signal consequently increases and thereby allows the quantification of the obtained PCR product. The Bio-Rad iQ5 software determines a threshold for the detection of the fluorescence. The number of cycles at which the fluorescence crosses this threshold is called the threshold cycle (C_t). Depending on the expression level of the analysed gene in each sample, the threshold is reached at a lower or higher number of cycles. In addition to the gene quantity, reaching of the threshold also depends to a great extent on the corresponding primers and the gene itself. Therefore, a standard curve (as described above) was established to determine the gene- and primer-specific amplification efficiency. As an example, an efficiency of 100% would mean an exact duplication of the PCR product with each cycle.

2.2.7 Western blot analyses

2.2.7.1 Preparation of cell lysates

Catecholamine-treated hiPSC-CMs were harvested for pellets as described above (see 2.2.1.5). The samples were stored at -80 °C until further use. After thawing the cell pellets on ice, 60-80 µl freshly prepared lysis buffer (see 2.1.3) were added into each tube depending on the pellet size. Each pellet was thoroughly resuspended before being incubated for 15 minutes on ice to avoid protein damage. Subsequently, the tubes were centrifuged for 10 minutes at 13 000 x *g* in a precooled centrifuge (5 °C) and the supernatant was transferred into a new Eppendorf tube. Pierce BCA Protein Assay Kit was used for measurement of the protein concentrations. Therefore, 5 µl of each sample were diluted in 95 µl DPBS. Triplicates of each diluted sample (25 µl respectively) were added into the appropriate wells of a non-sterile 96-well plate (nunc) along with 9 triplicates of the freshly prepared albumin standards. At last, 200 µl reaction mix were added into each well before the 96-well plate was incubated at 37 °C for 30 minutes. The protein concentrations were measured with a

microplate photometer at 562 nm (BioTek Instruments). The measured samples were diluted in blue loading buffer (see 2.1.3) and either used immediately or stored at -20 °C until further use.

2.2.7.2 SDS-polyacrylamide gel electrophoresis

For electrophoretic separation of the samples according to their molecular weight, SDS-polyacrylamide gel electrophoresis was performed. Depending on the analysed antibody and its size, the separation gel (see 2.1.3) was prepared with a concentration of 6-12 %. As soon as the gel was solid, the stacking gel (see 2.1.3) was poured on top. A comb was inserted into the stacking gel to create pockets for the samples. Those of the lysed protein samples previously stored at -20 °C were thawed on ice before all samples were denaturated by incubation at 37 °C for 30 minutes. Then, the samples along with the PeqGold protein marker V (see 2.1.3) were loaded into the pockets of the stacking gel. Each gel was submerged in an electrophoresis chamber filled with 1x running buffer (see 2.1.3). The gel electrophoresis was performed for 45 minutes at 50 V followed by another 90 minutes at 90 V.

2.2.7.3 Protein transfer

After the electrophoretic separation was finished, the proteins were electrically transferred onto a PVDF membrane. Protein transfer was performed semi-dry with the help of a Trans-Blot Turbo Transfer System (Bio-Rad). Three pieces of filter paper (each 0.8 mm) were submerged in cathode and anode buffer respectively. The PDVF membrane was incubated in methanol for 2 minutes before being washed for another 8 minutes in water. Everything was arranged inside the cassette of the Trans-Blot Turbo Transfer System as listed in **Table 14**. The standard program (2.5 A and 25 V) was run for 15 minutes.

Table 14. Transfer arrangement.

Filter paper (submerged in cathode buffer)
SDS-polyacrylamide gel
PVDF membrane
Filter paper (submerged in anode buffer)

2.2.7.4 Protein detection

The membrane was stained with Coomassie Brilliant Blue (see 2.1.3) to determine whether the transfer had been successful. After two minutes of staining, the membrane was destained using a PVDF destain solution and washed thrice with TBS-T buffer (see 2.1.3). To prevent unspecific binding between membrane and antibody, the PVDF membrane was blocked for one hour at room temperature with either 3 % BSA or 5 % nonfat dry milk, depending on the antibody. Thereafter, the membrane was incubated with a primary antibody (**Table 4**) at 4 °C overnight on a mechanical shaker. The membrane was subsequently washed with TBS-T buffer for 30 minutes before incubation with an HRP-conjugated secondary antibody (**Table 5**) at room temperature for one hour on a mechanical shaker. After another washing step with TBS-T for 30 minutes, the binding antibodies were visualised using the SuperSignal West Pico Chemiluminescent Substrate (see 2.1.3). The membrane was incubated with the substrate mix for 5 minutes. Meanwhile, HRP catalysed the oxidation of the luminol-based substrate by peroxide, which led to luminescence documented with a chemiluminescence detection system (ChemiDoc MP Imaging System, Bio-Rad).

2.2.8 Statistical analyses

Experimental data obtained from PCR or Western blot are shown as mean±SEM (standard error of the mean). The unpaired Student's t-test was applied to compare differences between two independent groups. For comparison of multiple groups, ANOVA (analysis of variance) was used. A value of p less than 0.05 was considered statistically significant (*=$p<0.05$, **=$p<0.01$, ***=$p<0.001$, ****=$p<0.0001$). All statistical analyses were performed with the help of GraphPad prism 6 or 7 software.

3 Results

3.1 Proof of pluripotency

Non-integrating systems such as Sendai viruses or plasmids were used for generation of the hiPSC lines applying previously described protocols (Okita *et al.* 2011, Churko *et al.* 2013). As part of this work, two newly generated hiPSC lines of patient 1 (passage range 6-10) were defrosted and cultivated for pluripotency characterization. The characterization served to show that the differentiation potential of the generated hiPSCs is similar to that of other pluripotent stem cells such as hESCs.

3.1.1 Morphology and alkaline phosphatase staining

The morphology of hiPSCs and hiPSC-colonies is similar to that formed by hESCs. The round-shaped cells form flat, sharply defined round colonies when cultivated on feeder-layer (**Fig. 6A, C**). All generated hiPSC lines showed a positive alkaline phosphatase staining (**Fig. 6B, D**).

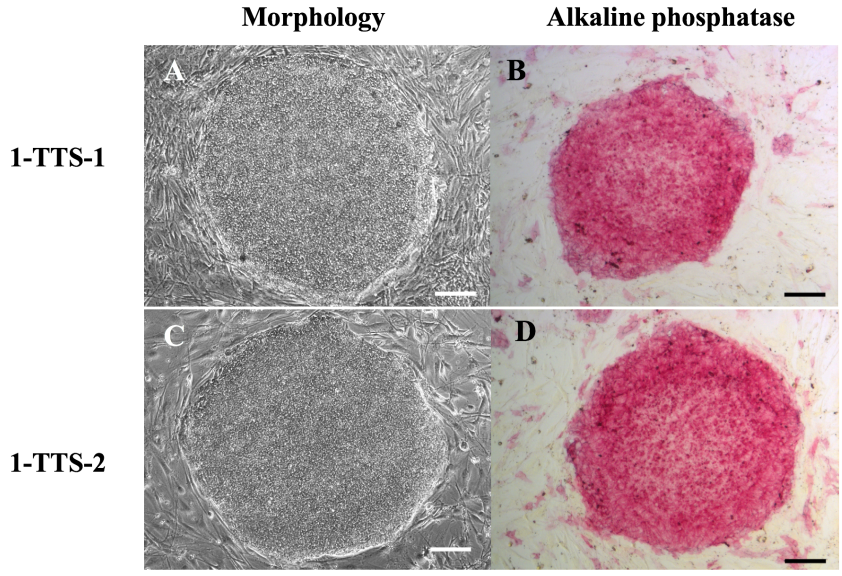

Figure 6. Morphology and alkaline phosphatase staining.

HiPSC-colonies cultivated on feeder layer (**A-D**) show a round shape. Alkaline phosphatase was expressed in both generated TTS-hiPSC lines as shown by the magenta-stained colonies (**B, D**). Scale bar 200 µm.

3.1.2 Expression of pluripotency related markers

Semi-quantitative RT-PCR was used to analyze the expression of different pluripotency related markers on mRNA level **(Fig. 7A)**. Additionally, immunofluorescence staining was performed to analyze the expression of those markers on protein level **(Fig. 7B)**.

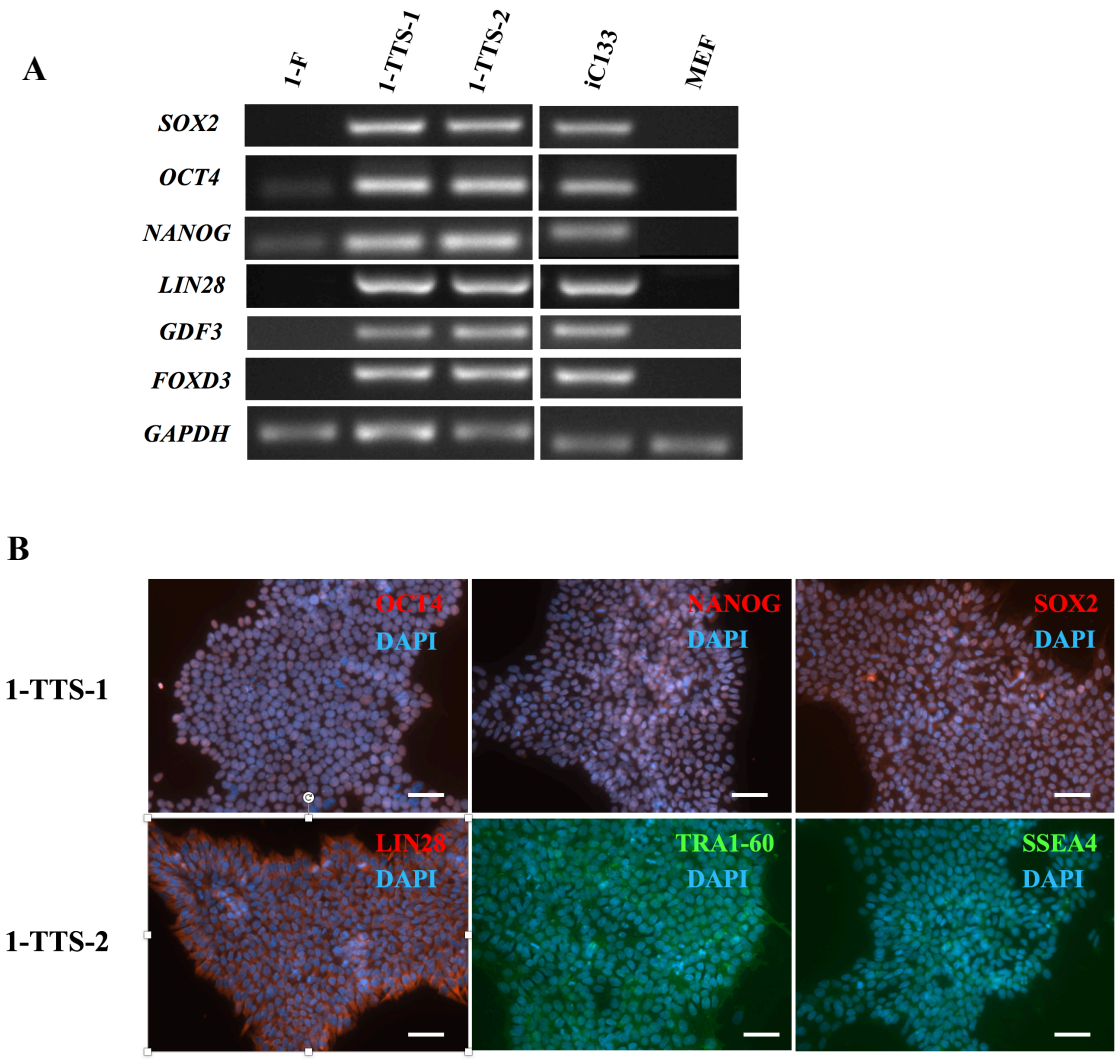

Figure 7. Gene expression analysis and immunostaining of two generated hiPSC lines of patient 1.

RT-PCR showed that the pluripotency-specific markers *SOX2, OCT4, NANOG, LIN28, GDF3* and *FOXD3* were upregulated in both cell lines of patient 1, whereas these genes were downregulated in their parental fibroblasts as well as the MEFs, who served as a negative control **(A)**. Previously published pluripotent cell line iC133 (Dudek et al. 2016) functioned as a positive control and GAPDH was used as housekeeping gene. HiPS cell line 1 of patient 1 showed a positive immunostaining for the pluripotency related proteins OCT4, NANOG, SOX2, LIN28, TRA1-60 and SSEA4 **(B)**. The TRA1-60 and SSEA4 are located in the cell membrane, whereas OCT4, NANOG and SOX2 are located in the cell nucleus and LIN28 is located in the cytoplasm. The cell nuclei were stained with DAPI (blue). Scale bar: 50 µm.

Both TTS-hiPSC lines of patient 1, as well as positive control cell line iC133, expressed similarly high levels of the pluripotency related markers *SOX2, OCT4, NANOG, LIN28, GDF3* and *FOXD3* on mRNA level, while these markers were not or only weakly expressed in their parental fibroblasts and the MEFs, which functioned as a negative control **(Fig. 7A)**. In addition to RT-PCR, immunofluorescence staining was performed **(Fig. 7B)**. TTS-hiPS cell line 1 of patient 1 stained positively for pluripotency related proteins OCT4, NANOG, SOX2, LIN28, TRA1-60 and SSEA4

(Fig. 7B). OCT4, NANOG and SOX2 are located in the nuclei of hiPSCs, whereas LIN28 is located in the cytoplasm. TRA1-60 and SSEA4 are located on the membrane surface. GAPDH was expressed similarly in all tested cells and served as control. No conspicuous differences between the two analyzed hiPSC lines were observed.

3.1.3 Differentiation potential *in vitro* and *in vivo*

A spontaneous differentiation protocol was used to determine the differentiation ability of the generated TTS-hiPSCs *in vitro* via embryoid body formation, while teratoma formation was used to proof the differentiation ability *in vivo*. For *in vitro* differentiation, the TTS-hiPSCs were cultivated in Iscove Medium on uncoated culture dishes so that the cell clusters known as embryoid bodies could form. On day 8, the embryoid bodies were transferred onto 0.1% gelatin-coated culture dishes and cultivated for another 25 days. For analysis of the differentiation on mRNA level, samples were taken at three different time points (day 0, day 8 and day 8+25) **(Fig. 4)**. Samples of both spontaneously differentiated TTS-hiPSC lines showed an increased gene expression of the markers representing the three germ layers **(Fig. 8)**.

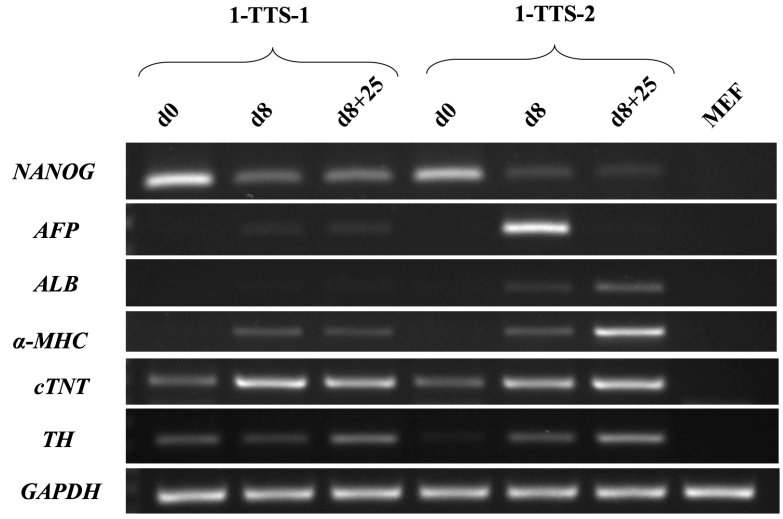

Figure 8. Gene expression analysis of in vitro differentiated TTS-hiPSCs.

Both TTS-hiPSC lines of patient 1 were differentiated spontaneously *in vitro*, and mRNA samples were taken at three different time points (day 0, day 8, day 8+25). The expression of all three germ layers was determined using ectodermal (*TH*), mesodermal (*α-MHC, cTNT*) and endodermal (*AFP, ALB*) markers. The pluripotency marker *NANOG* was initially upregulated in undifferentiated TTS-hiPSCs at day 0, but *NANOG* expression decreased with further differentiation. *GAPDH* was used as housekeeping gene. MEFs were used as a negative control.

The endodermal marker *AFP* was highly expressed at day 8 in 1-TTS-2 and weakly expressed in 1-TTS-1 during later stages of the differentiation. *ALB*, a late marker for hepatocytes, was particularly expressed at day 8+25 in 1-TTS-2. Practically no expression of *ALB* was detectable in 1-TTS-1. The mesodermal markers *cTNT* and *α-MHC* were especially expressed at day 8 and day 8+25 in both cell lines. *TH*, an ectodermal marker, was mostly expressed during the later stages of the differentiation process (day 8+25).

The *in vitro* differentiated TTS-hiPSCs were also fixated for immunofluorescence staining to analyze their differentiation potential on protein level **(Fig. 9A-F)**. Both TTS-hiPSC lines of patient 1 showed a positive staining for mesodermal α–SMA **(Fig 9A, D)**, endodermal AFP **(Fig 9B, E)** and ectodermal β-III-TUBULIN **(Fig 9C, F)**, therefore expressing markers for all three germ layers after spontaneous differentiation.

The *in vivo*-differentiation potential of the generated TTS-hiPSCs was determined via teratoma formation. Therefore, TTS-hiPSCs were injected subcutaneously into 8-week-old SCID mice. After two to three months, the injected TTS-hiPSCs formed teratomas, which were cut out of the mice, fixated and stained before being histologically analyzed **(Fig. 9G-L)**. Tissue of all three germ layers was detected in both TTS-hiPSC lines of patient 1: Neural rosettes **(Fig. 9I, L)** represented ectoderm and cartilage **(Fig. 9G, J)** represented mesoderm, while intestinal tissue **(Fig. 9H, K)** represented endoderm.

Taken as a whole, the previous data shows that the generated TTS-hiPSCs are pluripotent. They not only expressed pluripotent-specific markers on mRNA and protein level, but they were also able to differentiate spontaneously *in vivo* and *in vitro* into tissue of the three germ layers.

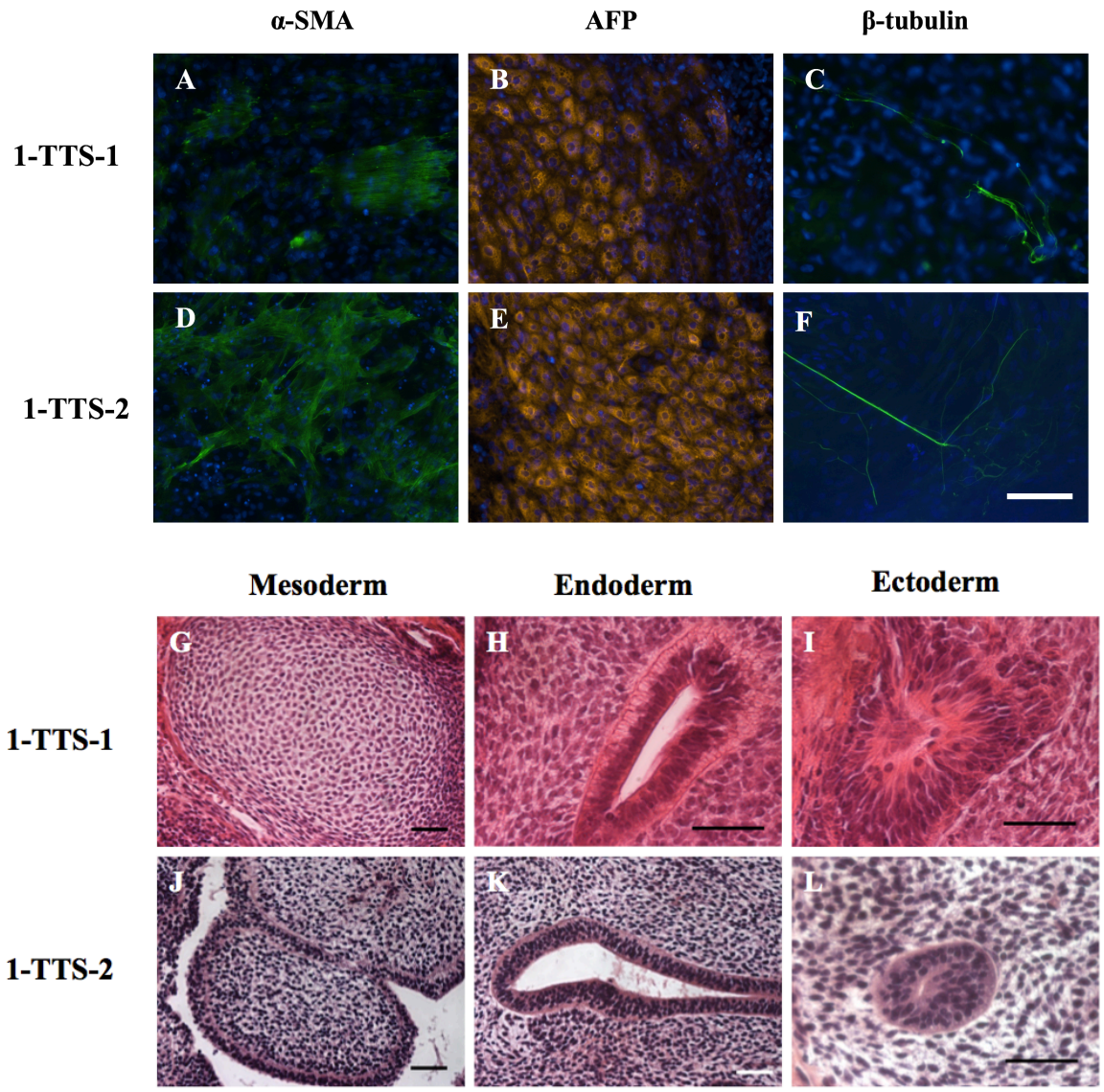

Figure 9. Immunofluorescence staining and teratoma formation of spontaneously differentiated TTS-hiPSCs.

Immunofluorescence staining of two *in vitro* differentiated TTS-hiPSC lines of patient 1 stained positively for mesodermal α–SMA **(A, D)**, endodermal AFP **(B, E)** and ectodermal β-III-TUBULIN **(C, F)**, thereby expressing specific proteins for all three germ layers. The cell nuclei were stained with DAPI (blue). Scale bar: 100 µm. Additionally, subcutaneously injected TTS-hiPSCs of patient 1 formed mature teratoma in SCID mice. The teratomas were cut out, fixated and histologically stained using Hematoxylin and Eosin Stain. Teratomas of both cell lines of patient 1 showed expression of three different germ layer-specific tissues. Mesoderm was represented by cartilage **(G, J)**, endoderm was represented by intestinal tissue **(H, K)** and ectoderm was represented by neuronal rosettes **(I, L)**. Scale bar: 50 µm.

3.1.4 Karyotyping

Long-term culture of hiPSCs is associated with the risk of chromosomal instability. In order to make sure that the cultivated hiPSCs did not develop numerical chromosome aberrations over time, karyotyping was performed with hiPSCs cultivated for 25 passages or more. The majority of cells examined displayed a diploid karyogram without numerical chromosome aberrations (46, XX), as exemplarily shown in **Figure 10**.

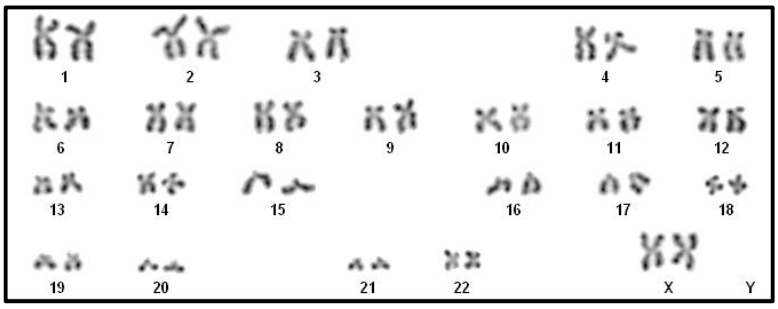

Figure 10. A representative karyogram of hiPSCs (1-TTS-1) cultivated for ≥ 25 passages.

The karyogram of 1-TTS-1 after long-term culture showed a diploid karyotype (46, XX) without numerical chromosome aberrations.

3.2 Generation of hiPSC-derived cardiomyocytes

HiPSCs were cultivated on Geltrex in Essential 8 Medium until they reached about 90% confluency before the process of directed cardiac differentiation was started. Cardio Differentiation Medium, supplemented first with CHIR99021 and then later with IWP2 to temporarily activate and subsequently suppress the Wnt-signaling pathyway, replaced the Essential 8 Medium. At day 8, the Cardio Differentiation Medium was in turn replaced with Cardio Culture Medium **(Fig. 5)**. First beating cardiomyocytes started to appear during the second week of cultivation (day 8-14). Around day 16, the generated hiPSC-CMs were digested and replated in a lower cell density. After three weeks of cultivation (around day 20), Cardio Culture Medium was replaced by Cardio Selection Medium (containing lactate, but leaving out glucose) to further purify the culture. A high percentage of pure beating cardiomyocytes was visually observed after selection. The cardiomyocytes were matured for three months before they were used for further experiments. Mature hiPSC-CMs showed a typical morphology of polyangular, oval to spindle-shaped cells **(Fig. 11B)**.

The expression of cardiac-specific markers was analysed on mRNA and protein level in order to proof that the directed differentiation of hiPSCs into cardiomyocytes had been successful. RT-PCR showed that the cultivated two-month old TTS-hiPSC-CMs expressed the cardiac-specific markers *ACTN2*, *α-MHC*, *β-MHC* and *cTNT* on mRNA level **(Fig. 11A)**. In contrast to the initial TTS-hiPSCs, mature TTS-hiPSC-CMs did no longer express pluripotent markers such as *SOX2* and

LIN28. Immunostaining of TTS-hiPSC-CMs with an antibody against α-actinin confirmed a successful cardiac differentiation on protein level **(Fig. 11C)**. The positive immunostaining for myofilament protein α-actinin also showed normally organized cross-striations in TTS-hiPSC-CMs **(Fig. 11C)**.

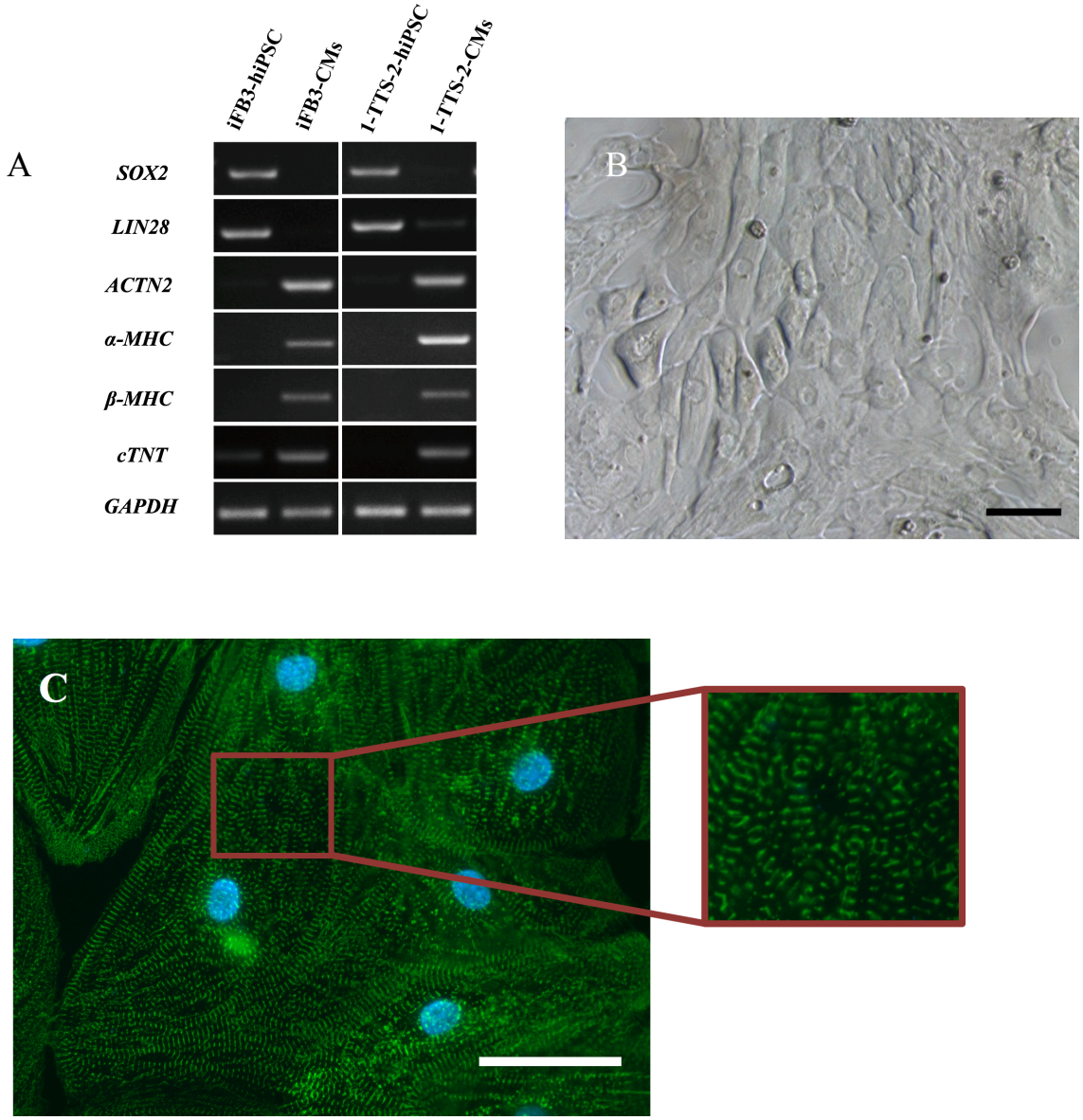

Figure 11. Gene expression analysis, morphology and immunofluorescence staining of mature TTS-hiPSC-derived CMs.

Both hiPSC lines of patient 1 were directly differentiated into cardiomyocytes for two months. The mRNA samples of these mature TTS-hiPSC-CMs expressed the cardiac-specific markers *ACTN2*, *α-MHC*, *β-MHC* and *cTNT*, as shown via RT-PCR **(A)**. Mature TTS-hiPSC-CMs did not express pluripotent markers such as *SOX2* and *LIN28*. *GAPDH* was used as housekeeping gene (data from S. Georgi). Cultivated TTS-hiPSC-CMs showed typical cardiomyocyte morphology **(B)**. Scale bar: 50 µm. Mature hiPSC-CMs of TTS patient 1 (1-TTS-2) stained positively for the myofilament protein α-actinin **(C),** thereby showing normally organized cross-striations. Cell nuclei were stained with DAPI (blue). Scale bar: 50 µm.

In summary, TTS-hiPSCs were successfully differentiated into mature, beating cardiomyocytes via a directed cardiac differentiation protocol. High purity of about 90% was achieved (data not shown). Cardiomyocyte differentiation was confirmed via high expression of cardiac-specific markers on mRNA level and positive immunostaining for sarcomeric structure protein α-actinin. No significant cell line-specific differences concerning sarcomeric structure, differentiation efficiency or expression of cardiac-specific markers on mRNA and protein level could be observed.

3.3 Stress induction in hiPSC-derived cardiomyocytes

In about 70 percent of the cases, TTS is triggered by emotional or physical stress (Lyon et al. 2016). Since the first publication back in 2005 revealed noticeably high catecholamine serum concentrations in TTS patients (Wittstein et al. 2005), TSS has been induced in several *in vitro* and *in vivo* models via exposure to high catecholamine concentrations (Paur et al. 2012, Shao et al. 2013, Ellison et al. 2007). However, all these models worked mainly with animal cardiomyocytes (rats, mice). Familial cases of TTS have been reported, suggesting a potential underlying genetic predisposition (Pison et al. 2004, Kumar et al. 2010, Subban et al. 2012) and reinforcing the need for a patient-specific disease model to study the pathomechanism of TTS which is still not sufficiently understood. Directly differentiated hiPSC-CMs of TTS patients offer the possibility to study the pathomechanism of TTS without ignoring possible genetic-based patient-specific differences compared to healthy controls.

In order to induce a TTS event in control- and TTS-hiPSC-CMs, 3-month-old CMs were treated with Epi (100 nmol/L, 500 µmol/L) and Iso (100 nmol/L, 5 mmol/L) for 2-20 hours. The chosen experimental conditions such as type of catecholamine, catecholamine concentration and length of treatment were based on publications of previous TTS disease models (Paur et al. 2012, Shao et al. 2013, Ellison et al. 2007) and our own establishment. Afterwards, mRNA samples of the treated cells were taken and analyzed for the expression of cardiac stress markers. Initially, expression of every stress marker was analyzed via RT-PCR. Promising stress markers were additionally analyzed via quantitative PCR for a more precise quantification of the changes in expression.

Clinical studies of TTS patients have shown a significant elevation of cardiac insufficiency related polypeptide hormone BNP in TTS patient serum during a TTS event (Madhavan et al. 2009). A TTS animal *in vitro* model by Ueyama also showed an upregulation of ANP in the myocardium after stress induction (Ueyama 2004). We therefore analyzed the expression of *NPPA* and *NPPB* in both control- and TTS-hiPSC-CMs after treatment with either Iso (100 nmol/L, 5 mmol/L) or Epi (100 nmol/L, 500 µmol/L) for 2 hours via quantitative PCR **(Fig. 12)**. Especially, treatment with 500 µmol/L Epi showed a significant increase of *NPPB* expression in both control- and TTS-hiPSC-CMs **(Fig. 12)**. Upon treatment with 500 µmol/L Epi or 5 mmol/L Iso, the expression of *NPPA* was significantly increased in control-hiPSC-CMs, too. On the other hand, no catecholamine

treatment of TTS-hiPSC-CMs showed a significant increase of *NPPA*. Overall, both stress markers showed a relatively modest increase and thus research for a more suitable stress marker continued.

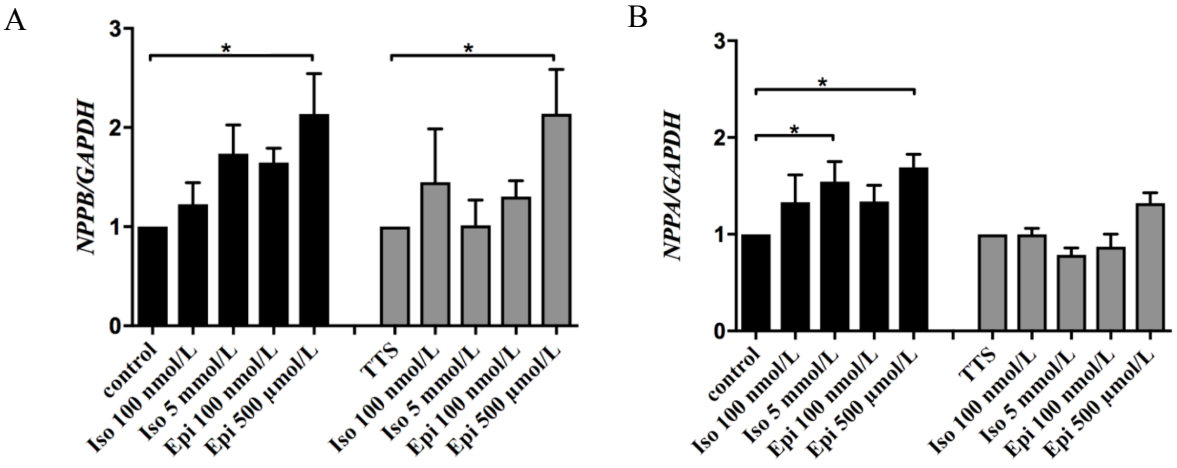

Figure 12. Expression of *NPPB* and *NPPA* in control- and TTS-hiPSC-CMs after catecholamine treatment.

Three-month-old hiPSC-CMs of both control and TTS patients were treated with Iso (100 nmol/L, 5 mmol/L) and Epi (100 nmol/L, 500 µmol/L) for 2 hours. The resulting mRNA samples were analyzed via quantitative PCR and showed a significant increase of *NPPB* expression **(A)** after treatment with 500 µmol/L Epi in both control- and TTS-hiPSC-CMs. The increase of *NPPA* after 5 mmol/L Iso-treatment was only significant for control-hiPSC-CMs. No significant increase of *NPPB* or *NPPA* expression was observed after Iso-treatment in TTS-hiPSC-CMs. *NPPB* and *NPPA* were normalized to *GAPDH*. Control: n=6 differentiation experiments from different cell lines of 3 healthy controls; TTS: n=5 differentiation experiments from different cell lines of 2 TTS patients. Data are shown as mean±SEM, *p<0.05 significant differences by one-way ANOVA for each group (TTS, control).

3.4 NR4A1 as a stress marker

3.4.1 Next Generation Sequencing

In order to find new β-adrenergic signaling-dependent stress markers specific for TTS-hiPSC-CMs, Next Generation Sequencing (NGS) was performed. Therefore, at least two-months old control- and TTS-hiPSCs were treated with 500 µmol/L Epi for 2 hours and compared to untreated samples, respectively. Transcriptome data obtained by the group of Dr. Streckfuß-Bömeke showed *NR4A1* expression as one of the most upregulated expressions after Epi treatment **(Fig. 13)**. *NR4A1* expression showed a 12-fold increase in TTS-hiPSC-CMs and a 13-fold increase in control-hiPSC-CMs after treatment with 500 µmol Epi respectively.

It has been recognized that NR4A1, an orphan nuclear receptor, plays an important role in cardiovascular diseases and might be a protective factor concerning β-adrenergic signaling-induced car-

diac hypertrophy and remodeling (Medzikovic et al. 2015, Yan et al. 2015). Previous studies showed that *NR4A1* expression markedly increased after β-adrenergic stimulation (Yan et al. 2015). Further work therefore concentrated on *NR4A1* as another potentially promising gene and stress marker in TTS.

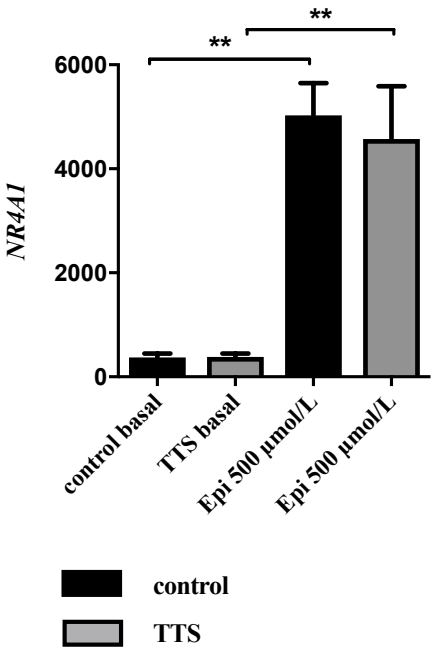

Figure 13. NGS data obtained after treating control- and TTS-hiPSC-CMs with 500 µmol/L Epi.

HiPSC-CMs of both control and TTS patients were treated with 500 µmol/L Epi. NGS was performed and expression of *NR4A1* in both samples was compared to untreated samples in each case. *NR4A1* expression was highly increased in both TTS- and control-hiPSC-CMs after Epi treatment. Control: n=3 differentiation experiments from different cell lines of healthy control 1 (1-C); TTS: n=5 differentiation experiments from different cell lines of 2 TTS patients. Data are shown as mean±SEM, *p<0.05; **p<0.01; ***p<0.001. The unpaired Student's t-test was used to compare differences between two independent groups. Data obtained by the group of Dr. Streckfuß-Bömeke.

3.4.2 Detailed analysis of *NR4A1* expression

In order to confirm the transcriptome data of NR4A1 as a stress marker in hiPSC-CMs, three different catecholamines were used for stress induction: epinephrine (Epi), isoprenaline (Iso) and phenylephrine (PE) **(Fig. 14)**. Control- and TTS-hiPSC-CMs were treated with each of the three catecholamines for 2 or 20 hours and the resulting samples were analyzed via semi-quantitative PCR. A dose-dependent increase of *NR4A1* expression was observed after 2-hour treatment for all three catecholamines (Epi, PE, Iso) **(Fig. 14)**. Almost every tested Epi concentration (10 µmol/L, 500 µmol/L, 1 mmol/L) applied for 2 hours significantly increased *NR4A1* expression (1.6-fold to 1.8-fold to 1.7-fold), whereby 500 µmol/L Epi-treatment achieved the highest upregulation (1.8-fold). Similarly, 2-hour Iso treatment (10 µmol/L, 5 mmol/L) significantly increased *NR4A1* expression (1.7-fold to 1.6-fold), although the dose-dependent *NR4A1* expression increase from lower to higher concentrations was not as pronounced. PE treatment also showed a dose-dependent increased of *NR4A1* expression for the tested 2-hour concentrations (100 nmol/L, 1 µmol/L, 10 µmol/L). However, the results were not statistically significant as only two differentiation experiments were used **(Fig. 14)**. For further experiments, solely Iso and Epi were used for catecholamine treatment of hiPSC-CMs.

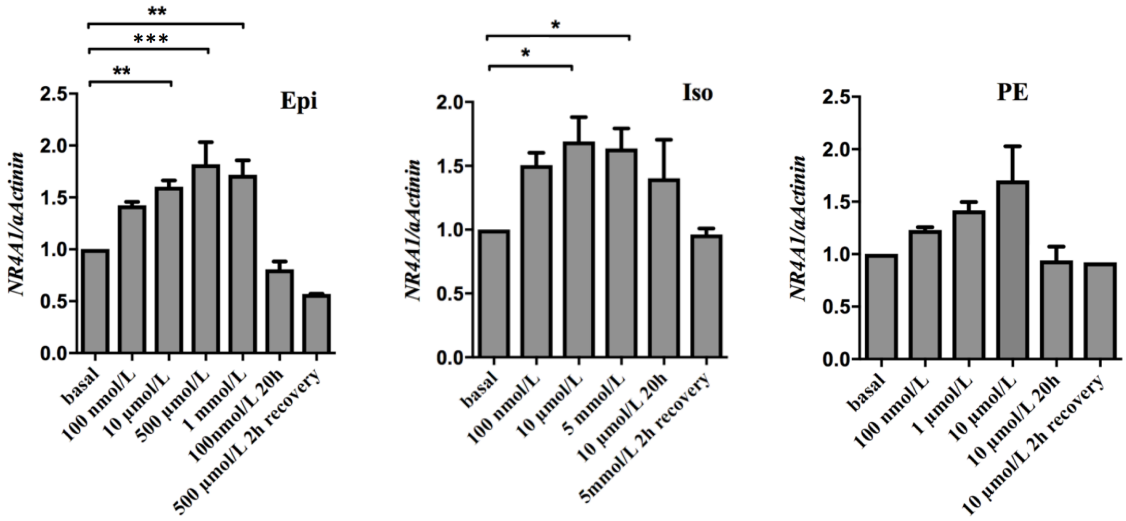

Figure 14. Gene expression of *NR4A1* in hiPSC-CMs after Epi, Iso and PE treatment.

Control and TTS-hiPSC-CMs were treated with different concentrations of Epi (100 nmol/L, 10 µmol/L, 500 µmol/L, 1 mmol/L), Iso (100 nmol/L, 10 µmol/L, 5 mmol/L) and PE (100 nmol/L, 1 µmol/L, 10 µmol/L) for 2 or 20 hours. *NR4A1* expression was analyzed via RT-PCR. An elevation of *NR4A1* expression was observed after treatment of hiPSC-CMs with catecholamines for 2 hours. Treatment with catecholamines for 20 hours did not result in a similar increase of *NR4A1* expression for any of the three catecholamines. HiPSC-CMs, which recovered for 3 weeks after catecholamine treatment, show *NR4A1* expression levels similar to those of untreated hiPSC-CMs. Control: n=2 differentiation experiments from different cell lines of healthy control 1; TTS: n= 2-3 differentiation experiments from different cell lines of TTS patient 1. Data are shown as mean±SEM, *p<0.05; **p<0.01; ***p<0.001 significant differences by one-way ANOVA for each group.

Extensive catecholamine treatment for 20 hours did not increase *NR4A1* activity significantly **(Fig. 14)** and was therefore discontinued. An acute, short treatment with catecholamines for 2 hours is more successful in inducing stress in hiPSC-CMs than a long catecholamine treatment for 20 hours.

In addition to inducing a TTS event in hiPSC-CMs, it was also important to show that the treated cells were able to fully recover from the stress exposure as the majority of TTS patients who survive the TTS event itself recover from the initial heart failure within a few months (Akashi et al. 2003, Lyon et al. 2016). After catecholamine treatment with subsequent washing out, the control- and TTS-hiPSC-CMs intended for recovery were further cultivated for three weeks in Cardio Culture Medium before mRNA samples were taken and analyzed alongside the other samples. Expression of *NR4A1* in the recovered cells matched the level of untreated hiPSC-CMs, thereby showing the reversibility of the stress induction in catecholamine treated hiPSC-CMs **(Fig. 14)**.

In order to more accurately quantify the increase of *NR4A1* expression after catecholamine treatment observed via semi-quantitative PCR, quantitative PCR was performed. TTS- and control-hiPSC-CMs were treated with Epi (100 nmol/L, 500 µmol/L) and Iso (100 nmol/L, 5 mmol/L) for

2 hours as described above in order to induce a TTS event. *NR4A1* expression levels were then quantified via quantitative PCR **(Fig. 15)**. In contrast to *NPPA* and *NPPB*, expression of *NR4A1* was highly elevated for every tested Epi and Iso concentration in both TTS- and control-hiPSC-CMs. Compared to untreated TTS-hiPSC-CMs, *NR4A1* expression increased 13-fold after treatment with 100 nmol/L Epi and even 30-fold after 500 µmol/L Epi treatment. Control-hiPSC-CMs also showed an increased *NR4A1* expression after Epi treatment, similar to the TTS-hiPSC-CMs, with a 13-fold increase after 100 nmol/L Epi and a 27-fold increase after 500 µmol/L Epi **(Fig. 15)**. Iso treatment showed a comparatively lower increase of *NR4A1* expression in both TTS- und control-hiPSC-CMs. However, treatment with either 100 nmol/L or 5 mmol/L Iso lead to a significantly higher increase of *NR4A1* expression in TTS-hiPSC-CMs compared to control-hiPSC-CMs. Expression of *NR4A1* increased 16-fold to 19-fold in TTS-hiPSC-CMs compared to an only 10-fold to 8-fold increase in control-hiPSC-CMs **(Fig. 15)**.

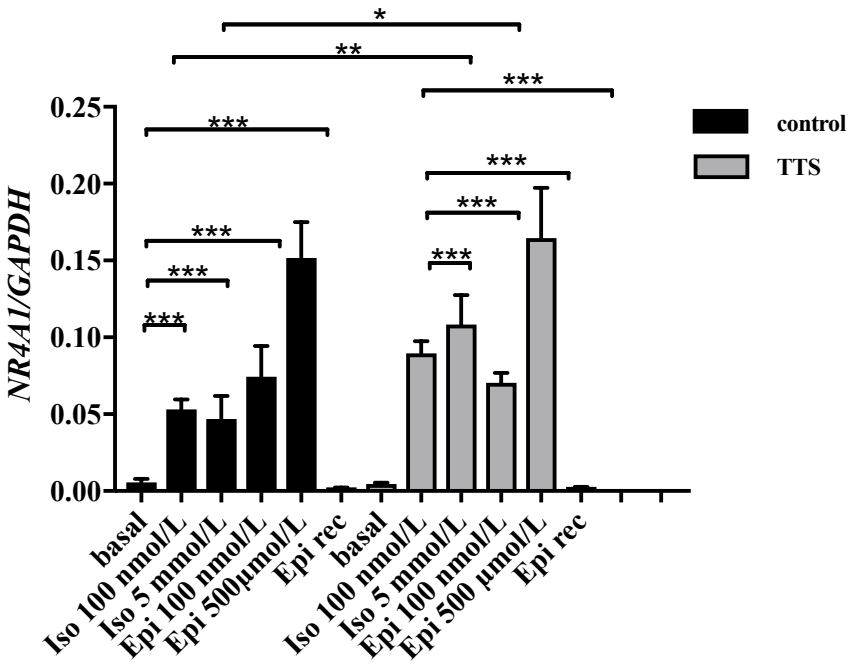

Figure 15. *NR4A1* expression in control- and TTS-hiPSC-CMs after Iso and Epi treatment.

TTS- and control-hiPSC-CMs were treated with Epi (100 nmol/L, 500 µmol/L) and Iso (100 nmol/L, 5 mmol/L) for 2 hours. *NR4A1* expression was analyzed via quantitative PCR. The cardiac stress-related gene showed a high increase after catecholamine treatment for all tested concentrations. The *NR4A1* increase was significantly higher in TTS-hiPSC-CMs compared to control-hiPSC-CMs after Iso treatment (100 nmol/L, 5 mmol/L). Treatment with epinephrine showed a *NR4A1* increase in both control- (13-fold to 27-fold) and TTS-hiPSC-CMs (13-fold to 30-fold). The increase of cardiac stress-related gene *NR4A1* was reversible after washing out and additional three weeks of cultivation (Epi/Iso rec). *NR4A1* was normalized to *GAPDH*. Control: n=6 differentiation experiments from different cell lines of 3 healthy controls; TTS: n=7 differentiation experiments from different cell lines of 2 TTS patients. Data are shown as mean±SEM, *p<0.05; **p<0.01; ***p<0.001, ****p<0.0001 significant differences by one-way ANOVA for each group (control, TTS) combined with Student's t-test.

NR4A1 expression three weeks after catecholamine treatment resembled the level of untreated TTS- and control- hiPSC-CMs **(Fig. 15)**. Therefore, the increase of *NR4A1* expression due to catecholamine treatment was reversible after washing out and additional three weeks of cultivation.

Overall, analysis of different cardiac-stress related genes after catecholamine treatment identified *NR4A1* as an important early marker for stress induction in hiPSC-CMs. TTS-hiPSC-CMs showed a significantly higher increase of *NR4A1* expression after Iso-treatment compared to control-hiPSC-CMs.

3.5 Influence of stress induction on sarcomeric structure

Immunostaining for the sarcomeric structure protein α-actinin was performed in order to analyze the influence of catecholamine treatment on sarcomeric structure. Untreated hiPSC-CMs along with hiPSC-CMs treated with either 500 µmol/L Epi or 5 mmol/L Iso for 2 hours were fixed and stained with α-actinin (see **2.1.4**). The catecholamine-treated hiPSC-CMs showed a regular sarcomeric structure with normally organized cross-striations and without any alteration when compared to untreated hiPSC-CMs **(Fig. 16)**, thereby confirming that treatment with high catecholamine concentrations did not visibly alter the sarcomeric structure.

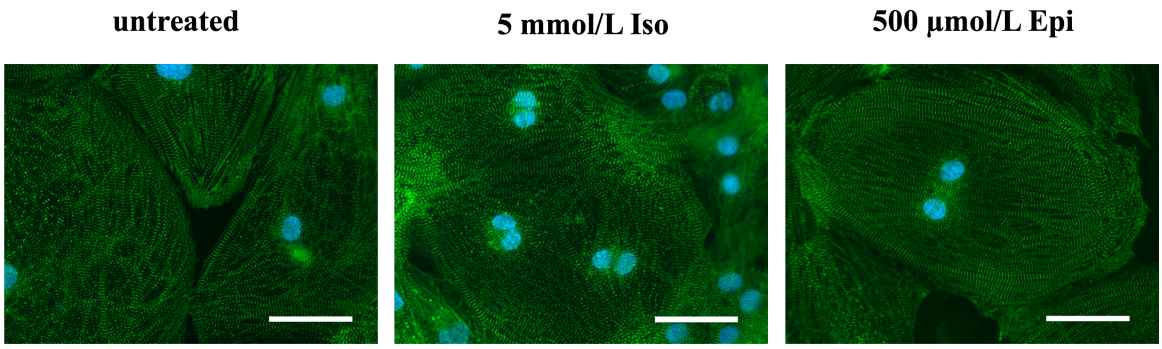

Figure 16. Immunostaining of TTS-hiPSC-CMs with or without catecholamine treatment.

Mature hiPSC-CMs of TTS patient 1 (1-TTS-2) were stained with an antibody against sarcomeric structure protein α-actinin (green). Neither treatment with 500 µmol/L Epi nor treatment with 5 mmol/L Iso showed an alteration of the sarcomeric structure compared to untreated TTS-hiPSC-CMs. Cell nuclei were stained with DAPI (blue). Scale bar: 50 µm.

3.6 Influence of catecholamine treatment on beta-adrenergic signaling

As NR4A1 belongs to the group of "orphan" nuclear receptors, the ligands controlling its activity have not yet been fully identified (Lanig et al. 2015). However, a number of previous publications have shown an increase of *NR4A1* expression after beta-adrenergic stimulation (Myers et al. 2009;

Söker and Godecke 2013; Grisanti et al. 2014). Having identified NR4A1 as an important early marker for stress induction in TTS-hiPSC-CMs, further examination of beta-adrenergic signaling in TTS- and control-hiPSC-CMs was required. One of the key players of this pathway is the PKA, whose activation can be measured using the phosphorylation status of its targets (**Fig. 2**). Therefore, phosphorylation of ryanodine receptor 2 at Serine 2808 (pRyR2-S2808) was analyzed via Western blot.

After treating control- and TTS-hiPSC-CMs with Epi (100 nmol/L, 500 µmol/L) and Iso (100 nmol/L, 5 mmol/L) for 2 hours, protein samples were taken for Western blot analysis. The samples were stained for RyR2 and pRyR2-S2808. After measuring the quantity of expressed protein using SuperSignal West Pico Chemiluminescent Substrate and a ChemiDoc MP Imaging System (Bio-Rad), phosphorylation at pRyR2-S2808 was normalized to RyR2 for each sample.

Both control- and TTS-hiPSC-CMs showed an increased phosphorylation of RyR2 at Serine 2808 for every tested catecholamine concentration **(Fig. 17A, B)**. Compared to untreated TTS-hiPSC-CMs, phosphorylation increased 3.3-fold to 6.4-fold after treatment with 100 nmol/L and 5 mmol/L Iso respectively. Control-hiPSC-CMs showed comparatively lower results as phosphorylation only increased 1.2-fold to 3.0-fold after Iso-treatment **(Fig. 17B)**. Quantity of phosphorylation after Epi-treatment provided similar results. PKA-dependent phosphorylation at S2808 increased 1.9-fold to 4.5-fold in TTS-hiPSC-CMs compared to untreated TTS-hiPSC-CMs, whereas control-hiPSC-CMs only showed a 1.2-fold to 1.3-fold increase of phosphorylation after treatment with 100 nmol/L and 500 µmol/L Epi. **(Fig. 17A)**.

Overall, phosphorylation of RyR2 at Serine 2808 and therefore PKA activity was elevated in both TTS- and control-hiPSC-CMs after catecholamine treatment. RyR2-phosphorylation was significantly higher in TTS-hiPSC-CMs compared to control-hiPSC-CMs after treatment with either 500 µmol/L Epi or 5 mmol/L Iso **(Fig. 17A, B)**.

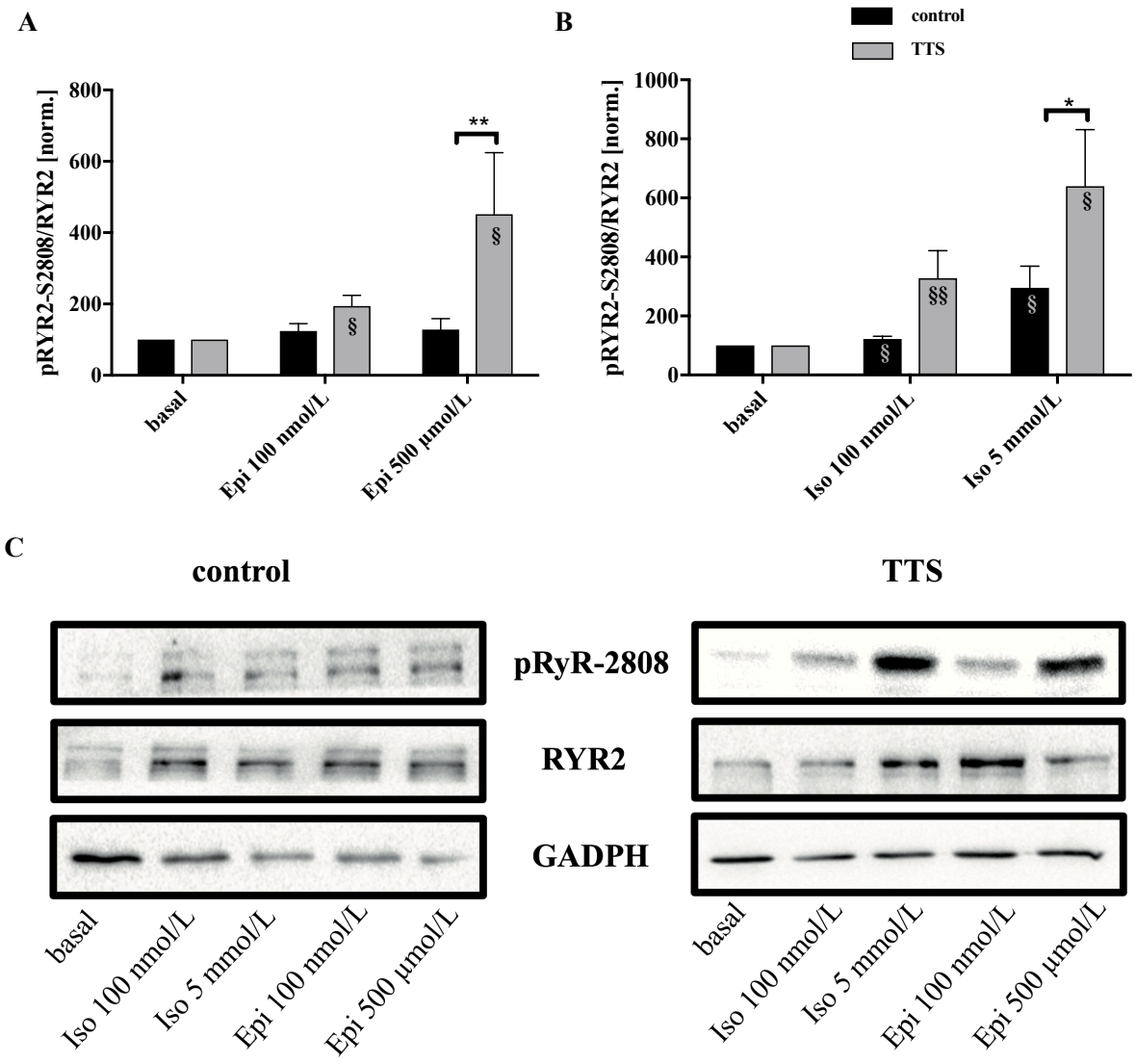

Figure 17. Phosphorylation of RyR2 at Serine 2808 in TTS- and control-hiPSC-CMs after catecholamine treatment.

TTS- and control-hiPSC-CMs were treated with Epi (100 nmol/l, 500 µmol/l) and Iso (100 nmol/l, 5 mmol/l) for 2 hours. The obtained protein samples were used for western blot analysis and stained with antibodies against RyR2 and pRyR2-S2808 **(C)**. After quantification, pRyR2-S2808 was normalized to RyR2 for each sample. Phosphorylation of RyR2 at Serine 2808 increased in both TTS- and control-hiPSC-CMs for every tested catecholamine concentration compared to untreated hiPSC-CMs in each case **(A, B)**. Phosphorylation increased significantly higher in TTS-hiPSC-CMs compared to control-hiPSC-CMs after treatment with 500 µmol/L Epi or 5 mmol/L Iso **(A, B)**. Control: n=7 differentiation experiments; TTS: n=7 differentiation experiments. Data is presented as mean±SEM of the ratio of normalized phosphorylated protein over total protein. * or § $p<0.05$; ** or §§ $p<0.01$; *** or §§§ $p<0.001$ significant differences by Multiple t-test and Sidak-Bonferroni method. §, significant differences of Iso/Epi-treated hiPSCM-CMs over basal conditions (analyzed via Student's t-test).

The prior experiments demonstrated an induction of beta-adrenergic signaling in TTS-hiPSC-CMs after catecholamine treatment via measurement of PKA activity using the phosphorylation status of its target RyR2. The extracellular signal-regulated kinase (ERK) is also known to be activated by β-adrenergic signaling-dependent phosphorylation (Yamazaki et al. 1997). Previous studies showed that ERK is involved in cardiac structural remodeling and that Epi treatment of human cardiomyocytes can lead to an increased ERK phosphorylation (Muslin 2008, d'Avenia et al. 2015). Therefore, TTS- and control-hiPSC-CMs were treated with Epi (100 nmol/L, 500 µmol/L) and Iso (100 nmol/L, 5 mmol/L) for 2 hours. The resulting protein samples were used for western blot analysis and stained with antibodies against ERK and pERK (see 2.1.4) **(Fig. 18)**. ERK was maximally phosphorylated in TTS-hiPSC-CMs after treatment with either 100 nmol/L Epi or Iso **(Fig. 18)**. However, higher catecholamine concentrations did not result in a further increase of ERK phosphorylation in TTS-hiPSC-CMs. In contrast, control-hiPSC-CMs rather showed a lowered ERK phosphorylation after catecholamine treatment (**Fig. 18**).

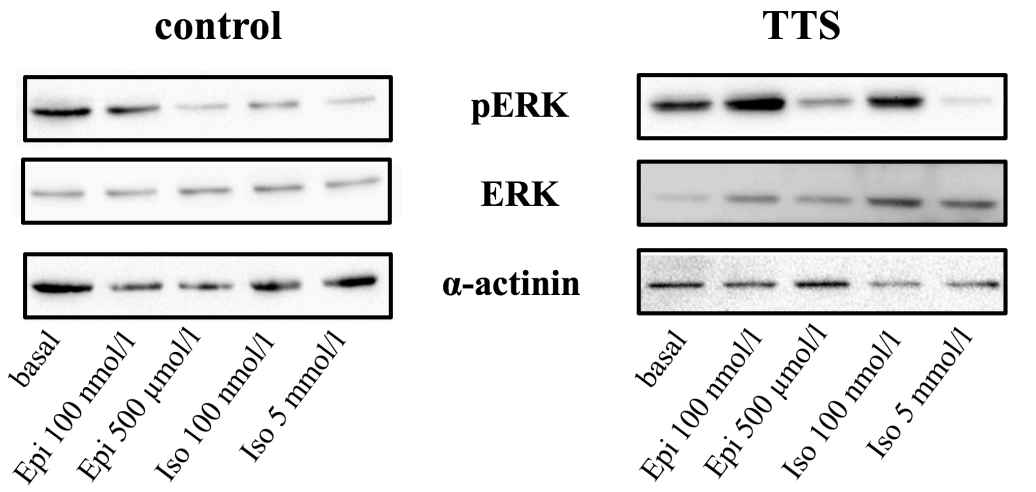

Figure 18. Phosphorylation of ERK in TTS- and control-hiPSC-CMs after catecholamine treatment.

TTS- and control-hiPSC-CMs were treated with Epi (100 nmol/L, 500 µmol/L) and Iso (100 nmol/L, 5 mmol/L) for 2 hours. The obtained protein samples were used for Western blot analysis and stained with antibodies against ERK and pERK. ERK was maximally phosphorylated in TTS-hiPSC-CMs after treatment with 100 nmol/L Epi or Iso. Control-hiPSC-CMs showed a lowered ERK phosphorylation compared to TTS-hiPSC-CMs. α-actinin was used as control.

3.7 Expression of possible NR4A1 targets after catecholamine treatment

After identification of NR4A1 as an important stress marker and knowing that NR4A1 expression increases after activation of beta-adrenergic signaling, further experiments concentrated on possible targets of NR4A1 and the influence of TTS on the metabolism, e.g. glucose utilization. One of the

pathways potentially affected by the increase in *NR4A1* expression is the hexosamine biosynthesis pathway, which is involved in posttranslational protein modification via glycosylation (Zraika et al. 2002). Glucosamine-fructose-6-phosphate aminotransferase isomerizing 1 (*GFAT1)* is the rate-determining enzyme of the hexosamine pathway and catalyses the synthesis of glucosamine-6-phosphate (Zhou et al. 1998). O-linked N-acetylglucosaminyltransferase *(OGT*) is also part of the hexosamine biosynthesis pathway and catalyzes protein glycosylation via transfer of N-acetylglucosamine to proteins (Bond and Hanover 2015). Expression of *GFAT* and *OGT* were analyzed via quantitative PCR. Therefore, control- and TTS-hiPSC-CMs were treated with Epi (100 nmol/L, 500 µmol/L) and Iso (100 nmol/L, 5 mmol/L) for 2 hours before the resulting mRNA samples were analyzed via quantitative PCR. Neither Epi (data not shown) nor Iso treatment led to a statistically significant increase or decrease of *OGT* or *GFAT1* expression in control- or TTS-hiPSC-CMs **(Fig. 19)**. Overall, stress induction via 2-hour catecholamine treatment did not influence mRNA expression of *GFAT1* and *OGT* in both TTS- and control-hiPSC-CMs.

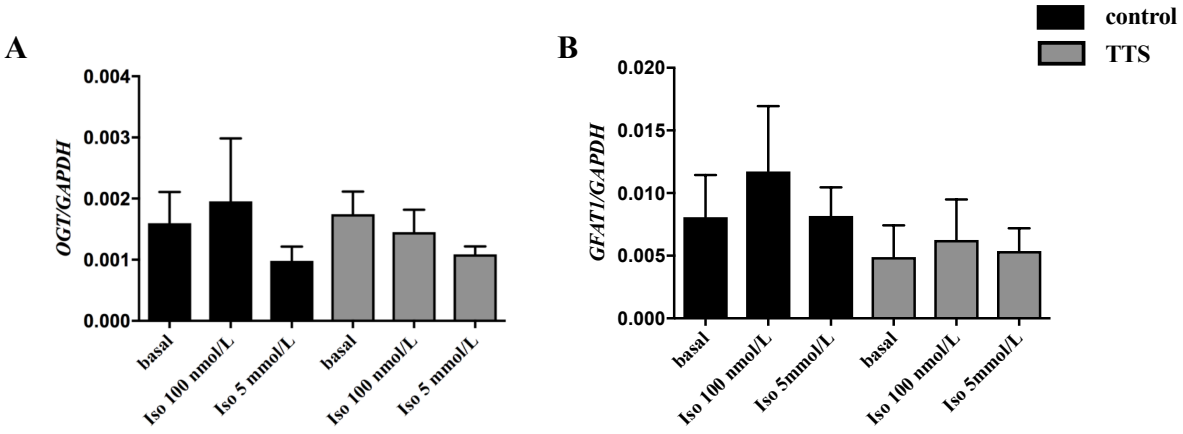

Figure 19. Expression of *GFAT1* and *OGT* after catecholamine treatment.

TTS- and control-hiPSC-CMs were treated with Iso (100 nmol/L, 5 mmol/L) and Epi (100 nmol/L, 500 µmol/L) for 2 hours. *OGT* **(A)** and *GFAT1* **(B)** expression were analyzed via quantitative PCR. Neither control- nor TTS-hiPSC-CMs showed a statistically significant increase or decrease of *OGT* or *GFAT1* expression after catecholamine treatment. *OGT* and *GFAT1* were normalized to *GAPDH*. Control: n=3 differentiation experiments of healthy control 1; TTS: n=3 differentiation experiments of 2 TTS patient. Mean±SEM, *p<0.05. One-way ANOVA was used to compare differences within each group (TTS, control).

4 Discussion

TTS is a heart disease first described in the early nineties, which is characterized by left ventricular dysfunction (Sato et al. 1990). It occurs predominantly in postmenopausal women, often after exposure to emotional or physical stress. In 2005, Wittstein and colleagues proposed high catecholamine concentrations as the primary cause of TTS (Wittstein et al. 2005). Several other hypotheses have been suggested along with a genetic predisposition (Ueyama et al. 2007, Kumar et al. 2010, Borchert et al. 2017). The aim of this thesis was the establishment of a catecholamine-dependent stress induction in TTS- and control-hiPSC-CMs to further explore TTS-specific stress markers as well as the phosphorylation status of PKA targets and the expression of NR4A1 targets after catecholamine treatment. Therefore, generated hiPSC lines from a TTS patient were successfully characterized to proof their pluripotency. Afterwards, the TTS-hiPSCs were directly differentiated into functional, beating CMs. Both TTS- and control-hiPSC-CMs were treated with different catecholamines in different concentrations for 2 or 20 hours and expression of potential cardiac stress markers was analyzed on mRNA level. *NPPA*, *NPPB* and *NR4A1* expression was significantly upregulated after catecholamine treatment, whereby *NR4A1* expression increased most impressively and statistically significantly higher in TTS-hiPSC-CMs compared to control-hiPSC-CMs after Iso-treatment. A short 2-hour catecholamine treatment was more effective in inducing stress in hiPSC-CMs than a long catecholamine treatment for 20 hours. Phosphorylation of RYR2 at Serine2808 was also statistically significantly higher in TTS- than control-hiPSC-CMs after treatment with 500 µmol/L Epi and 5 mmol/L Iso. ERK was maximally phosphorylated in TTS-hiPSC-CMs after treatment with 100 nmol/L Epi or Iso. Analysis of the expression of hexosamine biosynthesis pathway enzymes after catecholamine treatment showed no significant changes. Therefore, hiPSC-CMs from TTS patients are a feasible model to analyze the underlying mechanisms of TTS.

4.1 Successful generation of hiPSCs from TTS patients

In this study, semi-quantitative PCR confirmed the upregulated expression of *SOX2*, *OCT4*, *NANOG*, *LIN28*, *FOXD3* and *GDF3* on mRNA level in the two characterized hiPSC lines of TTS patient 1, while immunofluorescence staining additionally verified the expression of SOX2, OCT4, NANOG, LIN28, SSEA4 and TRA-1-60 on protein level **(Fig. 7)**. Early identification of the successful reprogramming was achieved via positive alkaline phosphatase stainings of the generated hiPSCs **(Fig. 6)**. The cultivated hiPSCs also showed a hESC-like morphology as the round cells formed flat, sharply defined round to polyangular colonies (depending on the form of cultivation). Overall, characterization of the two generated hiPSC lines of TTS patient 1 proved that the repro-

gramming of somatic cells into hiPSCs via introduction of pluripotency-related transcription factors had been successful.

The hiPSCs used during the work of this thesis were generated via Sendai virus or plasmid, which are both integration-free methods. No differences were observed between the plasmid- and Sendai virus-generated hiPSC lines during the hiPSC characterization or the followed experiments. As an additional control, an anonymized, previously published pluripotent cell line (iFB3) was used for experiments (Streckfuss-Bömeke et al. 2013). This cell line was generated with the STEMCCA lentivirus system, which combines all four initial factors (OCT4, SOX2, KLF4, C-MYC) in one "stem cell cassette" (Sommer et al. 2009). In contrast to plasmids or Sendai viruses, this is not an integration-free method as the lentivirus can randomly integrate into the host cell genome thereby altering transcription and potentially leading to gene function loss or oncogene activation (Okita et al. 2007, Medvedev et al. 2010). Although integration decreases as soon as the somatic cells turn into hiPSCs, the more elegant and effective integration-free methods are nowadays the preferred choice. No differences or anomalies were observed between the STEMCCA-generated iFB3 and the hiPSCs generated with integration-free methods (Sendai viruses, plasmids) during the work of this thesis and the conducted experiments.

The necessary reprogramming factors were introduced via the above-mentioned methods into the host cell genome, thereby leading to resumption of their expression and enabling the cell's return to a pluripotent state. Meanwhile, expression of somatic cell-specific genes is simultaneously suppressed (Boyer et al. 2005). The mechanism behind the reprogramming of human somatic cells into hiPSCs in its entirety is still being studied due to its complexity. The original set of transcription factors, also known as Yamanaka factors, included OCT4, SOX2, C-MYC and KLF4 (Takahashi et al. 2007). Due to their association with breast cancer and other human tumors (Pandya et al. 2004, Kuttler and Mai 2006) C-MYC and KLF4 were later replaced with the less carcinogenic transcription factors NANOG and LIN28 (Yu et al. 2007). Along with SOX2, OCT4 and NANOG, other pluripotency-related markers, such as LIN28, FOXD3, GDF3, TRA-1-60 and SSEA4 show an upregulated expression in undifferentiated pluripotent hESCs (Calloni et al. 2013).

The injection of hiPSCs into SCID mice led to teratoma formation, which is considered the hallmark of all pluripotent stem cells (Nelakanti et al. 2015). Light microscopy of the histological sections showed tissue of all three germ layers **(Fig. 9)** as the two analyzed cell lines of patient 1 expressed cartilage (mesoderm), intestinal tissue (endoderm) and neural rosettes (ectoderm). Apart from the successful spontaneous *in vivo* differentiation, TTS-hiPSCs also showed the same differentiation potential *in vitro* **(Fig. 8)**. Samples taken at three different time points showed that the spontaneously differentiated TTS-hiPSCs expressed markers for all three germ layers on mRNA and protein level. The hiPSC line 1-TTS-1 showed nearly no expression of endodermal markers (*AFP*, *ALB*) on mRNA levels. However, AFP expression was detectable on protein level and the

hiPSC of 1-TTS-1 were also able to differentiate *in vivo* into intestinal tissue, thereby proving that the hiPSC line 1-TTS-1 was able to differentiate into endoderm.

Whenever cells are cultivated for longer periods of time, there is a risk that this long-term cultivation might lead to an increase of chromosomal aberrations (International Stem Cell Initiative et al. 2011). These chromosomal aberrations could alter not only the hiPSC's differentiation ability but also the results of disease-specific experiments, especially if a genetic predisposition of the studied disease exists or is being discussed, as is the case here. In order to proof that long-term cultivated hiPSCs still possess a normal diploid karyotype, two hiPSC lines of TTS patient 1 (1-TTS-1 and 1-TTS-2) were cultivated for at least 25 passages and subsequently used for karyotyping as described above (see 2.2.5). The majority of analyzed TTS-hiPSCs presented a regular diploid karyotype without any apparent numerical chromosomal aberrations **(Fig. 10)**. Only a few analyzed samples (<5 %) showed a karyotype with 45 or 47 chromosomes. It is however very likely, that the majority of these observed numerical chromosomal aberrations are the product of chromosomal intermixture due to overlapping of the nuclei's content during application on the slide rather than actual chromosomal aberrations. Apart from that, it has to be noted that the performed karyotyping is unable to detect structural chromosomal aberrations, such as translocations, in the analyzed TTS-hiPSCs. For more precise results, elaborate methods such as fluorescence *in-situ* hybridization must be taken into consideration for future studies.

Overall, characterization of the two generated hiPSC lines of patient 1 confirmed their pluripotent state. The analyzed cell lines showed characteristics similar to hESCs and fulfilled the criteria of fully reprogrammed hiPSCs. In contrast to hESCs, cultivation of hiPSCs is less ethically problematic. HESCs are derived from the inner cell mass of a blastocyst, which would have formed the embryo in the further course of the embryogenesis (Thomson et al. 1998). In contrast, hiPSCs are generated from somatic cells, skin fibroblasts in the case of TTS patient 1.

4.2 Successful directed differentiation of hiPSCs into CMs

In order to study a cardiac disease such as TTS, hiPSCs needed to be differentiated into functional, mature CMs. Initially, hiPSC-CMs were generated via spontaneous differentiation protocols that resulted in EB formation. These three-dimensional aggregates differentiated into tissue of all three germ layers including CMs. However, this method was effortful and often inefficient due to the spontaneous aspect of the differentiation process (Zhang et al. 2009). Therefore, protocols for directed differentiation were developed that concentrated, among others, on the role of the wnt/β-catenin signaling pathway during human cardiac differentiation (Lian et al. 2012). As part of this work, hiPSCs were differentiated into CMs by applying a protocol published by Lian and colleagues in 2013 (Lian et al. 2013). HiPSCs were first treated with the GSK3-inhibitor CHIR99021

for two days and followed up by treatment with an IWP for another 48 hours. This induction and subsequent inhibition of the wnt/β-catenin signaling pathway differentiated hiPSCs into a two-dimensional monolayer of CMs. For the first 8 days, the differentiating hiPSC-CMs were cultivated in Cardio Differentiation Medium consisting of RPMI 1640 combined with recombinant human albumin and L-ascorbic acid 2-phosphate (Burridge et al. 2014). For the rest of the cultivation and maturation period, the hiPSC-CMs were cultivated in RPMI 1640 supplemented with B-27. Although this Cardio Culture Medium is more expensive and of animal origin, it is also more effective in terms of successful cardiac differentiation compared to Cardiac Differentiation Medium (Henze 2016). Previous experiences of the group of Dr. Streckfuß-Bömeke have shown that the combination of both media instead of exclusive use of just one medium achieved the best results. By applying a combination of both protocols, hiPSC-CMs were generated with about 85-95 % efficiency (data not shown). The high efficiency was also made possible through additional cardiac selection via temporary cultivation in a medium rich in lactate and deprived of glucose, which takes advantage of the CMs' ability to metabolize lactate and survive glucose deficiency compared to other cell types (Tohyama et al. 2013). The generated hiPSC-CMs expressed cardiac-specific markers, such as *α-MHC*, *β-MHC*, *cTNT* and the cardiac-specific α-actinin *ACTN2* on mRNA level **(Fig. 11A)**. The hiPSC-CMs also showed a positive immunostaining for sarcomeric-structure protein α-actinin, thereby confirming the success of the cardiac differentiation on protein level **(Fig. 11B)**. In addition, the immunostaining for α-actinin showed that the generated hiPSC-CMs possessed normally organized cross-striations. No differences were observed between the TTS- and control-hiPSCs or between cell lines generated with Sendai virus, plasmid or STEMCCA concerning their cardiac morphology, differentiation ability or efficiency. If differentiation efficiency differences were observed during the work of this thesis, they appeared randomly, even within the same hiPSC line, and could not be traced back to the reprogramming method, cell donor, original cell material (skin fibroblasts, perinuclear blood cells) or any other another conceivable variable. The generated hiPSC-CMs were cultivated for at least 2-3 months before the first experiments were performed, as previous studies have shown that longer cultivation periods significantly improved the maturation of the hiPSC-CMs (Lundy et al. 2013).

4.3 Generation of a humanized *in vitro* TTS-hiPSC-CMs model

As part of this work, TTS- and control-hiPSC-CMs were cultivated to induce a TTS event *in vitro* and develop a human patient-specific disease model to further study the pathophysiology of TTS. All TTS patients used during this work were females (age 62-70) with the apical type of ventricular dysfunction. Similar to the previously published animal *in vitro* models, TTS- and control-hiPSC-CMs were treated with high catecholamine concentrations to induce a TTS event.

The discovery of high catecholamine concentrations in the serum of TTS patients was the first breakthrough towards a better understanding of TTS. Based on this finding, different working groups were able to induce a TTS event via exposure to high catecholamine concentrations (Paur et al. 2012, Shao et al. 2013, Redfors et al. 2014). It is noticeable, that the majority of TTS disease models developed so far do not involve usage of human CMs. This is primarily due to the fact that human adult CMs are non-proliferative and difficult to cultivate.

Although animal disease models are generally able to induce a TTS event, no animal's physiology is identical to the human one. Animal disease models are also unable to explore patient-specific differences compared to healthy controls. However, these patient-specific differences play a key role in understanding the pathomechanism of diseases such as TTS, where a genetic predisposition has been suggested but the details are still unknown. In addition, screening for new potential drugs is also more reliable and promising when the cell source of the *in vitro* disease model is human and/or derived from an actual human patient.

HiPSC-CMs generated from TTS patients offer not only an endless source of human CMs (Lian et al. 2012), but also the possibility of a patient-specific disease model that takes into account the patient's genetic background and compares it to that of healthy controls. Usage of hiPSCs also doesn't lead to the ethical conflict the cultivation of hESCs entails.

4.3.1 Analysis of stress induction in hiPSC-CMs

During this work, we were able to show that treatment with high catecholamine concentrations led to stress induction in hiPSC-CMs. The level of stress in hiPSC-CMs was analyzed via expression of potential cardiac stress markers on mRNA levels. The first experiments of this work concentrated on ANP and BNP expression after catecholamine treatment, as elevated ANP and BNP concentrations had been observed in either a TTS disease model or in the serum of TTS patients (Ueyama 2004, Madhavan et al. 2009). *NPPB* expression in TTS- and control-hiPSC-CMs increased significantly after treatment with 500 µmol/L Epi. *NPPA* expression significantly increased upon treatment with 500 µmol/L Epi or 5 mmol/L Iso in control-hiPSC-CMs. However, catecholamine treatment of TTS-hiPSC-CMs did not result in a significant increase of *NPPA* expression **(Fig. 12)**. Compared to the later observed outstanding increase of *NR4A1* expression after catecholamine treatment, *NPPA* and *NPPB* expression fell below expectations. One of the reasons for the disparity between these results and the above-mentioned publications might be the hiPSC disease model itself. BNP secretion in the human hearts occurs in response to the stretching caused by high ventricular blood volumes and its serum concentration is therefore used to diagnose or assess heart failure (Vuolteenaho et al. 2005). It is likely, that the serum BNP elevation in TTS patients is a result of the left ventricular dysfunction and the resulting cardiac insufficiency. These complex correlations cannot be imitated by the hiPSC model used during this work and would require usage of an *in vivo* disease model. While hiPSC-CMs cultivated in multi-well plates allow the analysis of

the resulting cardiac insufficiency to a certain point, they cannot completely replace *in vivo* models so far.

In order to find new cardiac stress markers, transcriptome data were generated by NGS and revealed *NR4A1* as one of the most upregulated markers after catecholamine treatment in both TTS- and control-hiPSC-CMs **(Fig. 13)**. Semi-quantitative PCRs showed that *NR4A1* expression was highly elevated for every tested catecholamine concentration in both TTS- and control-hiPSC-CMs. Acute, short catecholamine treatment for 2 hours was more successful in inducing stress in hiPSC-CMs than long catecholamine treatment for 20 hours. This result is in line with other TTS *in vitro* disease models that were also able to induce a TTS event via short catecholamine treatment with similar catecholamines and concentrations (Paur et al. 2012, Shao et al. 2013). In accordance with the regressing ventricular dysfunction observed in TTS patients, hiPSC-CMs also showed a full recovery 3 weeks after catecholamine treatment **(Fig. 14)**.

The catecholamine-treated hiPSC-CMs showed a regular sarcomeric structure with normally organized cross-striations, thereby confirming that treatment with high catecholamine concentrations did not visibly alter the sarcomeric structure **(Fig. 16)**. In order to more accurately quantify the increase of *NR4A1* expression after catecholamine treatment, quantitative PCR was performed, which also showed highly increased *NR4A1* expression for every tested catecholamine concentration whereby Iso treatment led to a significantly higher upregulation of *NR4A1* in TTS-hiPSC-CMs than control-hiPSC-CMs **(Fig. 15)**. The strong increase of *NR4A1* after catecholamine treatment along with the significant differences between patient- and control-hiPSC-CMs suggest that NR4A1 might play a key role in further understanding the pathophysiology of the TTS.

NR4A1 is part of a group of highly conserved orphan nuclear receptors and has been known to be involved in various cellular stress events such as apoptosis (de Léséleuc and Denis 2006). It is still controversial, whether the increase of the transcriptional activity itself is sufficient for the pro-apoptotic effects of *NR4A1* or whether its translocation to the mitochondrium with the resulting release of cytochrome c is the decisive part (Cheng et al. 2011). Borchert and colleagues measured apoptosis in TTS- and control-hiPSCs after catecholamine treatment and did not observe a significant increase of apoptosis in both patient- and control-hiPSC-CMs (Borchert et al. 2017). Therefore, other pathways involving NR4A1 are probably of greater importance for the pathophysiology of the TTS. Studies have shown that the ligand-independent transcription factor also plays an important role in the lipid and glucose metabolism as it, among others, induces the expression of several genes involved in gluconeogenesis and lipolysis (Maxwell et al. 2005, Pei et al. 2006, Chao et al. 2007). A recent study showed elevated lipid accumulation in TTS-hiPSC-CMs after catecholamine treatment along with an increase of lipid transporter *CD36* (which transports fatty acids inside the cell) and a decrease of *CPT1C*, which not only transports fatty acids into mitochondria but also regulates beta-oxidation (Borchert et al. 2017). As the expression of *CD36* has, in addition, been shown to depend on *NR4A1* expression (Maxwell et al. 2005), these results suggest a contri-

bution of lipotoxicity to the TTS pathomechanism. However, further research is necessary to fortify this hypothesis and establish the possible mechanism behind the contribution of lipotoxicity to the TTS phenotype.

The significant differences in *NR4A1* expression observed in this study between patient- and control-hiPSC-CMs after Iso-treatment indicate an increased susceptibility of TTS-hiPSC-CMs to (isoprenaline-induced) stressful events. In line with this, Cheng and colleagues showed, that *NR4A1* expression, while decreasing after birth in postnatal mice cardiomyocytes, is upregulated following myocardial injury and pressure overload-induced hypertrophy. In addition, they identified NR4A1 as a contributor to cardiomyocyte apoptosis via its translocation to the mitochondrion in response to ischemia-reperfusion injury (Cheng et al. 2011). Our data are in line with a study of Yan and colleagues, in which *NR4A1* expression in the heart significantly increases after induction of β-adrenergic signaling (Yan et al. 2015). Induction of *NR4A1* might therefore serve to regulate glucose and lipid metabolism as a stress response to stressful situations. *NR4A1* overexpression has also been associated with a protective role concerning cardiac hypertrophy and dysfunction after Iso-treatment via inhibition of the NFATc3 (Nuclear factor of activated T-cells, cytoplasmic 3) and GATA4 (GATA-binding protein 4) transcriptional pathway (Yan et al. 2015). Therefore, NR4A1 should be considered as a therapeutic target in TTS as it might serve as an early stress sensor in TTS patients in the future.

4.3.2 Involvement of the β-adrenergic pathway in TTS

As mentioned above, NR4A1 is classified as an orphan nuclear receptor, meaning that its ligands have yet to be determined. However, previous publications have shown increased *NR4A1* expression after β-adrenergic stimulation (Myers et al. 2009; Söker and Godecke 2013; Grisanti et al. 2014). In order to further investigate the involvement of the β-adrenergic pathway in TTS, PKA-dependent RyR2-phosphorylation (at Serine 2808) in TTS- and control-hiPSC-CMs was measured via Western Blot. RyR2-phosphorylation and therefore PKA activity was elevated in both TTS- and control-hiPSC-CMs **(Fig. 17)**. In addition, RyR2-phosphorylation was significantly higher in TTS-hiPSC-CMs compared to control-hiPSC-CMs after treatment with either 500 µmol/L Epi or 5 mmol/L Iso, thereby suggesting β-adrenergic stimulation as a possible cause for the significantly higher *NR4A1* increase in TTS-hiPSC-CMs. The fact that catecholamine treatment also produced an increase of *NR4A1* expression and RyR2-phosphorylation in control-hiPSC-CMs (although not as significantly as in TTS-hiPSC-CMs) suggests that a TTS event might ultimately be inducible in every heart, whereby TTS patients are more likely affected due to their genetic predisposition.

Apart from the possible connection to NR4A1, β-adrenergic signaling has been in the focus of TTS research ever since Paur and colleagues published their theory of a G_s-G_i-switch of the β_2-adrenergic receptor in 2012 (Paur et al. 2012). Paur suggested, that the G_s-G_i-switch and the resulting cardiodepression function as a cardioprotective response to high catecholamine concentrations.

Their mouse model also revealed a β_2-gradient between apical and basal cardiomyocytes with higher β_2-adrenergic receptors and functional responses to catecholamine treatment in apical cardiomyocytes. This could be an explanation for the typically observed apical ballooning during a TTS event. Studies have shown that PKA and GRK phosphorylation of the β_2-adrenergic receptor enhance the receptor's coupling to G_i-proteins (Liu et al. 2009, Paur et al. 2012). In turn, L14Q polymorphism of GRK5 has been associated with TTS, which further underpins the hypothesis of a genetic predisposition in TTS patients (Spinelli et al. 2010).

The aspect of β-adrenergic signaling and its involvement in the pathophysiology of TTS is also of clinical relevance insofar as that beta-blockers are often part of the symptomatic treatment of a TTS event (Amsterdam et al. 2014). However, multiple cases of patients who developed TTS under beta-blocker treatment have been reported (Sharkey et al. 2010, Templin et al. 2015). In addition, Paur's TTS model showed an exacerbation of the catecholamine-induced negative inotropic effects under treatment with beta-blockers such as propranolol, which have additional β_2-agonistic effects (Paur et al. 2012). A large-scale study by Templin also revealed that treatment with beta-blockers was not associated with improved survival (Templin et al. 2015). Borchert and colleagues shed new light on the involvement of β-adrenergic signaling in the TTS pathomechanism as their experiments with β-adrenergic receptor blockers showed that the β_1- rather than the β_2-adrenergic receptor plays a greater role in the TTS system (Borchert et al. 2017).

4.3.3 ERK activation

ERK is an enzyme whose phosphorylation is known to dependent on beta-adrenergic signaling (Yamazki et al. 1997). Previous studies have shown that Epi treatment of human cardiomyocytes can lead to an increased ERK phosphorylation and that ERK is involved in cardiac remodeling (Muslin 2008, d'Avenia et al. 2015). In this study, ERK was maximally phosphorylated in TTS-hiPSC-CMs after treatment with 100 nmol/L Epi or Iso, whereas control-hiPSC-CMs showed a lowered ERK phosphorylation after catecholamine treatment **(Fig. 18)**. These findings are in line with data published by Jung and colleagues, who also observed a saturation of the ERK phosphorylation after treating hiPSC-CMs with 1 µmol/L isoprenaline (Jung et al. 2016). Further experiments are necessary to understand why higher catecholamine concentrations did not lead to a further increase of ERK phosphorylation and which role exactly ERK might play for the TTS pathomechanism.

4.3.4 Targets of NR4A1

After identifying NR4A1 as an important stress marker in TTS, subsequent experiments concentrated on possible targets of NR4A1. Against the background of NR4A1's involvement in glucose metabolism and β-adrenergic signaling, we analyzed two enzymes (GFAT1 and OGT) of the hexosamine biosynthesis pathway. It has been shown, that NR4A1-dependent activation of this path-

way negatively influences contractile function (Lehmann et al. 2018). The hexosamine biosynthesis pathway involves around posttranslational protein glycosylation (Zraika et al. 2002) and it has been suggested that GFAT activity is regulated by cAMP-dependent phosphorylation (Zhou et al. 1998; Schleicher and Weigert 2000). However, no significant differences were observed in *GFAT1* or *OGT* expression after catecholamine treatment in both TTS- and control-hiPSC-CMs **(Fig. 19)**. Although not statistically significant, Iso-treatment of TTS-hiPSC-CMs showed a downward trend of *OGT* expression. OGT catalyzes the addition of O-linked β-N-acetylglucosamine (O-GlcNAc) to serine or threonine residues. Different types of stress have been shown to induce *OGT* expression (Zachara et al. 2004), but the complex regulation of OGT is still largely unknown. However, high O-GlcNAc-levels have been attributed a cardioprotective effect (Jones et al. 2008), which leads to the suggestion that the above-mentioned decrease of *OGT* expression in TTS-hiPSC-CMs might contribute to the vulnerability of the TTS cardiomyocytes. Further research is necessary to determine whether and to which extent the hexosamine biosynthesis pathway is linked to the TTS pathomechanism.

Overall, these findings show significant differences between TTS- and control-hiPSC-CMs after catecholamine treatment and confirm the successful generation of a human *in vitro* disease model for TTS, thereby contributing to a better understanding of the potential TTS pathophysiology.

4.4 Limitations

During the work of this thesis, hiPSCs of four TTS patients and controls were treated with catecholamines and used for analysis. For even more reliable and representative results, additional hiPSC-CMs of patients and controls need to be analyzed to supplement the previous results. Alongside this additional number of experiments, an optimized selection and coordination of further TTS patients and controls might benefit the validity of the results. The TTS patients used during the work of this thesis were all females aged 60 to 72 years with the apical type of ventricular dysfunction. Although the healthy controls were females as well, they were either 25 or 52 years old and therefore significantly younger than the TTS patients. In addition, the age of the anonymous control iFB3 was unknown. For even more valid results, healthy controls with the same gender and age range as the TTS patients would be preferable if available. In order to consider the possible genetic background of the disease, healthy relatives of TTS patients fulfilling the aforementioned optimization of age and gender could be considered as ideal controls for further experiments.

The state of maturity of the cultivated hiPSC-CMs is another complex issue (Yang et al. 2014a; Jung et al. 2016), whose effect on the physiology of hiPSC-CMs is still mainly unknown. The hiPSC-CMs used for this thesis are less mature than those found in human adult hearts. Future research must ensure that expression and function of the studied signaling pathways in hiPSC-disease

models recapitulate human adult (patho)physiology, otherwise the collected data might lead to false conclusions.

During the work of this thesis, the influence of the catecholamine treatment on the sarcomeric structure was analyzed via immunostaining for the sarcomeric structure protein α-actinin. However, a fast Fourier transform analysis would have been more precise as it offers the possibility of a quantification and should therefore be considered for future experiments.

HiPSC lines generated from the same patient or control should produce nearly identical expression results as they are derived from the same origin. However, small differences have been noticed between the cell lines during the conducted analyses of this thesis. For example, different catecholamine-treated hiPSC lines of patient 1 did show small, random deviations for some of the used catecholamine concentrations. Therefore, further optimization of the cell culture is necessary to create as identical conditions as possible for all generated hiPSC-CMs so that differences in expression results will ultimately only be the product of the patient's own physiological and genetic background.

The *in vitro* disease model introduced in this thesis concentrated only on the use of hiPSC-CMs. However, it has been recognized, that the cause of TTS is probably multifactorial and involves a variety of components in a complex organ system rather than merely autonomous changes of CMs (see 1.2). Therefore, cultivation of hiPSCs into organoid cultures (Lancaster and Knoblich 2014) would be the next step towards an even more accurate *in vitro* disease model that concentrates on the creation of a tissue-like culture and as such includes different cell types rather than just one individual cell type (Borchert et al. 2017).

4.5 Future perspectives

The results of this study showed that hiPSC-CMs can serve as an *in vitro* disease model for studying the pathomechanism of TTS. Optimization and expansion of this *in vitro* disease model will be necessary in the future to produce even more valid results and to cover every aspect of the TTS pathophysiology. During this study, orphan nuclear receptor *NR4A1* showed a statistically significantly increased expression on mRNA level after catecholamine treatment. Further research concerning NR4A1 is necessary to fully establish its role in the pathophysiology of TTS and its potential as a future biomarker in daily clinical practice. Especially the analysis of NR4A1 targets offers a broad field of unknown possibilities and developments for future research.

The findings of this study showed that TTS-hiPSC-CMs are substantially different from control-hiPSC-CMs regarding catecholamine susceptibility and β-adrenergic signaling. Analysis of *NR4A1* expression and PKA-dependent RYR2-phosphorylation at Serine 2808 showed a significantly higher upregulation in TTS-hiPSC-CMs compared to control-hiPSC-CMs. These results indicate a

higher sensitivity of TTS-hiPSC-CMs to stressful events and suggest a possible genetic predisposition in TTS patients. The published SNPs in the cardiac genes *RBM20* and *CASQ2*, that were recently found in TTS patients (Borchert et al. 2017), as well as other already published SNPs concerning β-adrenergic receptors or GRK5 need to be thoroughly examined regarding their involvement in the TTS pathomechanism (Spinelli et al. 2010, Vriz et al. 2011). Further research is necessary to establish the extent of the genetic differences in TTS patients compared to healthy controls. In addition, the apical-basal gradient of β-adrenergic receptor density in the human heart still needs to be determined in order to further explore the role of the G_s-G_i-switch suggested by Paur and colleagues and its relevance for the pathophysiology of TTS.

Due to the high percentage of postmenopausal women among the TTS patients, lack of estrogen and its potential protective properties has been suggested as cause for TTS (Ueyama et al. 2003, Ueyama et al. 2007). Further research is necessary to understand the exact role of estrogen in the pathophysiology of TTS and to establish whether estrogen replacement therapy might even prevent or lessen the occurrence of TTS events. Here as well, TTS-hiPSC-CMs provide the unique opportunity to analyze the potential effects of estrogen with the use of a patient-specific *in vitro* disease model instead of the arduous and lengthy process of a clinical study. El-Battrawy and colleagues have already started this process with their publication about the protective effects of estradiol for isoprenaline-treated hiPSC-CMs on an electrophysiological level. Among others, estradiol prevented the prolongation of the action potential duration and weakened the enhancement of the late sodium current (El-Battrawy et al. 2018). Further research with hiPSC-CMs might illuminate additional aspects of the protective role of estrogen. This also applies to drug screening in search of an adequate medicamentous therapy. TTS therapy so far mainly consists of monitoring vital parameters and supportive care in form of heart failure medication (Amsterdam et al. 2014). With regards to the high rate of in-hospital complications (Templin et al. 2015), improvement of TTS therapy is urgently necessary and hiPSC-CMs could provide the necessary human *in vitro* model for these future experiments.

5 Summary

TTS is a cardiac disease characterized by left ventricular wall motion abnormalities, which occurs predominantly in postmenopausal women after exposure to physical or emotional stress. In 2005, Wittstein proposed high catecholamine concentrations as the main pathophysiological cause of TTS. This theory is supported by case reports of patients with pheochromocytoma or iatrogenic epinephrine overdose, who showed left ventricular dysfunction similar to TTS. However, various other hypotheses have been suggested and the pathophysiology of TTS is still not fully understood. Mutations in cardiac genes such as *RBM20* and the published familial cases of TTS indicate a genetic predisposition. The majority of TTS disease models published so far worked with animal cells and induced a TTS event via exposure to high catecholamine concentrations.

The aim of this thesis was to explore whether hiPSC-CMs from TTS patients can serve as a human *in vitro* disease model for TTS and to further study the pathophysiology of TTS. Therefore, generated hiPSC lines from a TTS patient were shown to be pluripotent by expression of pluripotency-related markers on mRNA and protein level, as well as spontaneous *in vivo* and *in vitro* differentiation. Afterwards, the TTS-hiPSCs were directly differentiated into functional, beating CMs that expressed cardiac specific markers on mRNA and protein level. Treatment with high catecholamine concentrations led to stress induction in TTS- and control-hiPSC-CMs. The level of stress in hiPSC-CMs was analyzed via expression of potential cardiac stress markers, whereby *NR4A1* showed the most impressive upregulation and also increased statistically significantly higher after Iso-treatment in TTS-hiPSC-CMs compared to control-hiPSC-CMs. Therefore, NR4A1 might serve as an early stress sensor in TTS patients in the future. A short 2-hour catecholamine treatment was more effective in inducing stress in hiPSC-CMs than a long catecholamine treatment for 20 hours. Similar to the regression of the ventricular dysfunction in TTS patients, hiPSC-CMs showed a full recovery 3 weeks after catecholamine treatment with *NR4A1* expression levels similar to those of untreated hiPSC-CMs. The analysis of the involvement of β-adrenergic signaling in the TTS pathomechanism showed an elevation of PKA-dependent RYR2-phosphorylation in both TTS- and control-hiPSC-CM after catecholamine treatment with significantly higher RYR2-phosphorylation in TTS-hiPSC-CMs after treatment with either 500 µmol/L Epi or 5 mmol/L Iso. ERK phosphorylation showed a saturation in TTS-hiPSC-CMs after treatment with 100 nmol/L Iso/Epi. Analysis of the expression of hexosamine biosynthesis pathway enzymes OGT and GFAT1 as targets of NR4A1 showed no significant changes.

Overall, these findings demonstrate significant differences between TTS- and control-hiPSC-CMs after catecholamine treatment and confirm that hiPSC-CMs can be used for the generation of a successful human *in vitro* disease model for TTS.

6 References

Abdelmoneim SS, Mankad SV, Bernier M, Dhoble A, Hagen ME, Ness SA, Chandrasekaran K, Pellikka PA, Oh JK, Mulvagh SL (2009): Microvascular function in Takotsubo cardiomyopathy with contrast echocardiography: prospective evaluation and review of literature. J Am Soc Echocardiogr 22 (11), 1249-1255

Ahmed KA, Madhavan M, Prasad A (2012): Brain natriuretic peptide in apical ballooning syndrome (Takotsubo/stress cardiomyopathy): comparison with acute myocardial infarction. Coron Artery Dis 23 (4), 259-264

Akashi YJ, Nakazawa K, Sakakibara M, Miyake F, Koike H, Sasaka K (2003): The clinical features of takotsubo cardiomyopathy. QJM 96 (8), 563-573

Akashi YJ, Tejima T, Sakurada H, Matsuda H, Suzuki K, Kawasaki K, Tsuchiya K, Hashimoto N, Musha H, Sakakibara M (2004): Left ventricular rupture associated with Takotsubo cardiomyopathy. Mayo Clin Proc 79 (6), 821-824

Akashi YJ, Goldstein DS, Barbaro G, Ueyama T (2008) Takotsubo cardiomyopathy: a new form of acute, reversible heart failure. Circulation 118 (25), 2754-2762

Amsterdam EA, Wenger NK, Brindis RG, Casey DE Jr, Graniats TG, Holmes DR Jr, Jaffe AS, Jneid H, Kelly RF, Kontos MC (2014): 2014 AHA/ACC Guideline for the Management of Patients with Non-ST-Elevation Acute Coronary Syndromes: a report of the American College of Cardiology/American Heart Association Task Force on Practice Guidelines. J Am Coll Cardiol 64 (24), e139-228

Anders MM, Comignani PD, Couce R, Prini N, Zerega AR, Santopinto M, Devetach G, Quinonez EG, Goldaracena N, McCormack L (2011): Takotsubo cardiomyopathy: a cardiac syndrome mimicking acute myocardial infarction in a liver transplant recipient. Cardiol Res 2 (2), 82-85

Banki N, Kopelnik A, Tung P, Lawton MT, Gress D, Drew B, Dae M, Foster E, Parmley W, Zaroff J (2006): Prospective analysis of prevalence, distribution, and rate of recovery of left ventricular systolic dysfunction in patients with subarachnoid hemorrhage. J Neurosurg 105 (1), 15-20

Bond MR, Hanover JA (2015): A little sugar goes a long way: The cell biology of O-GlcNAc. J Cell Biol 208 (7), 869-880

Borchert T, Hübscher D, Guessoum CI, Lam TD, Ghadri JR, Schellinger IN, Tiburcy M, Liaw NY, Li Y, Haas J (2017): Catecholamine-Dependent β-Adrenergic Signaling in a Pluripotent Stem Cell Model of Takotsubo Cardiomyopathy. J Am Coll Cardiol 70 (8), 975-991

Brouwers PJ, Wijdicks EF, Hasan D, Vermeulen M, Wever EF, Frericks H, van Gijn J (1989): Serial electrocardiographic recording in aneurysmal subarachnoid hemorrhage. Stroke 20 (9), 1162-1167

Brown KH, Trohman RG, Madias C (2015): Arrhythmias in takotsubo cardiomyopathy. Card Electrophysiol Clin 7 (2), 331-340

Burridge PW, Matsa E, Shukla P, Lin ZC, Churko JM, Ebert AD, Lan F, Diecke S, Huber B, Mordwinkin NM (2014): Chemically defined generation of human cardiomyocytes. Nat Methods 11 (8), 855-860

Bybee KA, Kara T, Prasad A, Lerman A, Barsness GW, Wright RS, RIhal CS (2004): Systematic review: transient left ventricular apical ballooning: a syndrome that mimics ST-segment evelation myocardial infarction. Ann Intern Med 141 (11), 858-865

Bybee KA, Motiei A, Syed IS, Kara T, Prasad A, Lennon RJ, Murphy JG, Hammill SC, Rihal CS, Wright RS (2007): Electrocardiography cannot reliably differentiate transient left ventricular apical ballooning syndrome from anterior ST-segment elevation myocardial infarction. J Electrocardiol 40 (1), e1-6

Calloni R, Cordero EA, Henriques JA, Bonatto D (2013): Reviewing and updating the major molecular markers for stem cells. Stem Cells Dev 22 (9), 1455-1476

Chao LC, Zhang Z, Pei L, Saito T, Tontonoz P, Pilch PF (2007): Nur77 coordinately regulates expression of genes linked to glucose metabolism in skeletal muscle. Mol Endocrinol 21 (9), 2152-2163

Chen G, Gulbranson DR, Hou Z, Bolin JM, Ruotti V, Probasco MD, Smuga-Otto K, Howden SE, Diol NR, Propson NE (2011): Chemically defined conditions for human iPSC derivation and culture. Nat Methods 8 (5), 424-429

Cheng Z, Völkers M, Din S, Avitabile D, Khan M, Gude N, mohsin S, Bo T, Truffa S, Alvarez R (2011): Mitochondrial translocation of Nur77 mediates cardiomyocyte apoptosis. Eur Heart J 32 (17), 2179-2188

Chesley A, Lundberg MS, Asai T, Xiao RP, Ohtani S, Lakatta EG, Crow MT (2000): The beta(2)-adrenergic receptor delivers an antiapoptotic signaling to cardiac myocytes through G(i)-dependent coupling to phosphatidylinositol 3'-kinase. Circ Res 87 (12), 1172-1179

Churko JM, Burridge PW, Wu JC (2013): Generation of human iPSCs fom human peripheral blood mononuclear cells using non-integrative Sendai virus in chemically defined conditions. Methods Mol Biol 1036, 81-88

d'Avenia M, Citro R, De Marco M, Veronese A, Rosati A, Visone R, Leptidis S, Philippen L, Vitale G, Cavallo A (2015): A novel miR-371a-5p-mediated pathway, leading to BAG3 upregulation in cardiomyocytes in response to epinephrine, is lost in Takotsubo cardiomyopathy. Cell Death Dis 6, e1948

de Léséleuc L, Denis F (2006): Inhibition of apoptosis by Nur77 through NF-kappaB activity modulation. Cell Death Differ 13 (2), 293-300

Deshmukh A, Kumar G, Pant S, Rihal C, Murugiah K, Mehta JL (2012): Prevalence of Takotsubo cardiomyopathy in the United States. Am Heart J 164 (1), 66-71

Desmet WJ, Adriaenssens BF, Dens JA (2003): Apical ballooning of the left ventricle: first series in white patients. Heart 89 (9), 1027-1031

Dick E, Rajamohan D, Ronksley J, Denning C (2010): Evaluating the utility of cardiomyocytes from human pluripotent stem cells for drug screening. Biochem Soc Trans 38 (4), 1037-1045

Diecke S, Lu J, Lee J, Termglinchan V, Kooreman NG, Burridge PW, Ebert AD, Churko JM, Sharma A, Kay MA (2015): Novel codon-optimized mini-intronic plasmid for efficient, inexpensive, and xeno-free induction of pluripotency. Sci Rep 5, 8081

Dote K, Sato H, Tateishi H, Uchida T, Ishihara M (1991): Myocardial stunning due to simultaneous multivessel coronary spasms: a review of 5 cases. J Cardiol 21 (2), 203-214

Dudek J, Cheng IF, Chowdhury A, Wozny K, Balleininger M, Reinhold R, Grunau S, Callegari S, Toischer K, Wanders RJ (2016): Cardiac-specific succinate dehydrogenase deficiency in Barth syndrome. EMBO Mol Med 8 (2), 139-154

El-Battrawy I, Zhao Z, Lan H, Schünemann JD, Sattler K, Buljubasic F, Patocskai B, Li X, Yücel G, Lang S (2018): Estradiol protection against toxic effects of catecholamine on electrical properties in human-induced pluripotent stem cell derived cardiomyocytes. Int J Cardiol 254, 195-202

Elesber A, Lerman A, Bybee KA, Murphy JG, Barsness G, Singh M, Rihal CS, Prasad A (2006): Myocardial perfusion in apical ballooning syndrome correlate of myocardial injury. Am Heart J 152 (3), e9-13

Elesber AA, Prasad A, Lennon RJ, Wright RS, Lerman A, Rihal CS (2007): Four-year recurrence rate and prognosis of the apical ballooning syndrome. J Am Coll Cardiol 50 (5), 448-452

Ellison GM, Torella D, Karakikes I, Purushothaman S, Curcio A, Gasparri C, Indolfi C, Cable NT, Goldspink DF, Nadal-Ginard B (2007): Acute β-adrenergic overload produces myocyte damage through calcium leakage from the ryanodine receptor 2 but spares cardiac stem cells. J Biol Chem 282 (15), 11397–11409

Fatima A, Yu G, Shao K, Papadopoulos S, Lehmann M, Arnáiz-Cot JJ Rosa AO, Nguemo F, Matzkies M, Dittmann S (2011): In vitro modeling of ryanodine receptor 2 dysfunction using human induced pluripotent stem cells. Cell Physiol Biochem 28 (4), 579-592

Feaster TK, Cadar AG, Wang L, Williams CH, Chun YW, Hempel JE, Bloodworth N, Merryman WD, Lim CC, Wu JC (2015): Matrigel mattress: a method for the generation of single contracting human-induced pluripotent stem cell-derived cardiomyocytes. Circ Res 117 (12), 995-1000

Frangieh AH, Obeid S, Ghadri JR, Imori Y, D'Ascenzo F, Kovac M, Ruschitzka F, Lüscher TF, Duru F, Templin C (2016): ECG Criteria to Differentiate Between Takotsubo (Stress) Cardiomyopathy and Myocardial Infarction. J Am Heart Assoc 5 (6), e003418

Fujikura J, Nakao K, Sone M, Noguchi M, Mori E, Naito M, Taura D, Harada-Shiba M, Kishimoto I, Watanabe A (2012): Induced pluripotent stem cells generated from diabetic patients with mitochondrial DNA A3243G mutation. Diabetologia 55 (6), 1689-1698

Fusaki N, Ban H, Nishiyama A, Saeki K, Hasegawa M (2009): Efficient induction of transgene-free human pluripotent stem cells using a vector based on Sendai virus, an RNA virus that does not integrate into the host genome. Proc Jpn Acad Ser B Phys Biol Sci 85 (8), 348-362

Galiuto L, De Caterina AR, Porfidia A, Paraggio L, Barchetta S, Locorotondo G, Rebuzzi AG, Crea F (2010): Reversible coronary microvascular dysfunction: a common pathogenetic mechanism in Apical Ballooning or Tako-Tsubo Syndrome. Eur Heart J 31 (11), 1319-1327

Ghasemi-Dehkordi P, Allahbakhshian-Farsani M, Abdian N, Mirzaeian A, Saffari-Chaleshtori J, Heybati F, Mardani G, Karimi-Taghanaki A, Doosti A, Jami MS (2015): Comparison between the cultures of human induced pluripotent stem cells (hiPSCs) on feeder- and serum-free system (Matrigel matrix), MEF and HDF feeder cell lines. J Cell Commun Signal 9 (3), 233-246

Gherghiceanu M, Barad L, Novak A, Reiter I, Itskovitz-Eldor J, Binah O, Popescu LM (2011): Cardiomyocytes derived from human embryonic and induced pluripotent stem cells: comparative ultrastructure. J Cell Mol Med 15 (11), 2539-2551

Gianni M, Dentali F, Grandi AM, Sumner G, Hiralal R, Lonn E (2006): Apical ballooning syndrome or takotsubo cardiomyopathy: a systematic review. Eur Heart J 27 (13), 1523-1529

Grisanti LA, Talarico JA, Carter RL, Yu JE, Repas AA, Radcliffe SW, Tang HA, Makarewich CA, Houser SR, Tilley DG (2014): Adrenergic receptor-mediated transactivation of epidermal growth factor receptor decreases cardiomyocyte apoptosis through differential subcellular activation of ERK1/2 and Akt. J Mol Cell Cardiol 72, 39-51

Guglin M, Notovorova I (2011): Neurogenic stunned myocardium and takotsubo cardiomyopathy are the same syndrome: a pooled analysis. Congest Heart Fail 17 (3), 127-132

Gunaseeli I, Doss MX, Antzelevitch C, Hescheler J, Sachinidis A (2010): Induced pluripotent stem cells as a model for accelerated patient- and disease-specific drug discovery. Curr Med Chem 17 (8), 759-766

Henze S: Induced pluripotent stem cell-derived cardiomyocytes as model for studying CPVT caused by mutations in RYR2. Naturwiss.Diss. Göttingen 2016

Heubach JF, Ravens U, Kaumann AJ (2004): Epinephrine activates both Gs and Gi pathways, but norepinephrine activates only the Gs pathway through human beta2-adrenoceptors overexpressed in mouse heart. Mol Pharmacol 65 (5), 1313-1322

Hochedlinger K, Yamada Y, Beard C, Jaenisch R (2005): Ectopic expression of Oct-4 blocks progenitor-cell differentiation and causes dysplasia in epithelial tissues. Cell 121 (3), 465-477

Hoffmann C, Leitz MR, Oberdorf-Maass S, Lohse MJ, Klotz KN (2004): Comparative pharmacology of human beta-adrenergic receptor subtypes – characterization of stably transfected receptors in CHO cells. Naunyn Schmiedebergs Arch Pharmacol 369 (2), 151-159

International Stem Cell Initiative, Amps K, Andrews PW, Anyfantis G, Armstrong L, Avery S, Baharvand H, Baker J, Baker D, Munoz MB (2011): Screening ethnically diverse human embryonic stem cells identifies a chromosome 20 minimal aplicon conferring growth advantage. Nat Biotechnol 29 (12), 1132-1144

Itskovitz-Eldor J, Schuldiner M, Karsenti D, Eden A, Yanuka O, Amit M, Soreq H, Benvenisty N (2000): Differentiation of human embryonic stem cells into embryoid bodies comprising the three embryonic germ layers. Mol Med 6 (2), 88-95

Jaguszweski M, Osipova J, Ghadri JR, Napp LC, Widera C, Franke J, Fijalkowski M, Novak R, Fijalkowska M, Volkmann I (2014): A signature of circulating microRNAs differentiates takotsubo cardiomyopathy from acute myocardial infarction. Eur Heart J 35 (15), 999-1006

Jones SP, Zachara NE, Ngoh GA, Hill BG, Teshima Y, Bhatnagar A, Hart GW, Marbán E (2008): Cardioprotection by N-acetylglucosamine linkage to cellular proteins. Circulation 117 (9), 1172-1182

Jung G, Fajardo G, Ribeiro AJ, Kooiker KB, Coronado M, Zhao M, Hu DQ, Reddy S, Kodo K, Sriram K (2016): Time dependent evolution of functional vs remodeling signaling in induced pluripotent stem cell-derived cardiomyocytes and induced maturation with biomechanical stimulation. FASEB J 30 (4), 1464-1479

Kadota S, Pabon L, Reinecke H, Murry CE (2017): In vivo maturation of human induced pluripotent stem cell-derived cardiomyocytes in neonatal and adult rat hearts. Stem Cell Reports 8 (2), 278-289

Katsuura S, Kuwano Y, Yamagishi N, Kurokawa K, Kajita K, Akaike Y, Nishida K, Masuda K, Tanahashi T, Rokutan K (2012): MicroRNAs miR-144/144* and miR-16 in peripheral blood are potential biomarkers for naturalistic stress in healthy Japanese medical students. Neurosci Lett 516 (1), 79-84

Kawahara E, Ikeda S, Miyahara Y, Kohno S (2003): Role of autonomic nervous dysfunction in electrocardiographic abnormalities and cardiac injury in patients with acute subarachnoid hemorrhage. Circ J 67 (9), 753-756

Kim D, Kim CH, Moon JI, Chung YG, Chang MY, Han BS, Ko S, Yang E, Cha KY, Lanza R, Kim KS (2009): Generation of human induced pluripotent stem cells by direct delivery of reprogramming proteins. Cell Stem Cell 4 (6), 472-476

Kogut I, Roop DR, Bilousova G (2014): Differentiation of human induced pluripotent stem cells into a keratinocyte lineage. Methods Mol Biol 1195, 1-12

Komamura K, Fukui M, Iwasaku T, Hirotani S, Masuyama T (2014): Takotsubo cardiomyopathy: Pathophysiology, diagnosis and treatment. World J Cardiol 6 (7), 602-609

Kumar G, Holmes DR Jr, Prasad A (2010): "Familial" apical ballooning syndrome (Takotsubo cardiomyopathy). Int J Cardiol 144 (3), 444-445

Kume T, Akasaka T, Kawamoto T, Yoshitani H, Watanabe N, Neishi Y, Wada N, Yoshida K (2005): Assessment of coronary microcirculation in patients with tako-tsubo-like left ventricular dysfunction. Circ J 69 (8), 934-939

Kuo BT, Choubey R, Novaro GM (2010): Reduced estrogen in menopause may predispose women to takotsubo cardiomyopathy. Gend Med 7 (1), 71-77

Kurisu S, Sato H, Kawagoe T, Ishihara M, Shimatani Y, Nishioka K, Kono Y, Umemura T, Nakamura S (2002): Tako-tsubo-like left ventricular dysfunction with ST-segment elevation: a novel cardiac syndrome mimicking acute myocardial infarction. Am Heart J 143 (3), 448-455

Kurisu S, Inoue I, Kawagoe T, Ishihara M, Shimantani Y, Nakama Y, Maruhashi T, Kagawa E, Dai K (2011): Incidence and treatment of left ventricular apical thrombosis in Tako-tsubo cardiomyopathy. Int J Cardiol 146 (3), e58-60

Kuttler F, Mai S (2006): c-Myc, genomic instability and disease. Genome Dyn 1, 171-190

Löffler G: Basiswissen Biochemie mit Pathobiochemie. 7. Auflage; Springer Medizin Verlag, Heidelberg 2008

Laflamme MA, Chen KY, Naumova AV, Muskheli V, Fugate JA, Dupras SK, Reinecke H, Xu C, Hassanipour M, Police S (2007): Cardiomyocytes derived from human embryonic stem cells in pro-survival factors enhance function of infarcted rat hearts. Nat Biotechnol 25 (9), 1015-1024

Lan F, Lee AS, Liang P, Sanchez-Freire V, Nguyen PK, Wang L, Han L, Yen M, Wang Y, Sun N (2013): Abnormal calcium handling properties underlie familial hypertrophic cardiomyopathy pathology in patient-specific induced pluripotent stem cells. Cell Stem Cell 12 (1), 101-113

Lancaster MA, Knoblich JA (2014): Generation of cerebral organoids from human pluripotent stem cells. Nat Protoc 9 (10), 2329-2340

Lanig H, Reisen F, Whitley D, Schneider G, Banting L, Clark T (2015): In silico adoption of an orphan nuclear receptor NR4A1. PLoS One 10 (8), e0135246

Lehmann LH, Jebessa ZH, Kreusser MM, Horsch A, He T, Kronlage M, Dewenter M, Sramek V, Oehl U, Krebs-Haupenthal J (2018): A proteolytic fragment of histone deacetylase 4 protects the heart from failure by regulating the hexosamine biosynthetic pathway. Nat Med 24 (1), 62-72

Lian X, Hsiao C, Wilson G, Zhu K, Hazeltine LB, Azarin SM, Raval KK, Zhang J, Kamp TJ, Palecek SP (2012): Robust cardiomyocyte differentiation from human pluripotent stem cells via temporal modulation of canonical Wnt signaling. Proc Natl Acad Sci U S A 109 (27), 1848-1857

Lian X, Zhang J, Azarin SM, Zhu K, Hazeltine LB, Bao X, Hsiao C, Kamp TJ, Palecek SP (2013): Directed cardiomyocyte differentiation from human pluripotent stem cells by modulating Wnt/β-catenin signaling under fully defined conditions. Nat Protoc 8 (1), 162-175

Liang P, Lan F, Lee AS, Gong T, Sanchez-Freire V, Wang Y, Diecke S, Sallam K, Knowles JW, Wang PJ (2013): Drug screening using a library of human induced pluripotent stem cell-derived cardiomyocytes reveals disease-specific patterns of cardiotoxicity. Circulation 127 (16), 1677-1691

Liang P, Sallam K, Wu H, Li Y, Itzhaki I, Garg P, Zhang Y, Vermglinchan V, Lan F, Gu M (2016): Patient-specific and genome-edited induced pluripotent stem cell-derived cardiomyocytes elucidate single-cell phenotype of brugada syndrome. J Am Coll Cardiol 68 (19), 2086-2096

Liu R, Ramani B, Soto D, De Arcangelis V, Xiang Y (2009): Agonist dose-dependent phosphorylation by protein kinase A and G protein-coupled receptor kinase regulates beta2-adrenoceptor coupling to G(i) proteins in cardiomyocytes. J Biol Chem 284 (47), 32279-32287

Litvinov IV, Kotowycz MA, Wassmann S (2009): Iatrogenic epinephrine-induced reverse Takotsubo cardiomyopathy: direct evidence supporting the role of catecholamines in the pathophysiology of the "broken heart syndrome". Clin Res Cardiol 98 (7), 457-462

Lundy SD, Zhu WZ, Regnier M, Laflamme MA (2013): Structural and functional maturation of cardiomyocytes derived from human pluripotent stem cells. Stem Cells Dev 22 (14), 1991-2002

Lyon AR, Rees PS, Prasad S, Poole-Wilson PA, Harding SE (2008): Stress (Takotsubo) cardiomyopathy - a novel pathophysiological hypothesis to explain catecholamine-induced acute mycoardial stunning. Nat Clin Pract Cardiovasc Med 5 (1), 22-29

Lyon AR, Bossone E, Schneider B, Sechtem U, Citro R, Underwood SR, Sheppard MN, Figtree GA, Parodi G, Akashi YJ (2016): Current state of knowledge on Takotsubo syndrome: a position statement from the taskforce on Takotsubo syndrome of the Heart Failure Association of the European Society of Cardiology. Eur J Heart Fail 18 (1), 8-27

M Lee Y, Zampieri BL, Scott-McKean JJ, Johnson MW, Costa ACS (2017): Generation of integration-free induced pluripotent stem cells from urine-derived cells isolated from individuals with Down syndrome. Stem Cells Transl Med 6 (6), 1465-1476

Madhavan M, Borlaug BA, Lerman A, Rihal CS, Prasad A (2009): Stress hormone and circulating biomarker profile of apical ballooning syndrome (Takotsubo cardiomyopathy): insights into the clinical significance of B-type natriuretic peptide and troponin levels. Heart 95 (17), 1436-1441

Marcovitz PA, Czako P, Rosenblatt S, Billecke SS (2010): Pheochromocytoma presenting with Takotsubo syndrome. J Interv Cardiol 23 (5), 437-442

Mátrai J, Chuah MKL, VandenDriessche T (2010): Recent advances in lentiviral vector development and application. Mol Ther 18 (3), 477-490

Maxwell MA, Cleasby ME, Harding A, Stark A, Cooney GJ, Muscat GE (2005): Nur77 regulates lipolysis in skeletal muscle cells. Evidence for cross-talk between the beta-adrenergic and an orphan nuclear hormone receptor pathyway. J Biol Chem 280 (13), 12573-12584

Medvedev SP, Shevchenko AI, Zakian SM (2010): Induced pluripotent stem cells: problems and advantages when applying them in regenerative medicine. Acta Naturae 2 (2), 18-27

Medzikovic L, Schumacher CA, Verkerk AO, van Deel ED, Wolswinkel R, van der Made I, Bleeker N, Cakici D, van den Hoogenhof MM, Meggouh F (2015): Orphan nuclear receptor Nur77 affects cardiomyocyte calcium homeostasis and adverse cardiac remodelling. Sci Rep 5, 15404

Miller JD, Ganat YM, Kishinevsky S, Bowman RL, Liu B, Tu EY, Mandal P, Vera E, Shim J, Kriks S (2013): Human iPSC-based modeling of late-onset disease via progerin-induced aging. Cell Stem Cell 13 (6), 691-705

Mori H, Ishikawa S, Kojima S, Hayashi J, Watanabe Y, Hoffmann JI, Okino H (1993): Increased responsiveness of left ventricular apical myocardium to adrenergic stimuli. Cardiovasc Res 27 (2), 192-198

Movahed A, Reeves WC, Mehta PM, Gilliland MG, Mozingo SL, Jolly SR (1994): Norepinephrine-induced left ventricular dysfunction in anesthetized and conscious, sedated dogs. Int J Cardiol 45 (1), 23-33

Mummery CL, Zhang J, Ng ES, Elliott DA, Elefanty AG, Kamp TJ (2012): Differentiation of human embryonic stem cells and induced pluripotent stem cells to cardiomyocytes: a methods overview. Cir Res 111 (3), 344-358

Muslin AJ (2008): MAPK signaling in cardiovascular health and disease: molecular mechanisms and therapeutic targets. Cli Sci (Lond) 115 (7), 203-218

Myers SA, Eriksson N, Burow R, Wang SC, Muscat GE (2009): Beta-adrenergic signaling regulates NR4A nuclear receptor and metabolic gene expression in multiple tissues. Mol Cell Endocrinol 309 (1-2), 101-108

Nelakanti RV, Kooreman NG, Wu JC (2015): Teratoma formation: a tool for monitoring pluripotency in stem cell research. Curr Protoc Stem Cell Biol 32, 1-17

Okita K, Ichisaka T, Yamanaka S (2007): Generation of germline-competent induced pluripotent stem cells. Nature 448 (7151), 313-317

Okita K, Matsumura Y, Sato Y, Okada A, Morizane A, Okamoto S, Hong H, Nakagawa M, Tanabe K, Tezuka K (2011): A more efficient method to generate integration-free human iPS cells. Nat Methods 8 (5), 409-412

Paige SL, Osugi T, Afanasiev OK, Pabon L, Reinecke H, Murry CE (2010): Endogenous Wnt/beta-catenin signaling is required for cardiac differentiation in human embryonic stem cells. PLoS One 5 (6), 11134

Pandya AY, Talley LI, Frost AR, Fitzgerald TJ, Trivedi V, Chakravarthy M, Chhieng DC, Grizzle WE, Engler JA, Krontiras H (2004): Nuclear localization of KLF4 is associated with an aggressive phenotype in early-stage breast cancer. Clin Cancer Res 10 (8), 2709-2719

Park ET, Gum JR, Kakar S, Kwon SW, Deng G, Kim YS (2008): Aberrant expression of SOX2 upregulates MUC5AC gastric foveolar mucin in mucinous cancers of the colorectum and related lesions. Int J Cancer 122 (6), 1253-1260

Paur H, Wright PT, Sikkel MB, Tranter MH, Mansfield C, O'Gara P, Stuckey DJ, Nikolaev VO, Diakonov I, Pannell L (2012): High levels of circulating epinephrine trigger apical cardiodepression in a beta2-adrenergic receptor/Gi-dependent manner: a new model of Takotsubo cardiomyopathy. Circulation 126 (6), 697-706

Pavin D, Le Breton H, Daubert C (1997): Human stress cardiomyopathy mimicking acute myocardial syndrome. Heart 78 (5), 509-511

Pei L, Waki H, Vaitheesvaran B, Wilpitz DC, Kurland IJ, Tontonoz P (2006): NR4A orphan nuclear receptors are transcriptional regulators of hepatic glucose metabolism. Nat Med 12 (9), 1048-1055

Pison L, De Vusser P, Mullens W (2004): Apical ballooning in relatives. Heart 90 (12), e67

Pollick C, Cujec B, Parker S, Tator C (1988): Left ventricular wall motion abnormalities in subarachnoid hemorrhage: an echocardiographic study. J Am Coll Cardiol 12 (3), 600-605

Prasad A, Lerman A, Rihal CS (2008): Apical ballooning syndrome (Tako-Tsubo or stress cardiomyopathy): a mimic of acute myocardial infarction. Am Heart J 155 (3), 408-417

Ramaraj R, Sorrell VL, Movahed MR (2009): Levels of troponin release can aid in the early exclusion of stress-induced (takotsubo) cardiomyopathy. Exp Clin Cardiol 14 (1), 6-8

Redfors B, Ali A, Shao Y, Lundgren J, Gan LM, Omerovic E (2014): Different catecholamines induce different patterns of takotsubo-like cardiac dysfunction in an apparently afterload dependent manner. Int J Cardiol 174 (2), 330-336

Reichenbach DD, Benditt EP (1970): Catecholamines and cardiomyopathy: the pathogenesis and potential importance of myofibrillar degeneration. Hum Pathol 1, 125-150

Rinaldi A, Vincenti S, De Vito F, Bozoni I, Oliverio A, Presutti C, Fragapane P, Mele A (2010): Stress induces region specific alterations in microRNAs expression in mice. Behav Brain Res 208 (1), 265-269

Rodin S, Domogatskaya A, Ström S, Hansson EM, Chien KR, Inzunza J, Hovatta O, Tryggvason K (2010): Long-term self-renewal of human pluripotent stem cells on human recombinant laminin-511. Nat Biotechnol 28 (6), 611-615

Roshanzamir S, Showkathali R (2013): Takotsubo cardiomyopathy a short review. Curr Cardiol Rev 9 (3), 191-196

Samuels MA (2007): The brain-heart connection. Circulation 116 (1), 77-84

Sankri-Tarbichi AG, Mathew PK, Matos M, Hsi D (2007): Stress-related cardiomyopathy. Heart Lung 36 (1), 43-46

Sato H, Tateishi H, Uchida T: Takotsubo-type cardiomyopathy due to multivessel spasm. In: Kodoma K, Haze K, Hon M (Hrsg.): Clinical aspect of myocardial injury: from ischemia to heart failure. Kagakuhyoronsya Publishing, Tokyo 1990, 56-64

Schleicher ED, Weigert C (2000): Role of the hexosamine biosynthetic pathway in diabetic nephropathy. Kidney Int Suppl 77, 13-18

Shao Y, Redfors B, Ståhlman M, Täng MS, Miljanovic A, Möllmann H, Troidl C, Szardien S, Hamm C, Nef H (2013): A mouse model reveals an important role for catecholamine-induced lipotoxicity in the pathogenesis of stress-induced cardiomyopathy. Eur J Heart Fail 15 (1), 9-22

Sharkey SW, Windenburg DC, Lesser JR, Maron MS, Hauser RG, Lesser JN, Haas TS, Hodges JS, Maron BJ (2010): Natural history and expansive clinical profile of stress (tako-subo) cardiomyopathy. J Am Coll Cardiol 55 (4), 333-341

Sharkey SW, Lesser JR, Maron MS, Maron BJ (2011): Why not just call it tako-tsubo cardiomyopathy: a discussion of nomenclature. J Am Coll Cardiol 57 (13), 1496-1497

Shimizu M, Kagawa A, Takano T, Masai H, Miwa Y (2008): Neurogenic stunned myocardium associated with status epileptics and postictal catecholamine surge. Intern Med 47 (4), 269-273

Soares-Filho GL, Felix RC, Azevedo JC, Mesquita CT, Mesquita ET, Valença AM, Nardi AE (2010): Broken heart or takotsubo syndrome: support for the neurohumoral hypothesis of stress cardiomyopathy. Prog Neuropsychopharmacol Biol Psychiatry 34 (1), 247-249

Söker T, Godecke A (2013): Expression of the murine Nr4a1 gene is controlled by three distinct genomic loci. Gene 512 (2), 517-520

Sommer CA, Stadtfeld M, Murphy GJ, Hochedlinger K, Kotton DN, Mostoslavsky G (2009): IPS cell generation using a single lentiviral stem cell cassette. Stem Cells 27 (3), 543-549

Song BG, Chun WJ, Park YH, Kang GH, Oh J, Lee SC, Park SW, Oh JK (2011): The clinical characteristics, laboratory parameters, electrocardiographic, and echocardiographic findings of reverse or inverted takotsubo cardiomyopathy: comparison with mid or apical variant. Clin Cardiol 34 (11), 693-699

Spinelli L, Trimarco V, Di Marino S, Marino M, Iaccarino G, Trimarco B (2010): L14Q polymorphism of the G protein coupled receptor kinase 5 is associated with left ventricular apical ballooning syndrome. Eur J Heart Fail 12 (1), 13-16

Stadtfeld M, Nagaya M, Utikal J, Weir G, Hochedlinger K (2008): Induced pluripotent stem cells generated without viral integration. Science 322 (5903), 945-949

Stauske M: Modelling genetic heart diseases with patient-specific induced pluripotent stem cells. Naturwiss.Diss. Göttingen 2014

Stover AE, Schwartz PH (2011): Adaptation of human pluripotent stem cells to feeder-free conditions in chemically defined medium with enzymatic single-cell passaging. Methods Mol Biol 767, 137-146

Streckfuss-Bömeke K, Wolf F, Azizian A, Stauske M, Tiburcy M, Wagner S, Hübscher D, Dressel R, Chen S, Jende J (2013): Comparative study of human-induced pluripotent stem cells derived from bone marrow cells, hair keratinocytes, and skin fibroblasts. Eur Heart J 34 (33), 2618-2629

Subban V, Ramachandran S, Victor SM, Gnanaraj A, Ajit MS (2012): Apical ballooning syndrome in first degree relatives. Indian Heart J 64 (6), 607-609

Sun N, Yazawa M, Liu J, Han L, Sanchez-Freire V, Abilez OJ, Navarrete EG, Hu S, Wang L, Lee A (2012): Patient-specific induced pluripotent stem cells as a model for familial dilated cardiomyopathy. Sci Transl Med 4 (130), 130ra47

Takahashi K, Tanabe K, Ohnuki M, Narita M, Ichisaka T, Tomoda K, Yamanaka S (2007): Induction of pluripotent stem cells from adult human fibroblasts by defined factors. Cell 131 (5), 861-872

Templin C, Ghadri JR, Diekmann J, Napp LC, Bataiosu DR, Jaguszewski M, Cammann VL, Sarcon A, Geyer V, Neumann CA (2015): Clinical Features and Outcomes of Takotsubo (Stress) Cardiomyopathy. N Engl J Med 373 (10), 929-38

Tohyama S, Hattori F, Sano M, Hishiki T, Nagahata Y, Matsuura T, Hashimoto H, Suzuki T, Yamashita H, Satoh Y (2013): Distinct metabolic flow enables large-scale purification of mouse and human pluripotent stem cell-derived cardiomyocytes. Cell Stem Cell 12 (1), 127-137

Toli D, Buttigieg D, Blanchard S, Lemonnier T, Lamotte d'Incamps B, Bellouze S, Baillat G, Bohl D, Haase G (2015): Modeling amyotrophic lateral sclerosis in pure human iPSC-derived motor neurons isolated by novel FACS double selection technique. Neurobiol Dis 82, 269-280

Tsuchihashi K, Ueshima K, Uchida T, Oh-mura N, Kimura K, Owa M, Yoshiyama M, Miyazaki S, Haze K, Ogawa H (2001): Transient left ventricular apical ballooning without coronary artery stenosis: a novel heart syndrome mimicking acute myocadial infarction. Angina Pectoris-Myocardial Infarction Investigations in Japan. J Am Coll Cardiol 38 (1), 11-18

Ueyama T (2004): Emotional stress-induced Tako-tsubo cardiomyopathy: animal model and molecular mechanism. Ann N Y Acad Sci 1018, 437-444

Ueyama T, Hano T, Kasamatsu K, Yamamoto K, Tsuruo Y, Nishio I (2003): Estrogen attenuates the emotional stress-induced cardiac responses in the animal model of Tako-tsubo (Ampulla) cardiomyopathy. J Cardiovasc Pharmacol 42, 117-119

Ueyama T, Ishikura F, Matsuda A, Asanuma T, Ueda K, Ichinose M, Kasamats K, Hano T, Akasaka T, Tsuruo Y (2007): Chronic estrogen supplementation following ovariectomy improves the emotional stress-induced cardiovascular responses by indirect action on the nervous system and by direct action on the heart. Circ J 71 (4), 565-573

Ueyama T, Kasamatsu K, Hano T, Tsuruo Y, Ishikura F (2008): Catecholamines and estrogen are involved in the pathogenesis of emotional stress-induced acute heart attack. Ann N Y Acad Sci 1148, 479-485

Vriz O, Minisini R, Citro R, Guerra V, Zito C, De Luca G, Pavan D, Pirisi M, Limongelli G, Bossone E (2011): Analysis of beta1 and beta2-adrenergic receptors polymorphism in patients with apical ballooning cardiomyopathy. Acta Cardiol 66 (6), 787-790

Vuolteenaho O, Ala-Kopsala M, Ruskoaho H (2005): BNP as a biomarker in heart disease. Adv Clin Chem 40, 1-36

Warren L, Manos PD, Ahfeldt T, Loh YH, Li H, Lau F, Ebina W, Mandal P, Smith ZD, Meissner A (2010): Highly efficient reprogramming to pluripotency and directed differentiation of human cells using synthetic modified mRNA. Cell Stem Cell 7 (5), 618-630

Wehrens XHT, Lehnart SE, Reiken S, Vest JA, Wronska A, Marks AR (2006): Ryanodine receptor/calcium release channel PKA phosphorylation: A critical mediator of heart failure progression. Proc Natl Acad Sci U S A 103 (3), 511-518

Wittstein IS, Thiemann DR, Lima JA, Baughman KL, Schulman SP, Gerstenblith G, Wu KC, Rade JJ, Bivalacqua TJ, Champion HC (2005): Neurohumoral features of myocardial stunning due to sudden emotional stress. N Engl J Med 352 (6), 539-548

Xu C, Inokuma MS, Denham J, Golds K, Kundu P, Gold JD, Carpenter MK (2001): Feeder-free growth of undifferentiated human embryonic stem cells. Nat Biotechnol 19 (10), 971-974

Yamazaki T, Komuro I, Zou Y, Kudoh S, Shiojima I, Hiroi Y, Mizuno T, Aikawa R, Takano H, Yazaki Y (1997): Norepinephrine induces the raf-1 kinase/mitogen-activated protein kinase cascade through both α1- and β-adrenoceptors. Circulation 95, 1260-1268

Yan G, Zhu N, Huang S, Yi B, Shang X, Chen M, Wang N, Zhang GX, Talarico JA, Tilley DG (2015): Orphan nuclear receptor Nur77 inhibits cardiac hypertrophic response to beta-adrenergic stimulation. Mol Cell Biol 35 (19), 3312-3323

Yang X, Pabon L, Murry CE (2014a): Engineering adolescence: maturation of human pluripotent stem cell-derived cardiomyocytes. Circ Res 114 (3), 511-523

Yang X, Rodriguez M, Pabon L, Fischer KA, Reinecke H, Regnier M, Sniadecki NJ, Ruohola-Baker H, Murry CE (2014b): Tri-iodo-l-thyronine promotes the maturation of human cardiomyocytes-derived from induced pluripotent stem cells. J Mol Cell Cardiol 72, 296-304

Ye L, Muench MO, Fusaki N, Beyer AI, Wang J, Qi Z, Yu J, Kan YW (2013): Blood cell-derived induced pluripotent stem cells free of reprogramming factors generated by Sendai viral vectors. Stem Cells Transl Med 2 (8), 558-566

Yu J, Vodyanik MA, Smuga-Otto K, Antosiewicz-Bourget J, Frane JL, Tian S, Nie J, Jonsdottir GA, Ruotti V, Stewart R (2007): Induced pluripotent stem cell lines derived from human somatic cells. Science 318 (5858), 1917-1920

Zachara NE, O'Donnell N, Cheung WD, Mercer JJ, Marth JD, Hart GW (2004): Dynamic O-GlcNAc modification of nucleocytoplasmic proteins in response to stress. A survival response of mammalian cells. J Biol Chem 279 (29), 30133-30142

Zhang J, Wilson GF, Soerens AG, Koonce CH, Yu J, Palecek SP, Thomson JA, Kamp TJ (2009): Functional cardiomyocytes derived from human induced pluripotent stem cells. Circ Res 104 (4), 30-41

Zhou J, Huynh QK, Hoffmann RT, Crook ED, Daniels MC, Gulve EA, McClain DA (1998): Regulation of glutamine: fructose-6-phosphate amidotransferase by cAMP-dependent protein kinase. Diabetes 47 (12), 1836-1840

Zraika S, Dunlop M, Proietto J, Andrikopoulos S (2002): The hexosamine biosynthesis pathway regulates insulin secretion via protein glycosylation in mouse islets. Arch Biochem Biophys 405 (2), 275-279

Zwi L, Caspi O, Arbel G, Huber I, Gepstein A, Park IH, Gepstein L (2009): Cardiomyocyte differentiation of human induced pluripotent stem cells. Circulation 120 (15), 1513-1523

Acknowledgements

I'd like to thank everybody, who supported me during the work on my thesis.

Special thanks go to

Prof. Dr. med. Gerd Hasenfuß for giving me the opportunity to work at the Clinic for Cardiology and Pneumology in Göttingen and thereby making this thesis possible in the first place.

PD Dr. rer. nat. Katrin Streckfuß-Bömeke for her outstanding support during my three years in the translational stem cell lab. She always took the time to discuss the ongoing work on my dissertation and I always valued her advice and work ethic highly.

Thomas Borchert for his excellent support, advice and friendship during the time we worked together on the TTS project.

Sandra Georgi for introducing me to the cell culture work and for providing technical assistance whenever I needed it.

Luis Haupt, Andrey Fomin and all the other colleagues of the translational stem cell lab, temporarily or permanent, with whom I enjoyed working in a friendly and productive atmosphere.